

NPS ARCHIVE
1966
PORTER, O.

INVESTIGATION OF NOISE CAUSED BY
FLOW CONTROL TO A PRESSURE REDUCING MAZE

by

Oliver H. Porter
Lieutenant
United States Navy

Massachusetts Institute of Technology

May, 1966

Thesis
P7426

DUDLEY KNOX LIBRARY
NAVAL POSTGRADUATE SCHOOL
MONTEREY, CA 93943-5101
1000 S. Highway 1
Monterey, CA 93943-5101



INVESTIGATION OF NOISE CAUSED BY
FLOW CONTROL TO A PRESSURE REDUCING MAZE

by
Oliver Howard Porter
B.S Central Michigan University
(1957)

Submitted in Partial Fulfillment of
the Requirements for the Degrees of

MASTER OF SCIENCE
in
MECHANICAL ENGINEERING

and

NAVAL ENGINEER

at the
Massachusetts Institute of Technology
June, 1966

NPS ARCHIVE

1966

PORTER, O.

~~11.2.66~~

~~5.74.66~~

ABSTRACT

INVESTIGATION OF NOISE CAUSED BY
FLOW CONTROL TO A PRESSURE REDUCING MAZE

by Oliver Howard Porter

Submitted to the Department of Naval Architecture and Marine Engineering on May 20, 1966 in partial fulfillment of the requirement for the degrees of Master of Science in Mechanical Engineering and Naval Engineer.

Hydrodynamic sound in a conventional pressure reducing valve is undesirable in the steam systems of naval ships and certain commercial power plants. To overcome this problem a steel ball maze has been proposed as a substitute for existing reducer valves.

The objective of this thesis is to investigate the noise producing effects of adding a flow control plug and seat to the maze. Theoretical analysis gives very little information as to the best configuration to use. An experimental investigation established that the noise introduced by at least those configurations tested was no more than 6 db (re 10^{-2} inches/sec²) and in some cases even reduced the noise produced in the maze.

The results are based on comparing the recorded narrow band frequency analysis of the signal from an accelerometer attached to the maze housing. Tests were run with maze inlet pressures varying between 300 and 600 psig while the reduced outlet pressure was held constant at 150 psig. Using air for the test simplified experimental procedures. Even though the results are all useful in themselves, designs and tests were made anticipating extrapolation to steam environments.

Further research work is continuing on these forms of pressure reducing devices. The work here substantiates the low noise attributes of the maze and proves that a flow regulation feature will not introduce excessive noise.

Thesis Supervisor: A.L. Hesselschwerdt
Title: Associate Professor of Mechanical Engineering

Thesis Advisor: P. Leehey
Title: Associate Professor of Naval Architecture

ACKNOWLEDGEMENTS

The author is indeed grateful to Professor Hesselschwerdt for the initial arrangements leading to this Thesis. During subsequent meetings his professional exactness and knowledge engendered a deep respect and desire for these attributes.

The realization of the objective here would have been impossible without the warm personal attention and the resources received from Mr. Paul Hayner and Mr. Larry Sharp of Sanders Associates.

Professor Leehey's vivid classroom presentations and the many informal discussions with him have been a continuing inspiration to gain a broader insight of the acoustic phenomena. His personal concern and patience during this thesis period has been especially appreciated.

The fact that final typing was accomplished so rapidly and smoothly can only be credited to the skill and patience of my devoted wife, Janeen.



TABLE OF CONTENTS

	Page
Chapter I Introduction	1
A. Background	1
B. Noise Definition	2
Chapter II Pressure Reducing Devices	8
A. Conventional Steam Valve	8
B. Reducing Maze	11
Chapter III Thesis Objective	15
Chapter IV Theoretical Investigation	18
A. Fluid Flow	18
B. Hydrodynamic Sound	25
Chapter V Experimental Investigation	35
A. General	35
B. Background Noise	36
C. Instrumentation Techniques	39
D. Variables	45
E. Procedure	48
Chapter VI Results	50
A. Theoretical	50
B. Experimental	51
Chapter VII Conclusion	57
Chapter VIII Recommendations	61
Appendix	
A. Steam Calculations	63
B. Fluid Properties	75
C. Experimental Apparatus	79
D. Data	87
E. Instrumentation	127
F. References	139



LIST OF FIGURES

Figure		Page
1	Typical Steam Reducer Valve Application	8-II
2	Cross Section of Typical Steam Reducer Valve	9-II
3	Proposed Maze Reducer	12-II
4	Analysis Regions for Axisymmetric Reducer Maze	19-IV
5	Elements of Ideal Flow	20-IV
6	Axisymmetric Relations	21-IV
7'	Unbounded Space	28-IV
7	Sketch of Experimental Apparatus	35a-V
8	Sketch of Plug and Stem	35b-V
9	Table Plug-Seat Combinations	46a-V
10	Proposed Seat Configuration	53-VI
A-1	Steam Reducing Valve Control Volume	63-A
A-2	Temperature Entropy Diagram	66-A
A-3	Steam Valve Interior Control Volume	69-A
A-4	Approximate Throat Velocities	74-A
B-1	Static Properties	76-B
C-1	Test Apparatus Arrangement	82-C
C-2	Calibrated Maze Characteristics	84-C
C-3	Plug-Seat and Maze Details	85-C
D-1	Run 1-10	94-D
D-2	Run 11-15	95-D
D-3a	Run 7,10,16,18	96-D
D-3b	Run 108,119,115,123	97-D
D-4	Run 20-23	98-D
D-5a	Run 81-84	99-D
D-5b	Run 85-88	100-D
D-5c	Run 75-80	101-D
D-6	Run 24-49	102-D
D-7	Run 105-126	105-D
D-8	Run 89-104	108-D
D-9	Run 1-5	111-D
D-10		112-D
to	Recorded Data	to
D-23		126-D
E-1	Frequency Response of Pick-Up System	128-E
E-2	Frequency Response of Sound Level Meter	128-E
E-3	Selectivity Curves for B & K Analyzer	130-E
E-4	Recorder Frequency Characteristics	130-E
E-5	Calibration Checks	132-E
E-6	Sound Level Meter Gain	138-E
E-7	Accelerometer/ SLM Db Conversions	137-E





INTRODUCTION

Chapter I

A. Background:

The need for the physical process of reducing a high pressure fluid to a lower pressure is ubiquitous in our modern society. The many devices that perform this process today have evolved through the years mainly from experience as guided by theoretical reasoning. These devices or pressure reducing valves have been designed with varying degrees of emphasis on such characteristics as thermodynamic efficiency, fluid flow properties, mechanical size and operation, complexity, cost, dependability, and reliability. However, in recent years applications for a quiet valve have appeared with the result of increased emphasis on acoustic behavior (1)

Problems as widely ranging as neighborhood noise discomfort from electric power plants (2) to protection of naval ships from enemy detection (3) could be significantly moderated by a quiet pressure reducing valve. This thesis as detailed in Chapter III delves into one aspect of a proposed substitute for the conventional pressure reducing valve. The next section develops the historical and analytical justification for this investigation. Although the author has chosen to present the background in terms of naval applications*, similar cases could be presented for the many other needs of a quiet reducing valve. For instance see Muller(2) or reference (5).

*The opinions expressed are the authors and do not necessarily reflect those of the Navy Department.

THEORY

CHAPTER I

The first part of the theory is devoted to the study of the properties of the functions which are defined by the following equations:

$$f(x) = \frac{1}{x} \int_0^x f(t) dt$$
$$f(x) = \frac{1}{x} \int_0^x f(t) dt$$

It is shown that these functions are continuous and differentiable, and that they satisfy the following properties:

1. $f(x) = f(1/x)$

2. $f(x) = f(x^2)$

3. $f(x) = f(x^3)$

4. $f(x) = f(x^4)$

5. $f(x) = f(x^5)$

6. $f(x) = f(x^6)$

7. $f(x) = f(x^7)$

8. $f(x) = f(x^8)$

9. $f(x) = f(x^9)$

10. $f(x) = f(x^{10})$

11. $f(x) = f(x^{11})$

12. $f(x) = f(x^{12})$

13. $f(x) = f(x^{13})$

14. $f(x) = f(x^{14})$

15. $f(x) = f(x^{15})$

16. $f(x) = f(x^{16})$

17. $f(x) = f(x^{17})$

18. $f(x) = f(x^{18})$

19. $f(x) = f(x^{19})$

20. $f(x) = f(x^{20})$

21. $f(x) = f(x^{21})$

22. $f(x) = f(x^{22})$

23. $f(x) = f(x^{23})$

24. $f(x) = f(x^{24})$

25. $f(x) = f(x^{25})$

26. $f(x) = f(x^{26})$

27. $f(x) = f(x^{27})$

28. $f(x) = f(x^{28})$

29. $f(x) = f(x^{29})$

30. $f(x) = f(x^{30})$

31. $f(x) = f(x^{31})$

32. $f(x) = f(x^{32})$

33. $f(x) = f(x^{33})$

34. $f(x) = f(x^{34})$

35. $f(x) = f(x^{35})$

36. $f(x) = f(x^{36})$

37. $f(x) = f(x^{37})$

38. $f(x) = f(x^{38})$

39. $f(x) = f(x^{39})$

40. $f(x) = f(x^{40})$

41. $f(x) = f(x^{41})$

42. $f(x) = f(x^{42})$

43. $f(x) = f(x^{43})$

44. $f(x) = f(x^{44})$

45. $f(x) = f(x^{45})$

46. $f(x) = f(x^{46})$

47. $f(x) = f(x^{47})$

48. $f(x) = f(x^{48})$

49. $f(x) = f(x^{49})$

50. $f(x) = f(x^{50})$

51. $f(x) = f(x^{51})$

52. $f(x) = f(x^{52})$

53. $f(x) = f(x^{53})$

54. $f(x) = f(x^{54})$

55. $f(x) = f(x^{55})$

56. $f(x) = f(x^{56})$

57. $f(x) = f(x^{57})$

58. $f(x) = f(x^{58})$

59. $f(x) = f(x^{59})$

60. $f(x) = f(x^{60})$

61. $f(x) = f(x^{61})$

62. $f(x) = f(x^{62})$

63. $f(x) = f(x^{63})$

64. $f(x) = f(x^{64})$

65. $f(x) = f(x^{65})$

66. $f(x) = f(x^{66})$

67. $f(x) = f(x^{67})$

68. $f(x) = f(x^{68})$

69. $f(x) = f(x^{69})$

70. $f(x) = f(x^{70})$

71. $f(x) = f(x^{71})$

72. $f(x) = f(x^{72})$

73. $f(x) = f(x^{73})$

74. $f(x) = f(x^{74})$

75. $f(x) = f(x^{75})$

76. $f(x) = f(x^{76})$

77. $f(x) = f(x^{77})$

78. $f(x) = f(x^{78})$

79. $f(x) = f(x^{79})$

80. $f(x) = f(x^{80})$

81. $f(x) = f(x^{81})$

82. $f(x) = f(x^{82})$

83. $f(x) = f(x^{83})$

84. $f(x) = f(x^{84})$

85. $f(x) = f(x^{85})$

86. $f(x) = f(x^{86})$

87. $f(x) = f(x^{87})$

88. $f(x) = f(x^{88})$

89. $f(x) = f(x^{89})$

90. $f(x) = f(x^{90})$

91. $f(x) = f(x^{91})$

92. $f(x) = f(x^{92})$

93. $f(x) = f(x^{93})$

94. $f(x) = f(x^{94})$

95. $f(x) = f(x^{95})$

96. $f(x) = f(x^{96})$

97. $f(x) = f(x^{97})$

98. $f(x) = f(x^{98})$

99. $f(x) = f(x^{99})$

100. $f(x) = f(x^{100})$

B. Noise Definition

Noise is very often defined as any unwanted sound or sounds. This elementary definition is accepted for its merits of simplicity and conciseness and will be specialized in this section, for the remaining paper, to sounds of particular origins and characteristics.

When fluids are in motion and interact with solid bodies sound can be generated. This sound is distinct from that produced by the vibration of a solid body. Although both types of sound producing mechanisms can exist simultaneously, only the former is considered here. Aerodynamic sound is this type and occurs when the interacting fluid is air.

The Helmholtz resonator (pop bottle whistle), Aeolian tones (wind hissing in power lines), and jet releases (steam from a locomotive or power station escaping into the air) are examples of everyday sounds produced by a fluid flowing in the presences of a solid body which does not vibrate.

Other examples not so widely known are boundary layer turbulence (fluid flow along a surface), flow transition processes (squeal of fluid passing through a partially opened valve), and others of no direct concern here.

All these flow sounds, often called hydrodynamic sounds, can be classified as noise when the "unwanted" aspect of the definition is satisfied. Psychological annoyance or hearing and communications interference are well known reasons for calling a sound, noise. A very important military reason is that of detection and identification.



Sounds corresponding to the above examples or their combinations are present on naval military ships in varying intensities. These sounds of fluid flow origin combine with sounds from other sources (i.e. solid body vibration, gears, etc.) to produce an overall sound radiation field about a ship. The component of this total ship-sound field due to fluid flowing internally (i.e. pipe flow) ~~and~~ is of particular interest here.

Essentially a ship is a closed steel container. Therefore most of the internal sounds escaping must be transmitted by the steel shell. For purposes here, disregard how it got there and assume a sound of intensity I_0 exists in the ship's shell. The coupling interface efficiencies between the steel and air or water media is of the order: (4)

$$1 \quad \tau \equiv \frac{I_{\text{transmitted}}}{I_0} \equiv \begin{array}{l} \text{Sound Power} \\ \text{Transmission} \\ \text{coefficient} \end{array}$$

For plain waves acoustic text books show this equal to:

$$1a \quad \tau \equiv \frac{4 \rho_s c_s \cdot \rho_m c_m}{(\rho_s c_s + \rho_m c_m)^2}$$

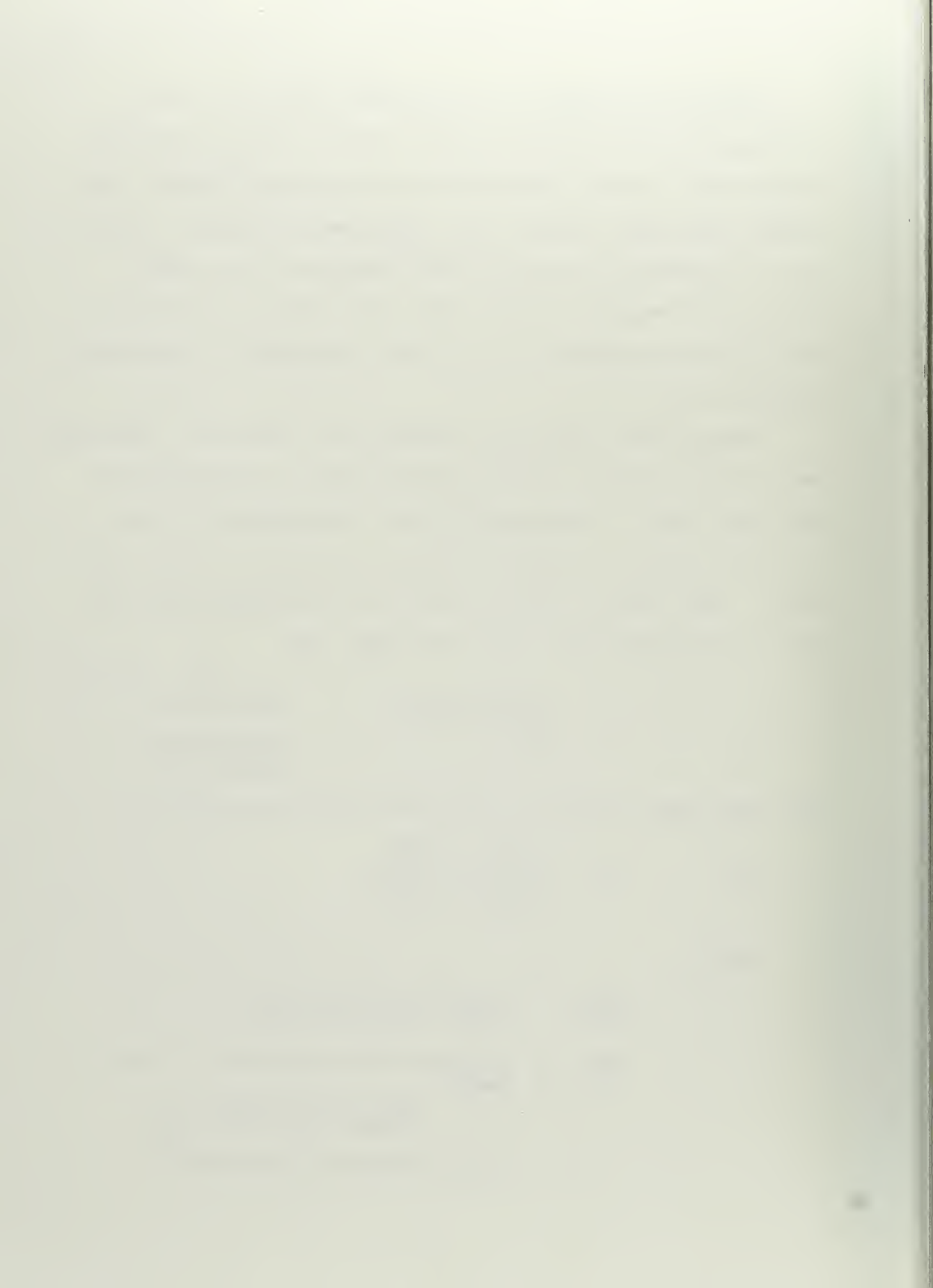
where:

$\rho_s c_s \equiv$ Characteristic impedance of the steel: $47 \cdot 10^6$ rayls

$\rho_m c_m \equiv$ Characteristic impedance of the media:

air = 415 rayls
water = $1.5 \cdot 10^6$ rayls

$I =$ Sound Intensity (watts/meter²)



These quantities substituted into equation 1a will give:

for the shell-air interface:

$$1b \quad \tau_{s-air} = \frac{(I_m)_{air}}{I_o} \approx 10^{-5}$$

and for the shell-water interface:

$$1c \quad \tau_{s-H_2O} = \frac{(I_m)_{H_2O}}{I_o} \approx 10^{-1}$$

Considering the radiation sound field of the ship to be essentially spherical at a sufficient range r , the sound intensity can be represented by:

$$2 \quad I = I_m \frac{\exp(-2r\alpha_m)}{r^2}$$

where:

I = sound intensity at r
 r = radial distance from ship
 I_m = initial intensity in media
 α_m = attenuation constant for media:

for air: $\alpha_{m_{air}} = 2 \times 10^{-11} (f^2)$ nepers/meter

for H_2O : $\alpha_{m_{H_2O}} = 24 \times 10^{-15} (f^2)$ nepers/meter

f = frequency of sound

Comparing the intensities of a sound wave traveling through air versus one traveling in water for a given intensity, I_o , existing in the steel shell an order of magnitude can be obtained:

$$2a \quad \frac{I_{H_2O}}{I_{air}} = \frac{(I_m)_{H_2O} \exp(-2r\alpha_{m_{H_2O}})}{(I_m)_{air} \exp(-2r\alpha_{m_{air}})}$$



Substituting into 2a from 1b and 1c:

$$\frac{I_{H_2O}}{I_{air}} = \frac{\tau_{s-H_2O}}{\tau_{s-air}} \cdot e^{+2r(\alpha_{mair} - \alpha_{mH_2O})}$$

$$2b \quad \frac{I_{H_2O}}{I_{air}} \approx 10^4 e^{2r\alpha_{mair}}$$

This relation shows that although there are two possible paths for internal sounds to radiate from a ship, the steel-water coupling is many orders better than the steel-air. The result is that most of the ship's sound field is carried through the water. Corresponding analysis for sounds originated on the outside of a ship (hull boundary layer turbulence, wave action, etc.) likewise shows water to be the dominate transmitting media.

The decay of this sound in water increases as the square of the frequency which appears in the attenuation constant of equation 2. Experience and test (3) have shown that frequencies can be neglected above 15 kcps as they are sufficiently attenuated by the water at any range of military consequence.

Spectrum analysis of these underwater radiations at a distance from the ship will show certain frequencies or frequency bands of the sound field to be very prominent. In fact a particular ship type usually has a unique profile of



of frequency plotted against intensity appropriatedly called "Ship's Signature."

The military importance of detecting and identifying a ship by its Signature thus creates an ironical specialization in the above definition of noise. The underwater sound from friendly ships can be classified as noise but the exact same sound from an enemy ship can not possibly fulfill the "unwanted" aspect of the noise definition.

Simultaneously with the developments in methods of underwater sound detection and analysis have been programs to eliminate or reduce the sources of noise from friendly ships.

Removing one dominate component has exposed other less intense sounds in the ships noise field. Today this elimination process has reached the point where fluid flow sounds in piping contribute a significant component to a ship's sound field.

The firm of Sanders Associates of Nashua, N.H. has recently developed for the Navy a hydraulic fluid control valve which operates without the objectionable flow noise of earlier valves. They, along with other agencies, are now attacking the problem of flow sounds in steam pressure reducing valves. This Thesis is a independent study undertaken in consonance with this development program at Sanders.

With the above background this section can be concluded



with an extended definition of noise as interpreted for this thesis: Noise is the unwanted sound in the frequency band 20-15,000 cps, which is produced in steam pressure reducing valves of naval ships.



PRESSURE REDUCING DEVICES

Chapter II

A. Steam Pressure Reducing Valves:

An universal application of the pressure reducing valve is in the auxiliary steam system of power plants. This system, figure 1, taps off the main steam header (600psig, 486°F Sat.) and supplies steam at 150psig for the condenser air ejectors, aeration system, and other ancillary reduced-pressure systems. The air ejectors and therefore the turbine efficiency are very sensitive to fluctuations in the 150psig pressure of the auxiliary system. For this reason the reducing valve must be capable of close regulation, the bounds of pressure variations depending on the particular power plant. Valve sizes also vary but a typical 1¼ inch valve can pass up to approximately 10,000 pounds mass of steam per hour.

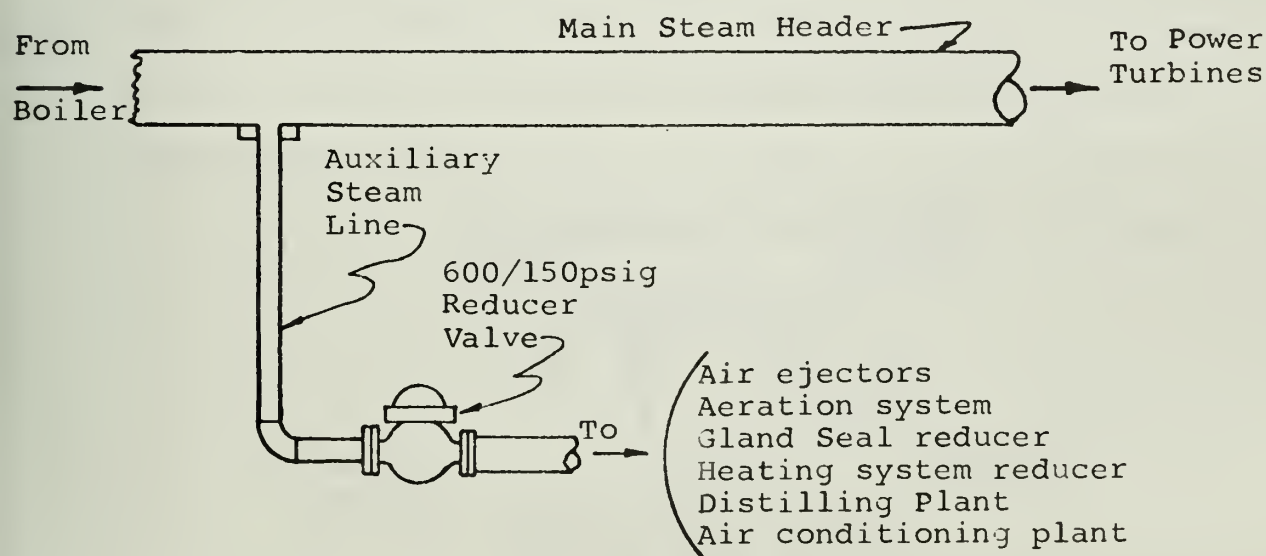
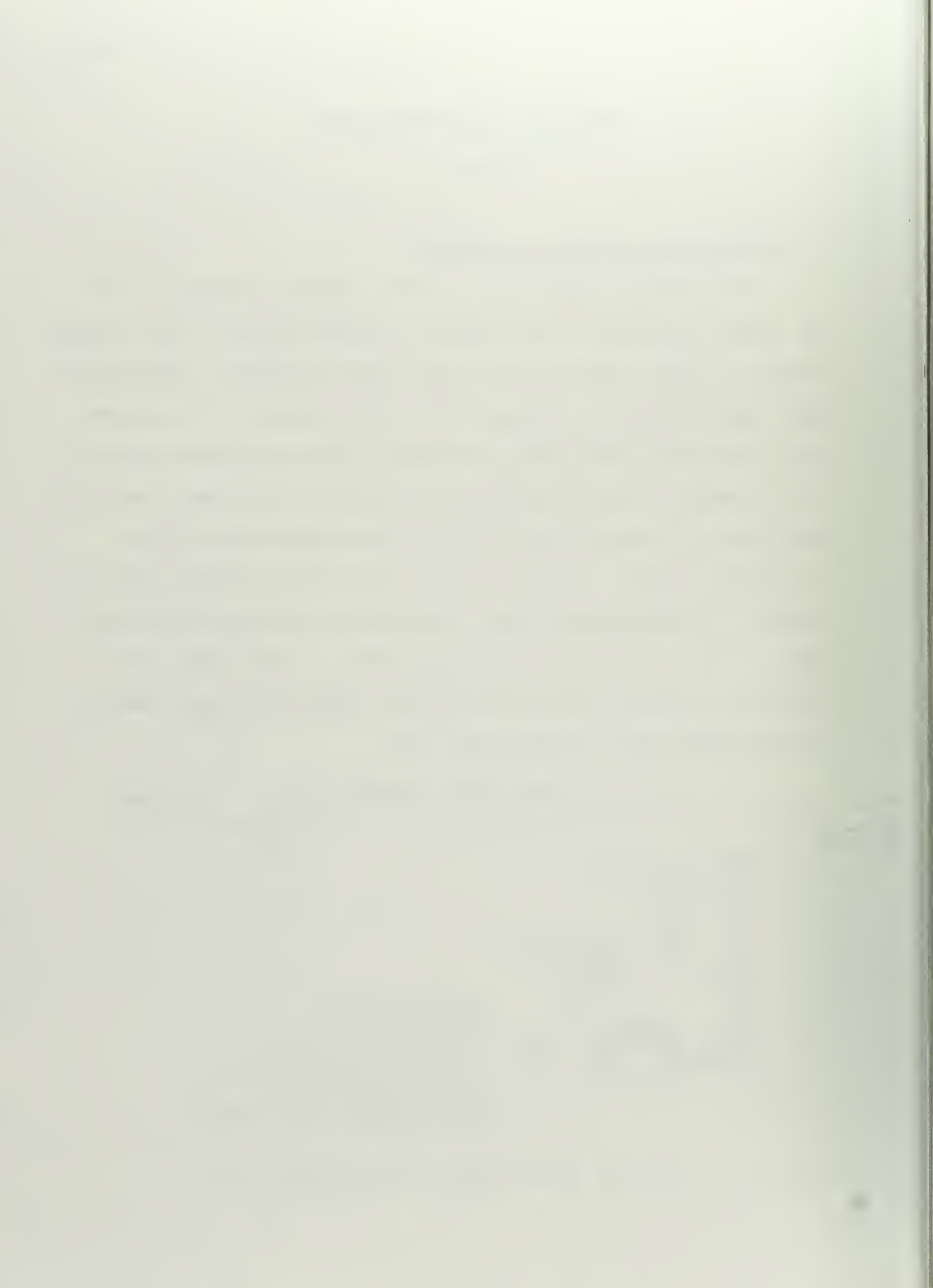


Figure 1 Typical Steam Reducer Valve Application



The internal configuration basically resembles the diagram of figure 2. The operating principles of the valve are easily understood. The valve plug, P, moves off its seat, S, whenever a differential force occurs across the diaphragm, D, . Ideally the valve plug opens just the correct amount to allow high pressure inlet steam to expand in the throat, t, at a rate sufficient to maintain the 150 psig outlet pressure. The velocity developed in the throat section is dissipated in the diffusion region, V. Obviously the differential force on the diaphragm must be related to the outlet pressure for automatic regulation. The actual details of how this is accomplished vary with each manufacturer's ingenuity and is well documented in the literature (6) (7) (8). However, the reducing valve is a distinct type of control valve. Whereas other control valves are usually designed to obtain outlet conditions (i.e. piston displacement, mass or volume flow rate, temperature changes, etc.) at a minimum of pressure loss across the device, pressure reducing control valves are deliberately designed for this loss.

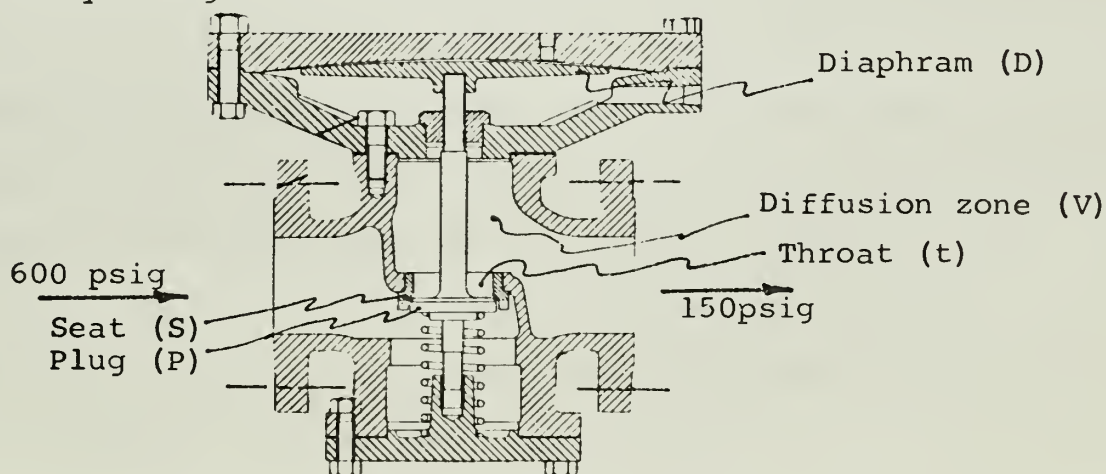


Figure 2

Figure 2 Cross Section of Typical Steam Reducer Valve



The detailed thermodynamic and flow behavior of the steam in passing through these valves is not as simple to analyze. In fact, valve designers are forced to semi-empirical methods when dealing with these properties (6,8,9,10,11,12). The elementary thermodynamic analysis of appendix A however, does show that the pressure reducing process is approximately a throttling process-i.e. a constant enthalpy process. Thermodynamically such a process represents the maximum degradation of theoretical useful energy of the steam. Thus a helpful conclusion is that any device that reduces pressure is as good thermodynamically (or really poor) as any other. Therefore thermodynamic restrictions do not influence a reducing valve configuration.

Review of published literature shows that very little is known about the velocity and pressure fluctuations of the fluid in passageways of the valve. Calculation of Appendix A do determine that the velocity in the throat region can reach the transonic range. The shock waves (and condensation effects) inherent in this flow range undoubtedly contribute to flow noise as well as to the problem of "wire drawing". It is interesting to note that Muller (2) finds this noise mechanism to be of 2nd order. This high velocity flow of the throat must be deaccelerated in the diffusion region, V, so that the flow leaves the valve with average pipe velocity. Chapter IV-B considers noise from such a diffusion region in which turbulent flow is known to dominate.



Further research with steam reducing valves is presently underway at MIT. As part of the background development for the objectives of this investigation, the significant characteristics of the steam pressure reducing valves are summarized:

- C1 Present reducing valves control outlet pressure by regulating the rate of mass flow (vice volume or temperature).
- C2 Any device that reduces pressure is admissible as an thermodynamic efficient reducing valve.
- C3 Internal flow velocities and pressure fluctuations are not precisely known.
- C4 Shock waves and flow turbulence can be present in reducing valves and apparently account for the noise produced.

B. Pressure Reducing Maze:

Fluid flow through porous media has been used for filtering out solid impurities of the flow for centuries (13). Only in recent years has it been used to filter or reduce sound in the flow. The very necessary family car appendage-the muffler where the pores have been expanded to cavities is based on the principle

The well known disadvantage of putting porous media in a fluid flow is the pressure loss produced. However, since this is the desired result in a reducing valve, such a media warrants further consideration.



Figure 3 is a sketch of an artificially manufactured porous media which hence forth is called a maze. The device is basically a diverging nozzle filled with solid spheres. The adaptation of such a packed bed of spheres into a suitable pressure reducer is under development at Sanders Associates as part of their solution to the steam reducer noise problem. The lengths, sphere size, and cross sectional areas can be determined analytically so as to give a desired pressure drop or flow rate (14). The over-riding restraint has been to keep the average velocities well below the speed of sound and thus eliminate large shock waves and possibly moderate the turbulent noise mechanism.

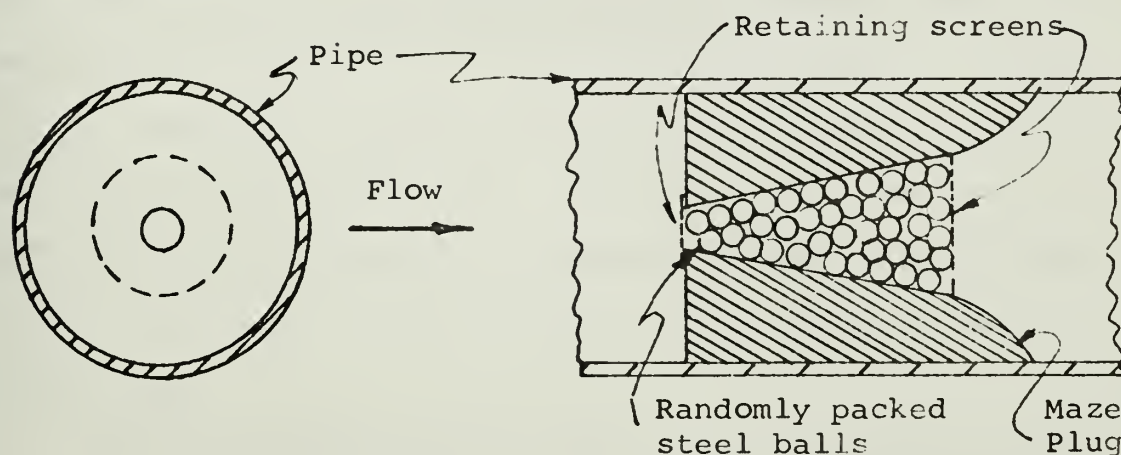


Figure 3 Proposed Maze Reducer

To determine the sound generated and to check the computed flow rates, experimental tests have been necessary. Accelerometers attached to the pipe through a thin plated diaphragm have been used to evaluate and compare the noise or acoustic output of these devices. For practical and

1. The first part of the document discusses the importance of maintaining accurate records of all transactions. It emphasizes that proper record-keeping is essential for the integrity of the financial system and for the ability to detect and prevent fraud. The text also mentions the need for regular audits and the role of independent auditors in ensuring the reliability of the data.

2. The second part of the document focuses on the challenges faced by organizations in implementing effective internal controls. It highlights the complexity of modern business environments and the need for a robust framework of controls to manage risks. The text suggests that organizations should adopt a risk-based approach to internal control design and implementation, focusing on the most significant risks to the organization's objectives.

3. The third part of the document discusses the importance of transparency and disclosure in financial reporting. It notes that providing clear and concise information to stakeholders is crucial for building trust and confidence in the organization. The text also mentions the need for organizations to comply with relevant regulatory requirements and to ensure that their disclosures are consistent and reliable.



4. The fourth part of the document discusses the importance of continuous improvement in financial reporting. It notes that the financial reporting process is not static and should evolve over time to reflect changes in the business environment and regulatory requirements. The text suggests that organizations should regularly review and update their reporting processes to ensure they remain effective and efficient.

5. The fifth part of the document discusses the importance of training and education for financial reporting staff. It notes that staff should have the necessary skills and knowledge to perform their duties effectively. The text suggests that organizations should provide ongoing training and education to their staff to ensure they are up-to-date with the latest developments in financial reporting.

economical reasons the initial development phases have been with scale models and using dry nitrogen gas as the fluid. Flow scaling effects have been assumed to be geometrically related but the scale effect on noise output has yet to be determined. Also the possible noise generating mechanism of steam condensation processes has not been reckon with in testing for the gained advantage of experimental simplification.

As a standard of comparison for the various mazes, a sharp edged orifice with similar flow and pressure drop characteristics was selected. Tests conducted at the same pressures using octave and narrow band analysis show the maze has on the order 30db less noise generation. (Figure D-12) Recently a limited test of a full scale maze with saturated steam indicated a similar trend. However difficulties in eliminating upstream and downstream flow noise at the test section prevented conclusive evaluation of the maze.

Additional development efforts with various configurations of manufactured porous media are continuing at Sanders. The very challenging research to perfect a given maze as a pressure reducer is not the purpose of this dissertation. Rather the characteristics of a particular maze configuration are accepted without question, at least for purposes of investigation. Referring to the characteristics of the



conventional reducer, II-A, it is apparent that item 2 and

3 apply directly to the maze, item 4 can somewhat be controlled by design, and item 1 does not apply i.e.; the maze by itself can not regulate the flow.



THESIS OBJECTIVE

Chapter III

Developmental work on the packed-sphere maze to date has been directed toward finding the design that generates the least noise. For such a pressure reducing maze to have utility it must be adaptable to a mass control device that will maintain the desired outlet pressure for varying inlet conditions.

From the previous discussions it is apparent that any configuration to control the mass flow rate of steam must possess at least these attributes:

- a. Contribute a negligible component to the overall noise generated by the maze.
- b. Conform to good steam valve design for minimum seat erosion and thus leakage (this essentially eliminates any continuous rubbing of sealing surfaces).
- c. Be amenable to automatic control.
- d. Occupy a minimum of space.
- e. Conform with conventional standards of simplicity, reliability, repairability, and durability.

The ways in which these attributes can be combined into a practical reducing valve are limited. One promising scheme combines a number of small mazes and would control the mass flow rate by passing the high pressure stream through a certain portion of the total number. This "module" valve



would then respond to fluctuating conditions by step changes as individual mazes or modules are opened to flow. The justification for using a number of small maze passageways is based on the supposition that the noise output is related in some direct way to the flow area and hence the size of the turbulence region. Most conventional valves vary the plug to seat opening for control whereas the "module" valve would have a poppet action of either fully open or completely shut. In either type of control action, the noise component caused by the plug-seat combination is not known.

The objectives established at the beginning of this thesis evolved from these considerations. These objectives were:

- a. Conceive and model a suitable mass control configuration for the maze reducer.
- b. Determine the component of radiated noise produced by this configuration.

During the course of developing these objectives it became evident that they could be applied to a multitude of designs. And that little, if any, theoretical or empirical analysis yet published would allow predicting their noise producing effect and therefore justify a particular configuration. Consequently an axisymmetric flow arrangement has been somewhat arbitrarily selected and analyzed. The factors that influenced this decision were:

- a. The possibility of finding a mathematical model of flow.



- b. It provided a vehicle for analysis of noise produced by flow around and into solid bodies in a closed conduct.
- c. Various plug/seat combinations could be easily made and tested.
- d. The effects of each combination could be attributed to that particular plug/seat configuration (i.e. variables from flow-wall interactions and scaling effects would be minimized.)
- e. The short time required to alter an existing test apparatus.
- f. The desired attributes described above are uniformly satisfied except possibly "a"(negligible noise).

From this decision, work has proceeded as discussed in the following chapters. During testing other possible configurations became apparent. These are briefly discussed in the Recommendation of Chapter VIII.

Even though the above objectives remain valid, a more concise and determinate goal description seemed appropriate after work had progressed. The initial objectives have therefore been consolidated into the following:

TO COMPARE THE NOISE PRODUCED BY VARIOUS PLUG-SEAT COMBINATIONS IN AXISYMMETRIC FLOW TO A MAZE PRESSURE REDUCER.



THEORETICAL INVESTIGATION

Chapter IV

A. Fluid Flow Model

Although the objective of this thesis is basically empirical some effort was devoted to finding a mathematical model for the flow through a maze in a straight pipe. Many mathematical models of valves have been formulated to predict and analyze dynamic performance of control valves (15). These treat the forces and displacement-flow rate parameters.

To predict or analyze a valve's noise performance, relationships dealing with velocities and pressure variances are required. As might be expected, even this simple axisymmetric flow device becomes extremely complicated mathematically. However, capitalizing on the assumptions of ideal fluid flow certain relations can be obtained. The following is a brief outline of a proposed approach to the modeling of this device.

The physical maze is conceptually divided into regions as shown in figure 4. The considerations here do not require an exact specification of the geometric dimensions. Naturally they would be considered in the detailed model.



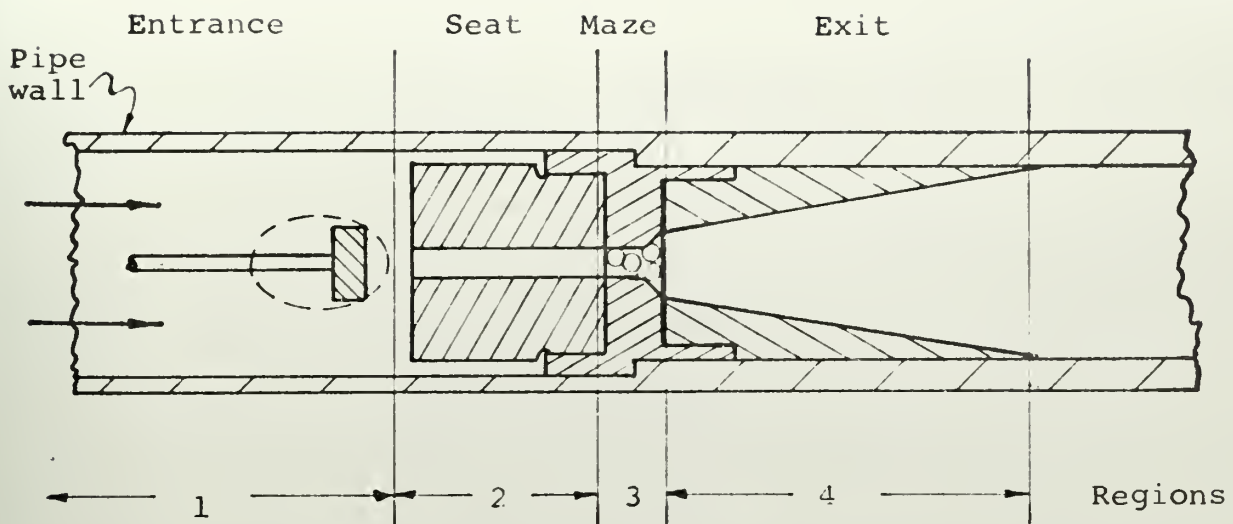


Figure 4 Analysis Regions for Axisymmetric Reducer Maze

It is proposed that using superposition and transformation principles, the flow in these regions can be synthesized from the elements of figure 5.

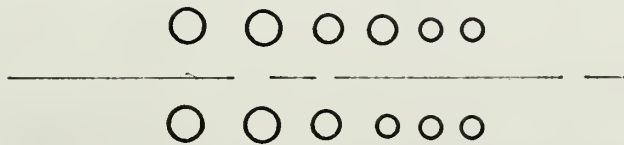
Since the average flow is everywhere axisymmetric, relationships are simplified by using two dimensional theory whenever possible. Conventional coordinates and basic expressions are given in figure 6.

Solutions to element 5a are readily obtained by slender body theory for many body shapes. M.M. Munk's (16) early work was on airship hull forms, Lamb (17) considers the general ellipsoid, J.L. Hess (18) has derived a potential for an arbitrary 3D body, while others have treated similar forms

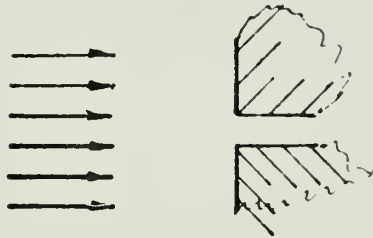




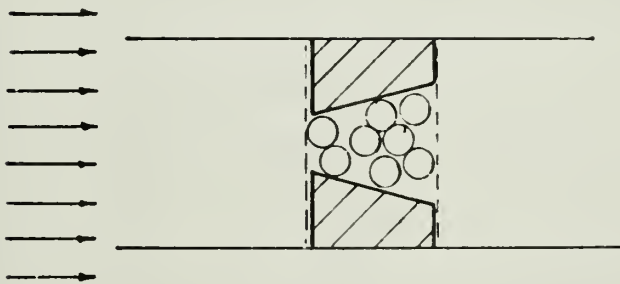
5a. Solid Body in Uniform Stream



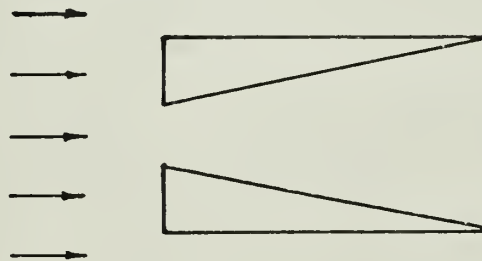
5b. Distributed Vortex Ring



5c. Entrance Orifice



5d. Porous Media



5e. Discharge Orifice

Figure 5 Elements of Ideal Flow



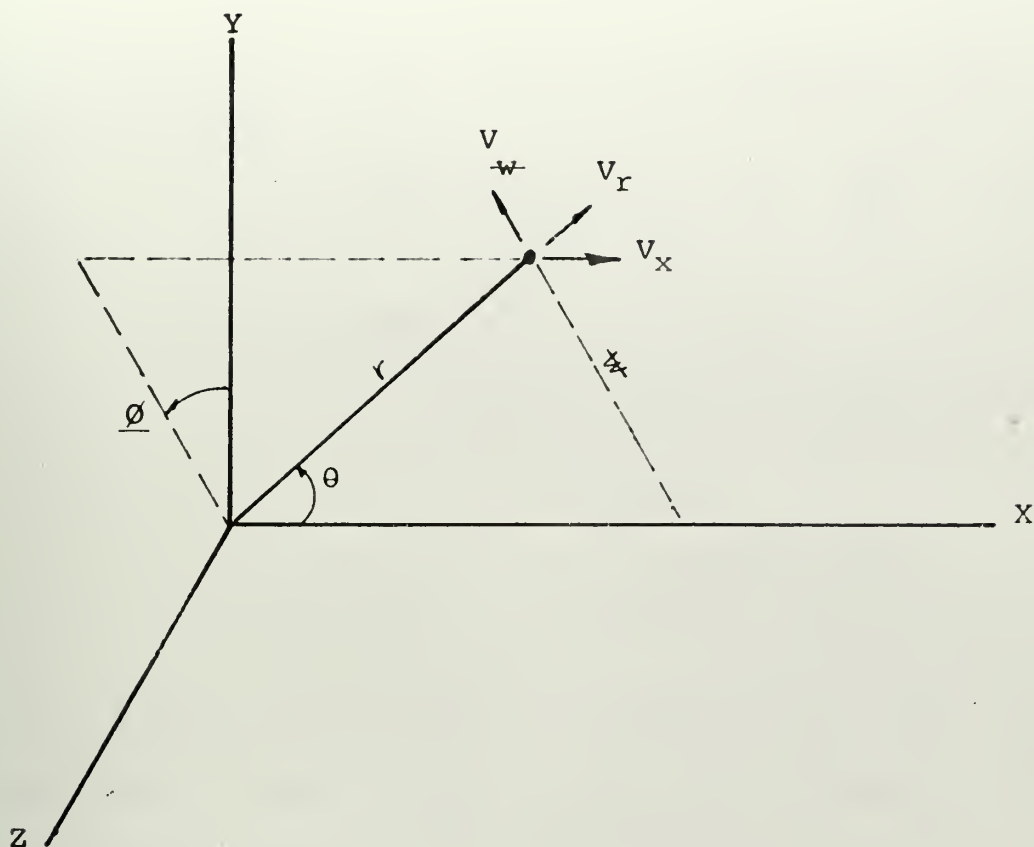


Figure 6a Axisymmetric, Cylindrical Coordinates

ϕ = velocity potential

ψ = stream function

\vec{v} = velocity vector = $\nabla \phi$

$$v_{\theta} = \frac{\partial \phi}{\partial \theta} = -\frac{\partial \psi}{\partial x}$$

$$v_x = \frac{\partial \phi}{\partial x} = \frac{\partial \psi}{\partial \theta}$$

$$\text{Continuity: } \frac{\partial \rho}{\partial t} + \frac{1}{\theta} \frac{\partial}{\partial \theta} (\theta \rho v_{\theta}) + \frac{\partial}{\partial x} (\rho v_x) = 0$$

Figure 6b Basic Axisymmetric Relationships

Figure 6 Axisymmetric Relations



A representative potential for an axisymmetric body is that given in Munk:

$$\phi = A\mu \left[\frac{1}{2} \rho \log \frac{\rho+1}{\rho-1} - 1 \right]$$

where A is a constant.

μ, ρ are coordinates defined by:

$$x = \mu \rho$$

$$y = \sqrt{1-\mu^2} \sqrt{\rho^2-1}$$

Element 5b simulates the conduct walls. This type of problem has been treated by using free streamlines (19) and distributed vortex rings. Birchhoff and Zarantonello (20) give the streamfunction of a vortex ring of radius "a":

$$\psi = (r_1^2 + r_2^2) (K/2r_1) - r_1 E$$

where:

$$r_1 = x^2 + (r+a)^2$$

$$r_2 = x^2 + (r-a)^2$$

K is the complete elliptic integral of the 1st kind

E is the complete elliptic integral of the 2nd kind

Integration of a distribution of the vortex rings would satisfy the pipe wall boundary conditions.

Conditions in region 1 of the reducer valves are therefore represented by superposing elements 5a and 5b. Region 2



corresponds to element 5c. Ehrick (21), Birkhoff (20), Robertson (19), and others treat the flow into and out of various valve configurations which would be appropriate here. Some of these involve transformation functions.

Mathematical relationships for flow in porous media have been generally empirically derived. However, for region 3 which is represented by element 5d, a potential function similar to those summarized in (19) is required. A complete mathematical description of this region may be quite complex. In which case simple sinks and sources at the inlet and outlet respectively would be necessary. These are easily expressed:

$$\phi_{\oplus} = \pm \frac{S}{4\pi r}$$

$$\psi_{\oplus} = \pm \frac{S}{4\pi} \cos \theta$$

where $\pm S$ = strength (-for source, + for sink)

The discharge element, 5e, simulating the valve region 4 can be treated in a corresponding matter to that of the inlet element 5c. Pipe boundaries and velocity, pressure and mass-flow boundary conditions between regions of course must be satisfied.

Even though each element has some type of analytic expression available in the literature, the possibility of obtaining a useable total expression is manifestly unlikely. However it is felt that each of these elements can be programmed into a computer and solved as sub routines and



and then through iteration methods matched together so as to obtain the optimum flow configuration for a given velocity flow rate. Such an undertaking would be no mean task, however the results would certainly be of interest to valve designers since each element could be specified according to each problem.



B. Hydrodynamic Sound

During recent years theoretical research on fluid-flow-solid body interaction phenomena has produced at least partial and often complete solutions to many sound problems caused by fluid flow. Although the theory is being applied to situations of greater complexity, the problem of predicting valve noise remains unanswered. The analysis and models of simple hydrodynamic sound theory however can provide at least qualitative information on valve noise.

M.J. Lighthill of the University of Manchester in 1952 & 1954 published (23) (24) his theory on aerodynamic sound which has become a popular starting point for subsequent sound analysis. The theory capitalizes on the simplicity found in Tensor notation and there is little reason to change here.

x or y \equiv space coordinate variable

x_i \equiv i^{th} coordinate ($i = 1, 2, 3$)

u_j \equiv j^{th} velocity component ($j = 1, 2, 3$)

τ_{ij} \equiv stress field tensor

ρ \equiv density

Expressed in this notation, the continuity equation has the form:

$$3 \quad \frac{\partial \rho}{\partial t} + \frac{\partial}{\partial x_i} (\rho u_i) = 0$$



Likewise the momentum equation is:

$$4 \quad F_i = \rho \frac{Du_i}{Dt} - \tau_{ij,j}$$

where:

F_i = Body force/volume

$\frac{Du_i}{Dt}$ = Substantial derivative

$$4a \quad \frac{Du_i}{Dt} = \frac{\partial u_i}{\partial t} + u_j \frac{\partial u_i}{\partial x_j}$$

Using 3,4,4a and combining terms the resulting expression is:

$$5 \quad F_i = \frac{\partial \rho u_i}{\partial t} + \frac{\partial}{\partial x_j} (\rho u_i u_j - \tau_{ij})$$

Lighthill in a simple but well directed move adds to both sides of 5 the term $c_0^2 \frac{\partial^2 \rho}{\partial x_i^2}$ and assumes no body forces to get a relation:

$$6 \quad \frac{\partial (\rho u_i)}{\partial t} + c_0^2 \frac{\partial \rho}{\partial x_i} = - \frac{\partial \tau_{ij}}{\partial x_j}$$

where:

$$\tau_{ij} = \rho u_i u_j - \tau_{ij} - c_0^2 \rho \delta_{ij}$$

c_0 = sound velocity in undisturbed fluid

Performing the operation $\frac{\partial}{\partial x_j}$ on 6 and $\frac{\partial}{\partial t}$ on 3

and subtracting gives:

$$7 \quad \frac{\partial^2 \rho}{\partial t^2} - c_0^2 \nabla^2 \rho = - \frac{\partial^2 \tau_{ij}}{\partial x_i \partial x_j}$$

where:

∇^2 = Laplacian operator



Now defining the wave operator

$$\square^2 = \left(\nabla^2 - \frac{1}{c^2} \frac{\partial^2}{\partial t^2} \right)$$

Lighthill's form of the wave equation is obtained:

$$8 \quad \square^2 \rho = \frac{1}{c_0^2} \frac{\partial^2 T_{ij}}{\partial x_i \partial x_j}$$

This expression was derived directly from the continuity and momentum relationships, 3 & 4, and therefore is appropriate in any fluid situation where these two equations hold. This wave equation subject to suitable boundary conditions has been solved in certain cases and in others approximate solutions have been found. Ultimately then, any solution to the noise mechanism of a pressure reducing valve must also be a solution of equation 8.

One particularly useful form of the solution to equation 8 is Kirchhoff's formula. This is derived mathematically as in Bateman (26) or Stratton (27). Consider^{the} fluid model shown in figure 7' where V is the volume space with a surface S present, $Q(x_i)$ is the point of interest, $P(y_i)$ is a variable point of integration, and r the distance between Q and P (i.e. $r = |x_i - y_i|$).



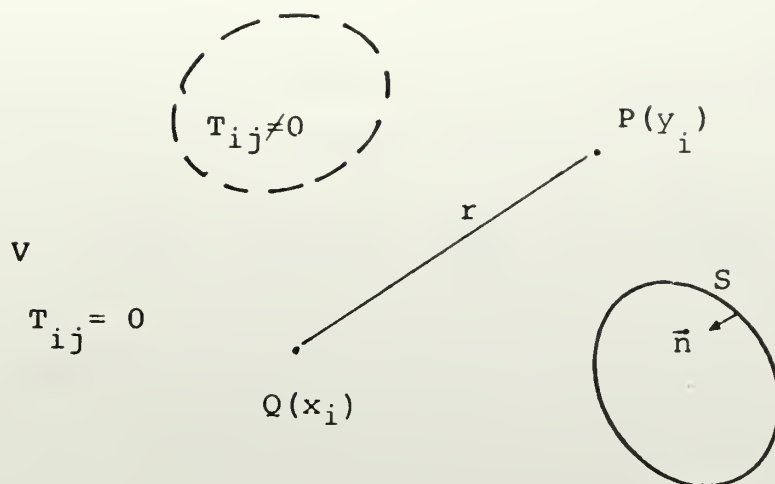


Figure 7' Unbounded Fluid Space

Kirchhoff's formula for equation 8 becomes:

$$\begin{aligned}
 &\text{For } Q \text{ in } V: 4\pi\rho_Q = \\
 &\text{For } Q \text{ on } S: 2\pi\rho_Q = \\
 &\text{For } Q \text{ not in } V: 0 =
 \end{aligned}
 \left\{ \begin{aligned}
 &\int_S \left\{ \frac{1}{r} \left[\frac{\partial \rho}{\partial n} \right] - \left[\rho \right] \frac{\partial}{\partial n} \left(\frac{1}{r} \right) + \frac{1}{rc} \frac{\partial r}{\partial n} \left[\frac{\partial \rho}{\partial t} \right] \right\} dS_p \\
 &+ \int_V \frac{1}{r} \cdot \frac{1}{c_0^2} \cdot \left[\frac{\partial^2 T_{ij}}{\partial y_i \partial y_j} \right] \cdot dV
 \end{aligned} \right.$$

where ρ_Q is the density at point Q

$\left[\right]$ is the retardation operator (i.e. t is replaced by $t-r/c$)



Lighthill considers the case of a turbulent region in an infinite fluid and so reduces equation 9 to:

$$10 \quad \rho(x_i, t) - \rho_o = \frac{1}{4\pi c_o^2} \int_V \frac{1}{r} \left[\frac{\partial^2 T_{ij}}{\partial y_i \partial y_j} \right] dV$$

where:

ρ_o (representing the undisturbed fluid)

is a constant which therefore satisfies the wave equation and hence for linear equations can be added to the solution.

Fundamental acoustic theory assumptions (4) give the relations:

$$p = c_o^2 (\rho - \rho_o)$$

$$11 \quad I = \overline{pu} = \frac{c_o^3}{\rho_o} \overline{(\rho - \rho_o)^2}$$

where:

p = acoustic perturbation pressure

I = acoustic wave intensity

\overline{pu} = ensemble average

Lighthill was able to mathematically manipulate equation 10 and with order of magnitude reasoning combine the relation with equation 11 to obtain:

12

$$I = \rho_o \left(\frac{d}{r} \right)^2 c_o^{-5} U^8$$



Which represents the intensity of sound reaching a far distant point (along r) from a turbulent wake region, characterized by d , in a uniformly flowing stream with velocity U . The mathematical behavior of the integrand of equation 10 permits identifying it as a quadrupole and thus the sound it represents as a quadrupole radiation. Expression 12 is valid only under the conditions stated (i.e. far field, infinite fluid, etc.) but extrapolating the strong noise intensity dependence on flow velocity to the noise reducer indicates at least that flow velocities play a dominant role in noise generation.

Curle (28) considers equation 8 in an infinite flowing fluid but allows a solid body to be present. Following his reasoning equation 9 becomes:

$$13 \quad p(x_i, t) - p_0 = \frac{1}{4\pi c_0^2} \int_V \left[\frac{\partial^2 T_{ij}}{\partial t^2} \right] \frac{(x_i - y_i)(x_j - y_j)}{c_0^2 r^3} dV - \frac{1}{c_0} \frac{\partial}{\partial t} \int_S \frac{(x_i - y_i)}{r^2} [P_i] dS$$

where:

$$P_i = \text{fluid stress vector} = \eta_j \tau_{ij}$$

By considering the case where the body characteristic length, d , is small with respect to, r , the distance to a far point of interest, x_i , and requiring that $d \ll \frac{c_0}{\omega}$ where ω is the circular frequency of sound, a first order approximation analysis gives:



a term corresponding to the quadrupole combination of equation 12 plus:

$$14 \quad I \simeq C_o^3 \left(\frac{\chi_i}{\chi} \right)^2 \frac{1}{\chi^2} e_o d^2 \left(\frac{U}{C_o} \right)^6$$

The integrals' mathematical behavior allows this sound component to be called dipole radiation. Equation 14 mainly shows the contribution of the surface integral of equation 13. As before this expression can not be considered valid for a reducer valve but it does indicate that the presence of a rigid body does not significantly change the noise dependence on the flow velocities involved.

When one considers the application of equation 9 to the case of an axisymmetric reducer valve or even simple pipe flow, the mathematical manipulations become nearly impossible. For instance the surface integral is evaluated with the variable point P on the surface in this case the interior pipe wall. Measurements are conveniently made on the wall therefore the density and hence pressure fluctuation are desired there too. Point Q would then also be on the interior surface and looking at the 2nd term of equation 9b the task of evaluating $\frac{\partial}{\partial n} \left(\frac{1}{r} \right)$ as P is varied over all the interior surface can be appreciated. Simplification by limiting processes or symmetry are admissible but being in the near field these methods fail.



Perhaps another form of the solution to Lighthill's wave equation other than Kirchhoff's formula will be developed which can be used for axisymmetric situations. Unable to find such a deterministic model of axisymmetric (and other complex) flows, investigators have applied probability techniques with some success. Models of the physical phenomena are now called random processes and described not by values at any instant of time but by certain probability distributions and averages such as means, moments, spectra, correlation functions, etc.

These models, then presuppose fluctuating components in the flow. In fluid mechanics such fluctuations are called turbulence vice laminar flow where velocities have a regular, continuous distribution. Turbulent motion has been characterized at each point by a mean velocity to which is added an irregular fluctuating velocity. Note that although velocity is used other fluid properties such as pressure and density which are directly related to velocity have a very similar behavior.

The irregular motion is thought to be connected with particles or masses of fluid crossing over from their average line of flow into adjacent regions in which the average velocity may be considerably different. Mixing Length Theory introduced by Prandtl (29) argues that the size of the average fluid mass which crosses over is about the same order of magnitude as the length traversed before the mass loses its identity.



Such cross over of mixing masses is really a momentum transfer phenomena. If the total velocity at a point is u_i then in turbulent motion:

$$u_i = \overline{u_i} + u'_i$$

where: $\overline{u_i}$ = average velocity

u'_i = fluctuating component of velocity

The transfer of momentum across a plane would be:

$$\overline{u'_i u'_j}$$

Batchelor (30), Townsend (31), and Hinze (32) statistically treat turbulent flow for many applications including some simple pipe flows. The averages, spectral densities and correlation expressions presented in these books, show promise for utilization with the axisymmetric maze.

However, internal pressures or other fluctuating quantities must first be equivalently determined or averaged before any meaningful conclusions can be obtained. The problem then becomes initially experimental.

Theoretical investigations of this chapter have been concerned with models of sound in turbulent flow since this mechanism appears to be dominate in the axisymmetric maze. Even so, other sources of sound may be present such as shock



waves, and vortex motions.

Although for the objectives here, turbulence has received consideration; subsequent work must treat these other modes as well.



EXPERIMENTAL INVESTIGATIONS

Chapter V

A. General

The overall experimental apparatus is sketched in figure 7. This represents the best arrangement scheme found for having minimum background noise at the test section, while still permitting interchanging plug-seat combinations at the maze. The sketch also shows the hook-up of instrumentation as used on this project.

Air from the laboratories 2000 psig system enters the apparatus through a solenoid valve and filter. A six foot rubber isolation hose joins this valve to the inlet test section. Also attached to the test section is a conventional high=pressure, right angle disc valve whose plug and seat have been removed. The screw mechanism of this valve is used to vary the plug-seat gap at the reducing maze by means of an extended stem. (Figure 8)

The inlet and outlet test sections are 5000 psig pressure, 1 inch OD, steel tubing with a wall thickness of .125 inch. Another 6 foot isolation hose joins the outlet of the test section to a calibrated flow measuring maze. After the calibrated maze, the tubing diameter is reduced to 3/4 inch. The required back pressure on the test section is maintained by adjustment of a specially constructed nozzle inside the 3/4 inch tube and a conventional orifice valve on the end. The detailed description of each component is given in appendix C.



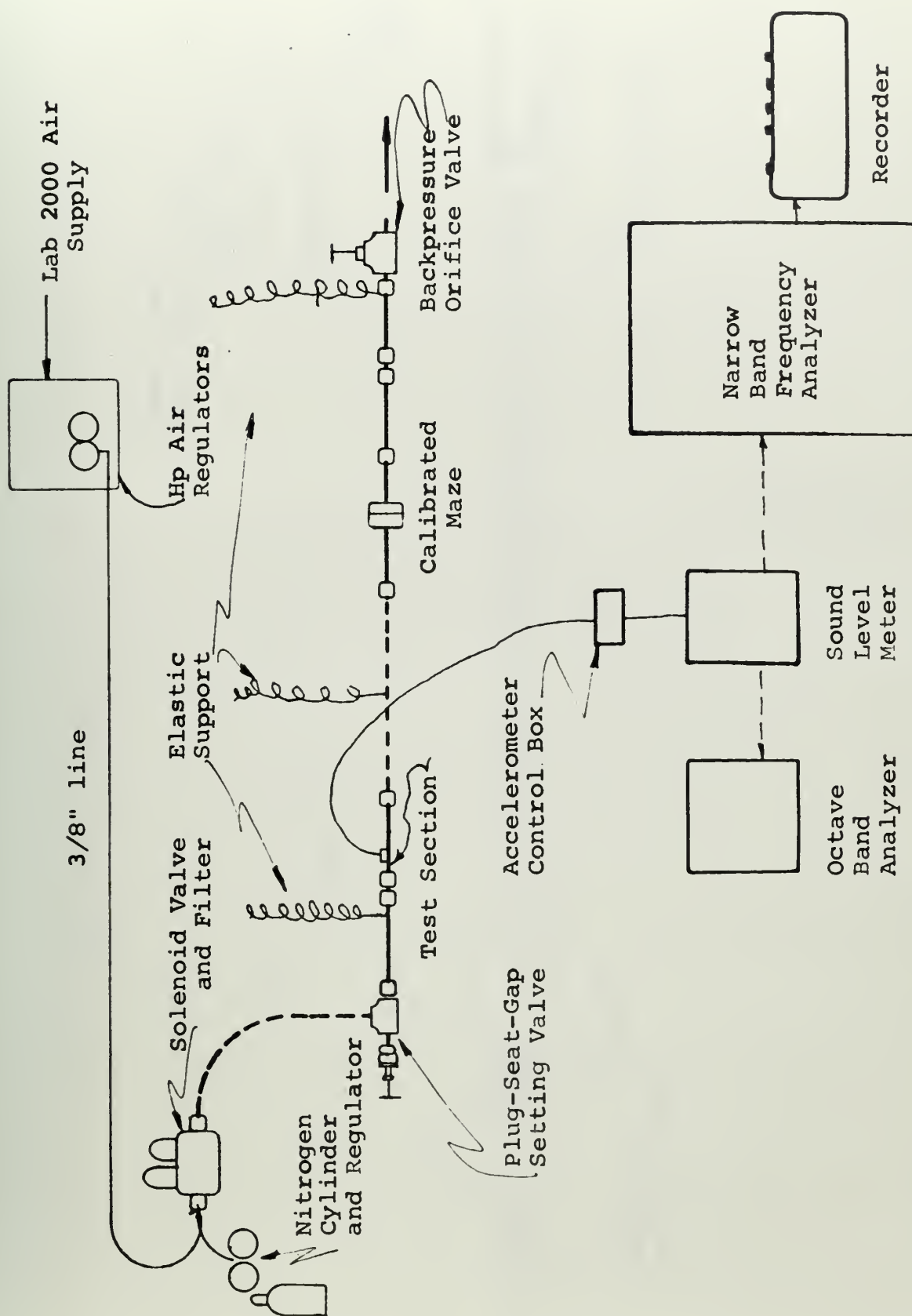


Figure 7 Sketch of Experimental Apparatus



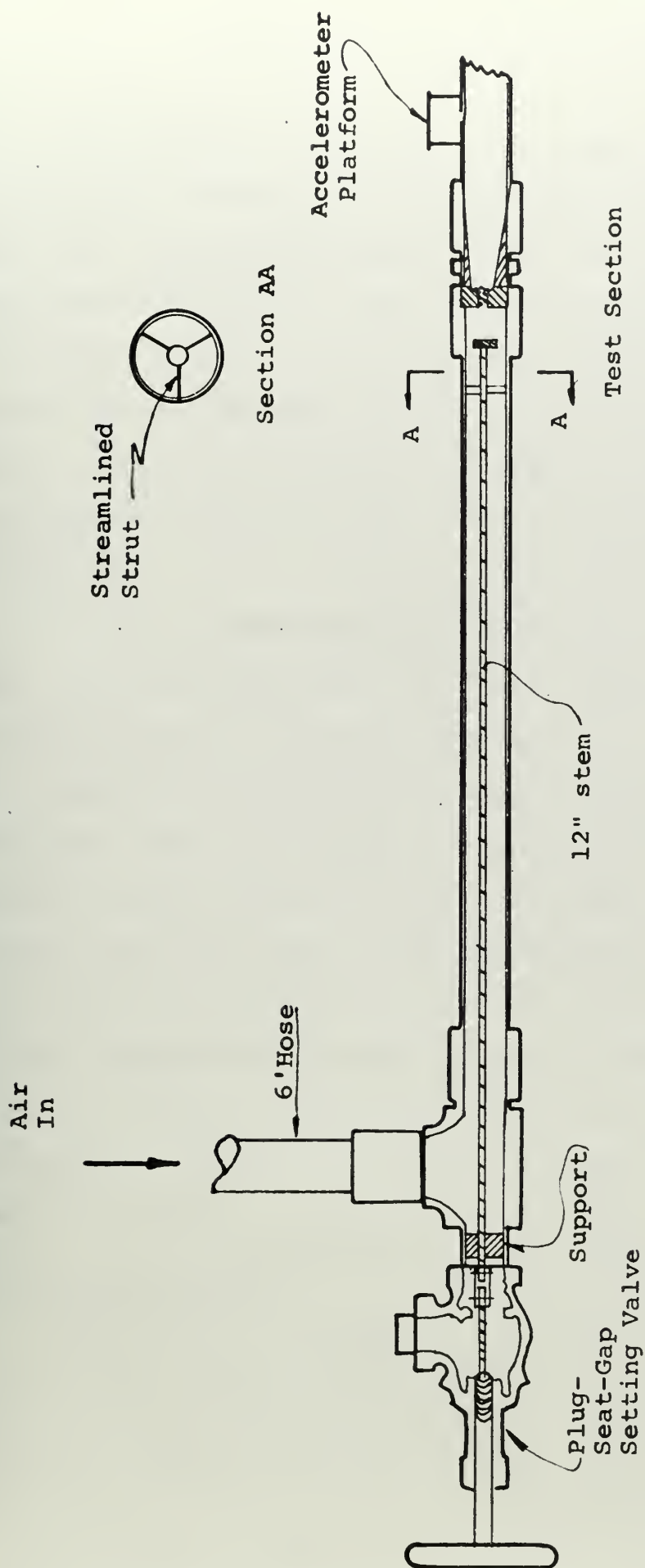


Figure 8 Sketch of Plug and Stem



Instrumentation consists of 3 static pressure gauges, initially a thermocouple for stagnation temperatures, and the sound analyzing equipment. The "inlet" pressure gauge provided the parameter used to vary the flow and therefore pressure difference across the test section. The "outlet" gauge reading was held constant at 150 psig throughout the test. Temperature readings were taken by means of a copper-constantan thermocouple probe in the flow stream. Initial temperatures for all pressure ranges varied no more than 1.5° F. and so subsequently only periodic checks were made. When the outlet pressure is 150 psig air flow rate through the calibrated maze is given by figure C-2.

Appendix E briefly describes the sound analysis equipment used. The signal from an Endevco accelerometer pickup was fed through a control box into the GR 1551-C Sound Level Meter (SLM). The broadband level of this signal was read on the SLM meter. From the output of the SLM either octave or narrow band frequency analysis was performed. Data for each run consisted of the 3 pressures, flow rate, broadband noise level, and either octave or narrow band analysis levels.

B. Background Noise:

Ideally the only source of flow noise would be from the plug-seat-maze combination under evaluation in the test section. However to obtain the desired inlet and outlet



pressures at the test section, some type of regulation is necessary in both the upstream and downstream air line. Conventional orifice or globe valves are known to be noisy when regulating flow. No little effort was expended in reducing the component of these "regulation" generated sounds that reached the test section.

To this end various arrangements were assembled and accelerometer readings taken along the pipe length. These readings were taken on the same structural point whenever possible. The important pipe arrangements considered are shown in Figure C-1. The first (PI) is basically the set-up received from Sanders Associates. This was selected as the starting point: a) since it had been proven workable, b) so that the results here could be correlated with Sanders development work, c) and because no simpler flow arrangement could be found. This arrangement scheme also gives straight-axisymmetric flow and thus offers the possibility of analytical expression as discussed in ~~III~~^V-A.

The Octave band levels for inlet pressures of 300 and 550 psig are plotted in figures D-6, 7 and 8 for each station along arrangements PI, PIII, and PV (Nomenclature code in Appendix D). Figure D-13 is a similar plot for arrangement PVI using narrow band analysis. The effect of discharging under water, arrangement PII, was very apparent in the low frequency bands as seen in Figure 2, runs 11 and 12.



The octave band results from arrangements PII, PIV, and PVI were very similar to PI, PV, and PV, respectively and have not been included.

In addition to these comparison checks made by traversing each arrangement axially, comparison checks were also made at the test section (station 4). Figure D-5 is a typical result. As is evident in figure D-5, these checks do not show a significant effect caused by varying the piping arrangements. Apparently the strong noise from the maze itself completely dominates all sound components produced outside the test section. However, prudent reasoning does justify keeping the "regulation noise" reaching the test section to a minimum. This occurs for the arrangement which has a plot with the highest noise peak at the test section. Figure D-13 shows the final arrangement, PVI, to have this desirable peak at station 4 for almost all frequencies. Since the accelerometer rested on different structures at each station these results are only relative and should be interpreted with care.

Laboratory ambient noise (for no air flow), both airborne and structureborne, is shown in the upper half of figure D-10 for a typical test period. Conversely, an extremely noisy background is shown in figure D-11 (lower) which was recorded while an adjacent (30 feet away) experiment using a large electric water pump was operating. Of course test runs were not made when this condition prevailed. Also shown in these



two figures (D-10 and 11) are levels recorded with a microphone 3 inches away from the test section when it was reducing air flow pressure. Note that these airborne recordings are referenced to sound pressure vice acceleration as for the structural borne noise.

For the plug-seat combination on the outlet side of the maze, arrangement PVII had to be used. Accelerometer checks of this arrangement did not show significant variance from arrangements PV or PVI.

To minimize the possibility of ambient structure borne noise influencing the test data, each piping arrangement was hung with elastic shock cord from a steel frame resting on a wooden bench top. The 6 foot inlet rubber hose isolated the 2000 psig lab air from the test section. The 6 foot outlet hose seemed to help isolate the test section from the downstream back pressure regulation valves.

C. Instrumentation Technique:

The nature of the objective motivating this thesis (Chapter III) indicates the need for a comparative parameter. To evaluate each plug-seat combination for its noise generating or suppressing characteristics, such a parameter must be related to this noise and should be quantifiable. For this pipe flow process four such parameters are available. Their characteristics follow:

1. Externally radiated acoustic pressure:

For airborne noise, conventional microphones



convert the acoustic pressure fluctuations into electrical signals. These signals can then be analyzed with the many techniques used in commercial acoustics. The results of this analysis then permits an evaluation of each combination. However the particular situation of this experiment introduces two significant drawbacks of this parameter:

- a. Presence of noise in the atmosphere produced other than in the pressure reducing test section. This includes not only the laboratory ambient noise but also the noise generated at the upstream and downstream flow regulating regions of the piping apparatus. Figure D-11b is a typical laboratory background airborne noise. Figure 11 c & d are recordings of the total laboratory ambient and the entire test apparatus airborne noise.
- b. Coupling effects between the sound source in the reducer to the pickup microphone outside. The wall of the pipe may attenuate certain frequencies or produce additional ones through resonate modes. These effects are especially dependent upon the apparatus used.

Other factors that must be carefully considered but are not necessarily serious limitations of



airborne measurements are: directional sensitivity, upper and lower sound pressure threshold, frequency response characteristics, and temperature variation effects of the pickup device.

2. Internal acoustic pressures:

With a suitable pressure-sensitivity pick-up device, electrical signals can be generated and analyzed as with the microphone system.

Although this technique overcomes the drawbacks of the exterior microphone it also presents noteworthy difficulties:

- a. Since the internal air is under a pressure of 150 to 600 psig, the pickup device must be capable of withstanding these static pressures while simultaneously remaining sensitive to acoustic pressures in the range of 10^{-4} to 10^{-10} psig. When the fluid is steam, the high temperature environment imposes another serious condition.
- b. Physical location with respect to the flow stream, the sensing face dimension, and the frequency response characteristic determine the amount of focusing, masking and distortion introduced into the analysis by the pickup.



Given a satisfactory pickup device, this method of obtaining a comparative parameter is obviously the ideal since the pressure fluctuations are in fact the noise of interest. Such pickups are commercially available but their special properties are reflected in their cost.

3. Internal flow velocity fluctuations:

With a velocity probe, such as the hot resistance wire, flow structure can be determined. This method is especially meaningful when correlation and spectral density analysis is used. This method usually gives the general or averaged character of the fluctuating flow, but of no less importance for comparisons. Even though theoretically promising, this technique is practically limited by the problem of manipulating a probe internally so as not to distort the true velocity field.

4. Structureborne motions:

As noted in Chapter I-B, the significant component of flow noise radiated from a ship is through the structure. Therefore pickups sensitive to either displacement, velocity, or acceleration attached to the pipe could be expected to give a representative parameter of the flow noise. These devices or accelerometers generate electric signals



amenable to analysis as in the microphone case. Since an accelerometer senses motion, which by Newtons Law, is the result of a force or equivalently a pressure acting, the accelerometer output must be related in some matter to the internal flow sound. An absolute relationship must involve the mass and shape of the body undergoing motion. However as long as the structure whose motion is being determined does not change, comparison of magnitudes should reflect only changes in the acoustic pressure forcing field. In addition to this configuration constraint, the structure may also attenuate or accentuate certain frequencies so that the measured motion amplitudes and the internal pressure fluctuations may not follow the same pattern.

Each of the above parameters was considered for use in this investigation. The desirable internal pressure parameter would have been used had suitable pick-up devices been accessible. Commercially such specialized units are produced but of course are very costly. The next best parameter was judged to be the structural motions. Special arrangements allowed the use of a General Radio Vibration pick-up system which was operated in the acceleration mode.



Other instruments used in the comparative^{ity} analysis are shown in figure 8. All instrument characteristics are given in appendix E. The accelerometer, its control box, and the Sound Level Meter (SLM) were used for all data runs. The output from the SLM was analyzed on either a GR 1550-A Octave Band Analyzer by manual manipulation or on a Bruel and Kjaer (B&K) Frequency Analyzer and with a B&K Automatic Recorder. The instrument settings held constant for all data except where noted are described in Appendix E. As suggested in the manufacturers instruction manual, the B&K analyzer and recorder were operated in a mode "equivalent to the averaging time of "FAST" on sound level meters". Attenuator settings varied but the effect has been eliminated by refering all plots to the same reference (Acceleration reference; 10^{-2} inches/sec, microphone pressure reference; .0002 ubar). The graphs from the narrow band analyzer and automatic recorder have been reduced in size for presentation whereas the Octave Band Analyzer data is plotted.



D. Variables

With the test apparatus arrangement and comparing parameter determined as discussed in V-B and C, relative noise of various plug-seat combinations at different pressures was evaluated. For any particular series of runs (indexed in Appendix D) only one variable was changed. Other than the runs to check background conditions, this variable was either: 1. Inlet pressure, 2. Plug-seat combination, 3. Plug to seat gap, or 4. Maze to plug-seat location. The range and selection of each variable is described below:

1. Inlet pressure:

Initial runs were taken at 50 or 100 psig increments from 200 to 600 psig inlet pressure. The plots of the noise at each increment were found to be almost identical except for a slight increase in magnitude for higher pressures. This increase of intensity with pressure however is not linear as figure D-5c shows. Consequently to conserve time, runs were made at 300 and 600 psig and later only at 600 psig; the noise at intermediate pressures is assumed to be some fraction of the intensity at 600 psig in these later runs. The important flow rates were determined by the differential pressure across the calibrated maze and the calibration chart of Appendix C. These pressure variations effects are recorded in figures D-1, 2, 3, 4, 5, 12, 14, 15, 16, 17, & 18.



2. Plug-seat combinations:

The shape and dimensions of each plug and seat can be found in Appendix C, Figure 9 summarizes the combinations used. Individual plug and seat dimensions were not varied. The initial choice of dimensions was based on scaling existing valves and on the empirically derived relations of Beard (33), Valstar (34), Ross (35), Sylee (36), and Blackburn (15). Particular care was used in smoothing all flow surfaces so as to minimize scaling effects from roughness. The upstream seats have a smaller diameter opening than the downstream so as to conform to the maze openings. Plug and seat combinations were selected that could be used for actual steam valves. Noise produced by the maze and seat alone are shown in figures D-2, 3, 4, 5, 11, 12, 14, 17, 18, 21, and 22. The effect of adding a plug upstream can be determined by comparing these figures with D-15, 16, 17, 18, 19, and 20 and adding one downstream with figure D-23.

3. Plug to seat gap:

One proposal for a mass control scheme, mentioned in III would use a poppet type valve. Of interest in the design of such a valve is the relationship of plug displacement or gap opening to the noise produced at that opening. Rather



Plug \ Seat	None	Disc	Stream Lines	Cone
Sharp edge	D21			
Square edge	D14	D16	D19	
Radius edge	D14	D15	D19	
Borda tube	D18	D18	D20	
Taper	D13			
Cone	D12		D20	D17

Figure 9a Plug-Seat Upstream

Plug \ Seat	None	Disc	Stream Lines
Square	D22/21	D23	
Radius	D22/21		
Taper	D10/21		
Cone	D22/21		D23

Figure 9b Plug-Seat Downstream

Figure 9 Table Plug-Seat Combinations



than complicate the tests to obtain a continuous relation two points were chosen for comparison, one corresponding to just off the seat and the other at the fully open position. In each case the close opening was determined by tightly closing the valve and then backing off the plug just sufficient to give the flow rate of the maze along. This turned out to be about $1/16$ of an inch for all tests. The recordings of figures D-15, 16, 17, 18, 19 & 20 for the plug upstream and figure D-23 for the plug downstream were made this way. Better techniques for determining gap openings less than $1/16$ " would be necessary to evaluate a plug's configuration for "close up" noise effects.

4. Maze and plug seat location:

The question of which side of the maze to locate the plug-seat combination was also considered. Intuitively one expects the downstream side where the pressure is 2 to 4 times less to be the optimum location for low noise. This seems especially true if the noise is of shock wave or turbulent origin, since the theoretical results of Lighthill and Curle show turbulent noise to have a strong dependence on flow velocities. The above referenced recordings for various plug-seat combinations can be compared for this effect

1. The first part of the document discusses the importance of maintaining accurate records of all transactions and activities. It emphasizes the need for transparency and accountability in financial reporting.

2. The second part outlines the various methods used to collect and analyze data, including surveys, interviews, and focus groups. It also discusses the challenges associated with data collection and analysis.

3. The third part presents the results of the study, showing the distribution of responses and the key findings. It includes tables and graphs to illustrate the data.

4. The fourth part discusses the implications of the findings for policy and practice. It suggests ways in which the results can be used to inform decision-making and improve outcomes.

5. The fifth part concludes the document by summarizing the main points and highlighting the limitations of the study. It also suggests areas for future research.

of inlet-outlet location. Figures D-21, 22, and 23 when compared to the remaining recordings show the effect of this variable.

E. Procedure:

The piping apparatus was developed for room temperature fluids although ultimate application of the maze will include steam. Since the MIT Projects Laboratory has a 2000 psig air supply, this media offered the most convenience at no apparent sacrifice of accuracy. This air supply was thus piped through a reducing-regulator and approximately 15 feet of 3/8 inch tubing to a solenoid valve and filter of the test apparatus. The work at Sanders has been with dry bottled nitrogen and to ensure that the fluids produced similar effects a number of comparison runs were made (Figure D-4 and 10 are typical). Figure B-1 compares the static properties of air, nitrogen, and also steam. The nitrogen gas was reduced at the cylinder by pressure regulating valves and piped directly into the solenoid valve in place of the Lab. air for the air-nitrogen comparison runs.

When preparations for a run had been made, the following sequence was followed: Air was cut in at the upstream lab-reducer-regulator and adjusted until the test section "inlet" pressure gauge read the desired amount (usually either 300 or 600 psig). The backpressure orifice valve was then adjusted to give a reading of 150 psig on the "outlet" gauge. (There was less than 1/2 psig drop from this "outlet" gauge



to the inlet of the calibrated maze so that pressure gauges P_{out} and P_i can be considered the same). Generally the two pressures across the maze could be maintained with very little attention after the initial setting.

Then the B & K recorder was switched to automatic and the output from the accelerometer was recorded by frequency and intensity at about a 6% bandwidth. During the recording, the broadband level of the SLM and the pressure differential across the calibrated maze were logged.

The SLM attenuator setting was adjusted prior to starting so as to keep the recording within the chart scale. For the majority of runs 80 db attenuation was used. When the Octave Band Analyzer was used, the air flow adjustment was as above but the various Octave bands were switched and the readings logged by hand. Using the automatic recording equipment each run required 2-3 minutes. With the manual Octave Band Analyzer each run required 7-8 minutes.



RESULTS

Chapter VI

A. Theoretical

A proposed mathematical model of the ideal flow in an axisymmetric valve has been briefly described in IV-A. Extensive literature review and study of basic potential theory indicates that this model is theoretically possible. The utility of a valve model in design work is apparent, but practicality must depend upon further development.

The manipulation of this mathematical model by hand would be extremely tedious if at all possible. When programed on a computer such a model would permit optimization of many flow parameters.

Theoretical treatment of the sound generated in an axisymmetric flow of a maze reducer has been necessarily limited to qualitative arguments of significance to the objectives established in Chapter III. Solutions for noise produced by turbulence in an infinite media show a 8th power dependence on the free stream velocity. When rigid bodies are present another noise component exists which depends on the free stream velocity to the 6th power. The complexities of modeling axisymmetric flow problems as deterministic expressions has forced investigators to find simpler models. Random process models, although still involved, do offer some hope of becoming practically useful,



even though these models require empirical data from which averages and correlation can be made.

The most significant result of the theoretical investigation has been that predictions about noise effects for any particular flow configuration in the reducer maze can not be made at this time. As in the past, these effects must be determined empirically.

B Experimental

A maze pressure reducer has been combined with various plug-seat configurations and the resulting noise analyzed. To do this a portion of the multitude of piping arrangements possible have been checked for desirable noise characteristics. All findings indicate that the test section must be separated by at least 6 feet of rubber hose and possibly more from the upstream as well as the downstream flow regulating devices. Other measures to reduce background noise included using a minimum number of elastic supports for the test section piping, adding a second maze near the flow regulators downstream, and the selection of structural motion vice airborne pressures for the comparing parameter.

Sound instrumentation initially consisted of the accelerometer, a Sound Level Meter and a Octave Band Analyzer. This allowed adequate comparisons of the piping arrangements but did prove to be a very slow method of analysis. Later the availability of an automatic analyzer and recorder greatly increased the experimental effectiveness by reducing the time per run, performing a much narrower frequency

analysis and by eliminating manual plotting.

Combinations of 6 seat and 3 plug geometries were tested at a pressure of 600 psig in all cases and at 300 psig. in a few. The readings at 600 were found to be representative of those at 300 and differed in magnitude by an order of 5 db at low frequency and 10 db at high frequency. No single combination was a standout however one did show better over all characteristics. The general tendencies noted were:

1. No plug on either side of maze

- a. The sharp edged inlet and square edged outlet seats produced the lowest noise combination.
- b. The cone and radius seats on the inlet side were slightly noisier at low frequencies than the other 4 seats.
- c. Distinctive peaks near 850, 1700, 3500, 4500, 8600, and 20,000 cps appeared with almost every combination. These apparently are characteristic of the maze.

The supposition that any turbulence upstream will be suppressed by the narrow confines of the Borda or square edge seats has not been substantiated by the recordings. Likewise the added labor of fairing the inlet side of the maze can not be justified on a noise elimination basis. In fact, not having solid boundaries leading into the maze appears desirable. The square edge seat may have given this action and thus would account for the "smoothing" off of the peaked frequency areas in figure D-21. The outlet square edged



seat also accounted for a low frequency db reduction of the order 6. Since the low frequency component has some relation to the larger turbulent eddies, suppressing the outlet flow could explain this attenuation effect. Figure 10 is a proposed configuration incorporating these features.

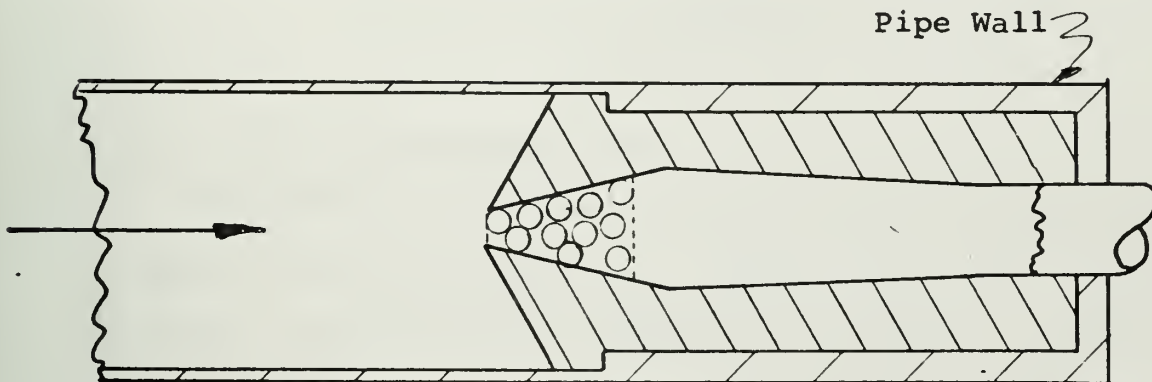
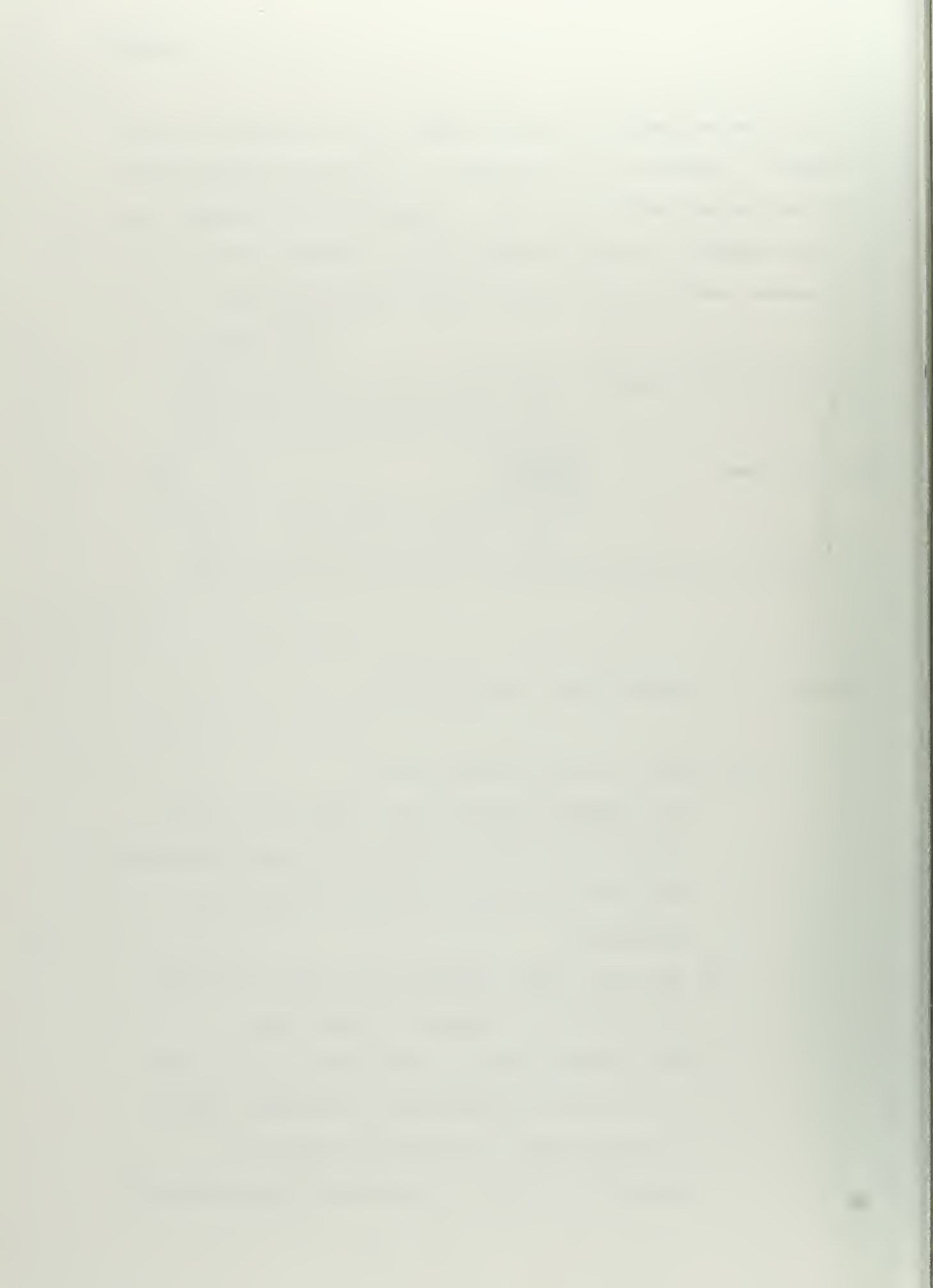


Figure 10 Proposed Seat Configuration

2. With plug on inlet side of maze

- a. The combination of a disc plug and a radius seat are by far the quietest at all frequencies. This is true at both large and small gap openings.
- b. The next best combination is the disc plug and either the square or borda seat.
- c. The streamlined and cone plugs and the cone seat in each combination had higher noise levels whereas the disc plug had the opposite effect of "flattening" especially the



peaked frequencies.

- d. With any plug at the 1/2 inch gap opening the noise recording is almost identical to the case of no plug at all. On some the plug did increase the high frequency noise. In this case the streamline and cone plugs accentuated the peaks while the disc plug attenuated them.

A somewhat unexpected conclusion then is that upstream turbulence may be beneficial. The disc as a blunt body would be well suited for creating such a flow. In addition, having solid confinement upstream, as in the no plug case, seems to increase especially the low frequency noise. The actual flow and noise mechanisms involved here are not clear but apparently incoming turbulent flow suddenly forced into a maze produces less noise than a laminar gradually converging inlet flow. The degree of upstream turbulence certainly can not be large otherwise it would be producing its own noise.

3. With plug on outlet side of maze

- a. Neither of the two combinations tested had a distinct advantage.
- b. The disc plug did seem to flatten the high frequencies while the streamline plug again accentuated them. However at low frequencies the streamline plug was 4-5 db quieter.



These results indicate that the peaked areas can be reduced by introducing turbulence but at the expense of adding 1-2 db of low frequency noise.

Considering all 3 categories, one must conclude at this stage that the disc-sharp edge inlet seat and the square edge outlet seat gives the best combination. With a disc added to figure 10 this configuration would represent the next combination to test.

The testing at Sanders has been done with bottles of dry nitrogen supplying the flow. Because of the unlimited supply of high pressure air available to the author this media was used for most of the testing done for this thesis. To allow comparisons, a number of runs were made using nitrogen. Figures D-4 and 10 are typical results. As can be seen the nitrogen media produces a significant increase in the noise, especially at low frequencies. The static properties of the fluids are very similar (figure B-1) and so should behave acoustically the same. A possible explanation of the difference is the relative location of the high pressure regulators used.

The HP regulator for the laboratory 2000 psig air was located on a gauge board about 15 feet upstream. The pipe between this regulator and the solenoid valve was 3/8"OD tubing. When nitrogen was used this 3/8 inch line was disconnected and the nitrogen bottle regulator attached directly to the solenoid valve. This nearness to the

inlet rubber hose may have allowed the nitrogen regulator noise to reach the test sections.

CONCLUSION

Chapter VII

A. Theoretical

The lack, at the present time, of a workable mathematical model of the fluid flow process in a valve, even the simplest type, precludes theoretical analysis of configuration effects. The problem of finding a valve with particular characteristics such as a pressure reducer must now be solved, as in the past, by trial and error methods.

The initial considerations for such a mathematical model have been presented. The proposed model is based on ideal, or potential flow but eventual inclusion of real fluid behavior seems possible. The use of computer programs would permit such a model to be of practical value while still retaining an accurate representation of the real process.

The formulation of a mathematical model of valve noise must consider Lighthill's form of the wave equation. The application of solutions for this equation to axisymmetric flow would be extremely complicated for the present form of these solutions. However, extrapolating the 6th and 8th power velocity effects from the solutions that have been found, indicates that the most important consideration in making valves quiet is to keep flow velocities low when turbulence is present.



The difficulties of constructing a suitable deterministic model have led to models based on probability expressions and averages. These models are dependent on empirical data from particular flows but when once obtained, the mathematical expressions are often valid for similar processes.

Thus, the general conclusion is that because present mathematical models of pressure reducing processes are inadequate, questions concerning configuration effects on noise output must be answered empirically.

B. Experimental

The objective of this thesis has been "To compare the noise produced by various plug/seal combinations in axisymmetric flow to a maze pressure reducer." Comparison by theoretical means has been limited. Published material found, generally treats aspects of fluid flow other than noise effects introduced by configuration changes. Fulfillment of the object has been possible then only by an experimental investigation.

The apparatus used and the instrumentation techniques have been described. Numerous modifications to the test apparatus, although changing the acceleration readings at points along the inlet and outlet section, had very little effect on the noise measured at the maze. This indicates the accelerations existing at station 4 over the maze are almost entirely characteristic of the maze and its immediate

structure.

The increased noise (BB 2 db and about 5 db at low freq.) when using nitrogen vice air was unexpected since the static properties of the two gases are almost identical. The explanation may lie not with the gas composition but rather with the physical location of the high pressure regulators used in each case.

Flow rates throughout the tests were measured, however these rates were permitted to vary for each series of runs in preference for maintaining the desired inlet and outlet pressures. The mass flow characteristic of the maze was thus not considered as stated in Chapter II-B. Future work must consider the sizing or number of modules necessary to satisfy system mass flow. Even though the objective concerns noise, the effect on mass flow rate for various gap openings was noted. As compared to the case of no plug, flow rates were reduced with the plug present only when the plug was within $\frac{1}{2}$ diameter (here .137") travel of fully shut. Noise effects were detected at all gap openings (max. variance of about 5 db) and in some cases acted to reduce the noise from the case of no plug at all present.

The physical parameter chosen for comparisons (structural acceleration) was dictated by background levels and economic considerations. Without contrary evidence, the assumption has been implied that the data results for this parameter are representative of the actual sound pressures existing in the internal flow. Regardless of the validity of this

assumption by the use of axisymmetric flow and by changing only one variable at a time relative evaluation of different configurations could be made. From approximately 200 test runs, the combination of a disc plug and sharp edged seat on the inlet side of the maze reducer was found to produce less noise relative to the other configurations. The noise difference was seldom more than 4-6 db for any frequency.

This indicates an even more important conclusion in that apparently the configurations required to control the flow do not significantly increase and on occasion even decrease the noise of the maze reducer. It must be emphasized that this applies when the plug does not significantly restrict the flow(i.e. for open and shut action vice regulating action, which is unsteady).

This work has established that the order of magnitude of noise introduced by plug/seat combinations in axisymmetric flow to pressure reducer mazes is 6db(re 10^{-2} inches/sec²). The tests have also substantiated the low noise attributes of the packed ball maze as a pressure reducer.

RECOMMENDATIONS

Chapter VIII

As pointed out in Chapter IV analytic models are needed for both the fluid flow and the noise behavior in valves. The axisymmetric valve is particularly promising for mathematical modeling. Further research and development work is needed in these areas.

The accelerometer provides an adequate technique for comparison, but for analytic expression, the true sound field existing in the fluid flow must be determined. With a well constructed test apparatus and sensitive transducers, both of which are attainable, pressure fluctuations in the stream itself could be evaluated. In the author's opinion this type of information, presented in a meaningful form, will help tremendously in understanding pipe or valve flow noise.

Since the ball maze contributes the major noise component, improvement in its configuration would offer the greatest return. The data runs at 100 psig increments (Figure D-5) show the strongest noise to be associated with the greater pressure reduction (i.e. 600 & 150). In the lower reducing realm (300 & 150) the noise has decreased at a rate faster than $\frac{1}{2}$ as is established by interpreting D-5. All evidence points to the velocity as being the prime mechanism of noise. To capitalize on this behavior, other than axisymmetric flow devices should be designed and tested with particular regard to the velocities occurring. The effect of swirl or

rotational motion has not been treated at all.

The phenomenon of turbulence suppression needs further investigation. The question of whether it is better to dissipate turbulence in the fluid only or do it by imposing solid boundaries has not been answered. Imposing the boundary may suppress the eddies but results from these tests indicate this may introduce more noise into the wall structure.

Finally, the obvious should be mentioned. Either repeating or conducting similar tests with pressure reducing mazes using steam as the media must be accomplished to ascertain the effects of 2 phase flow.

APPENDIX A

STEAM CALCULATIONS

1. THERMODYNAMIC ANALYSIS:

The steady flow energy equation for the control volume (Figure A-1) about a steam pressure reducing valve is:

$$A-1 \quad Q = W + w(h_{out} - h_{in}) + \frac{w(v_{out}^2 - v_{in}^2)}{2g_o J} + \frac{wg(z_{out} - z_{in})}{Jg_o}$$

where

Q = net heat added to control volume (BTU)

W = net work done by control volume (BTU)

h = enthalpy (BTU/lb_m)

w = mass flow rate (lb_m/sec)

g = acceleration of gravity (ft/sec²)

v = fluid velocity (ft/sec)

z = elevation (ft)

g_o = gravitational constant (lb_m·ft/lb_f·sec²)

J = Joules constant (778.16 ft·lb_m/BTU)

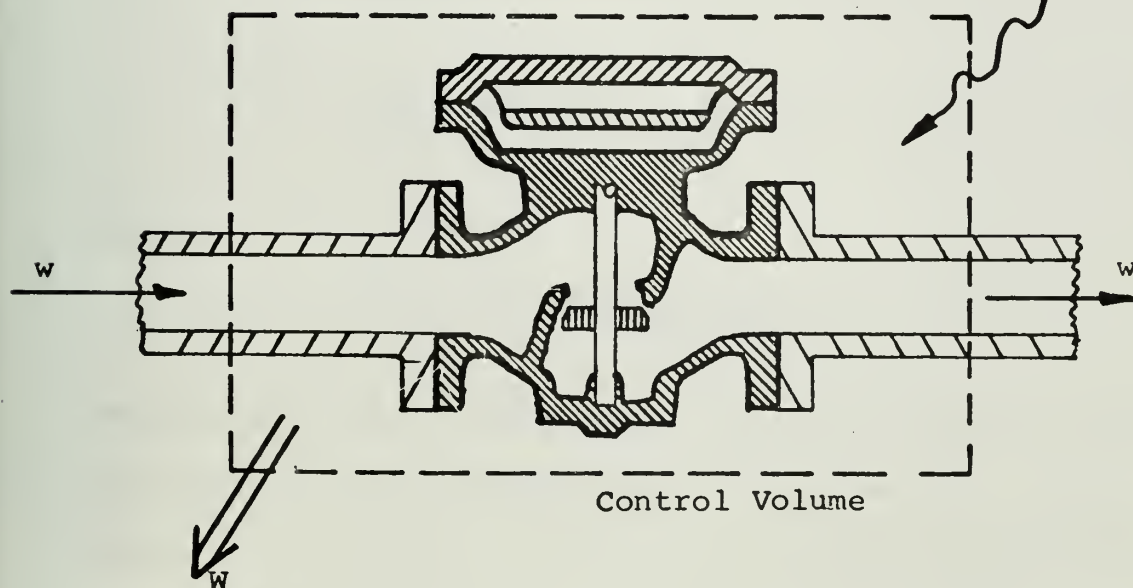


Figure A-1 : Steam Reducing Valve Control Volume

Consider a typical installation:

Inlet conditions:

$$\begin{aligned} \text{Pipe diameter} &= 1.25'' = .104 \text{ feet} \\ w &= 7000 \text{ lb}_m/\text{hr} \\ P &= 600 \text{ psig} \\ T &= 490^\circ\text{F} \end{aligned}$$

Outlet conditions:

$$\begin{aligned} \text{Pipe diameter} &= 1.500'' = .125 \text{ feet} \\ w &= 7000 \text{ lb}_m/\text{hr} \\ P &= 150 \text{ psig} \\ T &= \text{to be determined} \end{aligned}$$

From section A-2:

$$\begin{aligned} v_{in}^2 &= 3.2 \times 10^4 (\text{ft/sec})^2 \\ v_{out}^2 &= 17.4 \times 10^4 (\text{ft/sec})^2 \end{aligned}$$

From the steam tables:

$$\begin{aligned} h_{in} &= 1206.7 \text{ BTU/lb}_m \\ s_{in} &= \text{entropy} = 1.4492 \text{ BTU/}^\circ\text{R} \cdot \text{lb}_m \end{aligned}$$

Following assumptions are made:

$$W = 0$$

$$\begin{aligned} z_{in} &= z_{out} \\ Q &= 0 \end{aligned}$$

Steam systems are generally heavily insulated.
Experience has shown this to be a valid assumption.

Equation A-1 now becomes:

$$h_{in} - h_{out} = \frac{v_{out}^2 - v_{in}^2}{2g_o J} = \frac{(17.4 - 3.2) 10^4}{2 \times 32.2 \times 778.16} = 3.02 \approx 0$$

Compared with the enthalpy term, the kinetic energy term is negligible and when disregarded, the steady flow energy equation reduces to:

A-2

$$h_{in} = h_{out}$$



The outlet state can now be determined from the Steam Tables with $P_{out} = 150\text{psig}$ and $h_{out} = 1206.7 \text{ btu/lbm}$:

	370°F	T_{out}	380°F
h_{out}	1201.4	1206.7	1207.5
s_{out}	1.5782	<u>1.5845</u>	1.5856

By interpolation: $T_{out} = 386.6^\circ\text{F}$

The valve inlet and outlet states are now completely known and can be sketched on the Temperature-Entropy coordinates of figure A-2. The actual path between these two states is complex and not readily determined. This has been signified by the dashed, wavy line.

The severity of the degradation of energy by the pressure reducing process can be found by determining the increase in unavailable energy, E_u (22).

$$\text{A-3} \quad E_u = T_o(s_b - s_a)$$

where states a and b are the "dead" states at the reservoir sink temperature T_o .

From figure A-2 and the definition of E_u :

$$E_u = T_o(s_{out} - s_{in})$$

$$E_u = 530(1.5845 - 1.4492)$$

A-4

$$E_u = 72 \text{ BTU/lbm}$$

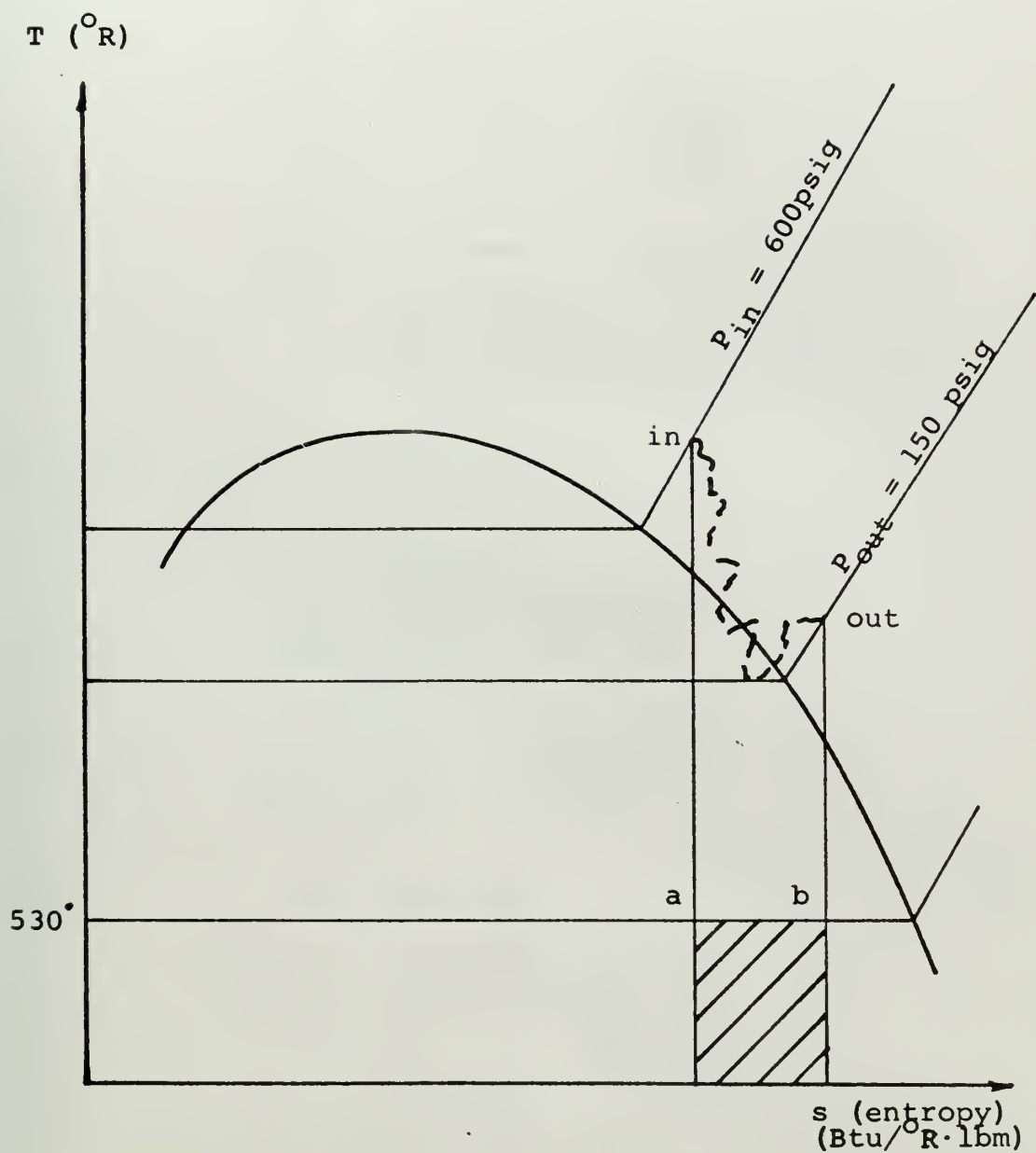


Figure A-2 Temperature-Entropy Diagram



2. Pipe Flow Velocities

The average velocities in the inlet and outlet pipes of a typical steam reducing valve can be determined from the continuity equation:

$$V = \frac{w}{\rho A} = \frac{wq}{A} = \frac{w \cdot q \cdot 4}{\pi D^2}$$

where: V = average velocity (ft/sec)
 w = mass flow rate (lbm/sec)
 ρ = density (lbm/t³)
 A = cross sectional area (ft²)
 q = specific volume (ft³/lbm)

Representative conditions are:

i) Inlet:

$P_{in} = 600$ psig
 $T_{in} = 490^{\circ}\text{F}$ (4° superheat)
 $q_{in} = 0.7768$ ft³/lbm
 $\text{Dia}_{in} = 1\frac{1}{4}" = .104$ feet
 $w = 7000$ lbm/hr

$$V_{in} = \frac{7000}{3600} \frac{.7768 \times 4}{\pi (.104)^2}$$

A-5

$$V_{in} = 178. \text{ ft/sec}$$

$$V_{in}^2 = 31,700 \text{ (ft/sec)}^2$$

$$Re \equiv \frac{\text{Dia} \cdot V_{in}}{\nu} = \frac{.104 \times 178}{9.7 \times 10^{-6}}$$

$$Re = 1.2 \times 10^6$$

ii) Outlet:

$$P = 150 \text{ psig}$$

$$T_{\text{out}} = 358^{\circ}\text{F (sat)}$$

$$q_{\text{out}} = 2.638 \text{ (ft}^3/\text{lbm)} \text{ for } .877 \text{ quality}$$

$$\text{Dia} = 1\frac{1}{2} = .125 \text{ feet}$$

$$w_{\text{out}} = w_{\text{in}} = 7000 \text{ lbm/hr}$$

$$v_{\text{out}} = \frac{7000}{3600} \cdot \frac{2.638 \cdot 4}{\pi (.125)^2}$$

A-6

$$v_{\text{out}} = 418, \text{ ft/sec}$$

$$v_{\text{out}}^2 = 174,000 \text{ (ft/sec)}^2$$

$$\text{Re} = \frac{D_{\text{out}} \cdot v_{\text{out}}}{\nu} = \frac{.125 \times 418}{2.43 \times 10^{-5}}$$

$$\text{Re} = 2.15 \times 10^4$$

3. Isentropic Throat Velocities:

An interior control volume is imagined as shown by the dashed lines in figure A-3 and the steady flow energy equation applied. Here the inlet condition is an arbitrary plane upstream of the valve and the outlet condition corresponds to the throat section. Q is again assumed to be negligible by considering a typical, well insulated system. By inspection $W=0$ and elevations, z , are assumed equal. The energy equation, A-1, then becomes:

$$\frac{v_{\text{in}}^2 - v_{\text{out}}^2}{2q_{\text{OJ}}} = h_{\text{out}} - h_{\text{in}}$$

A-7

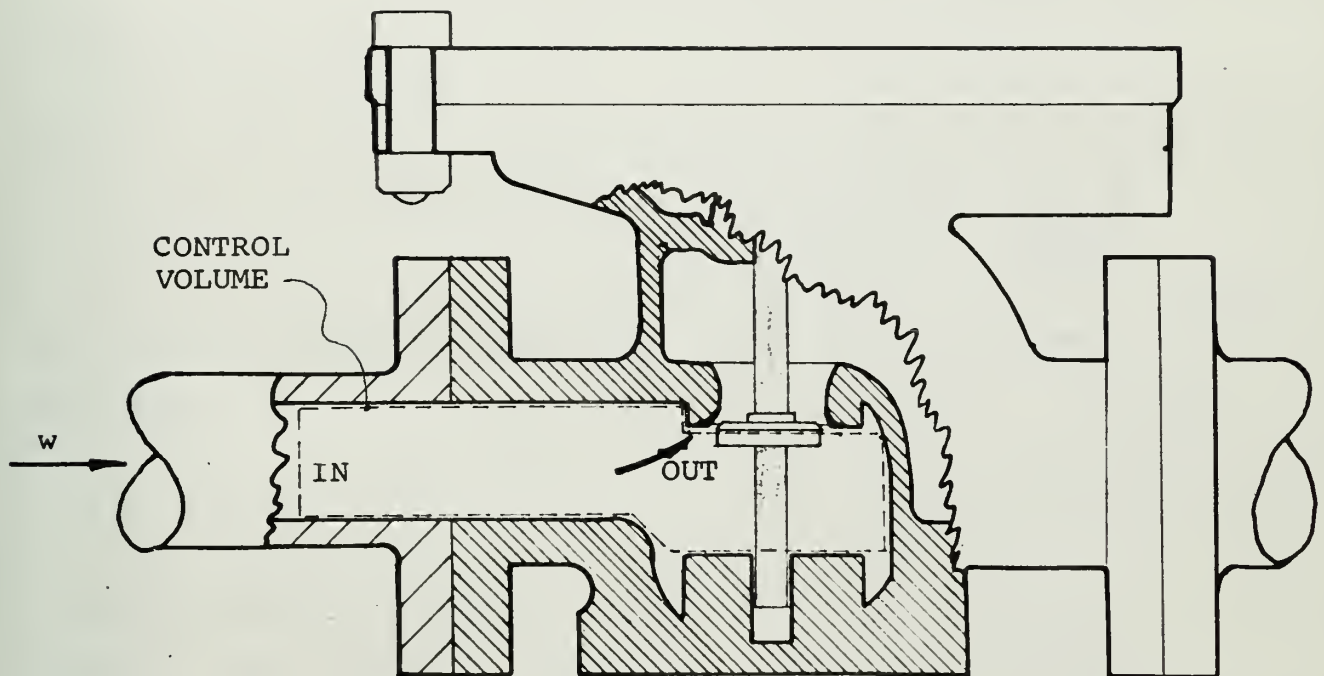


Figure A-3 Steam Valve Interior Control Volume

Conservation of mass is expressed by

$$A-8 \quad W = \frac{V_{in} A_{in}}{q_{in}} = \frac{V_{out} A_{out}}{q_{out}}$$

where q = specific volume (ft^3/lbm)

A = cross sectional area (ft^2)

Eliminating V_{in} from A-7 with the aid of A-8:

$$A-9 \quad V_{out} = 233.7 \sqrt{\frac{h_{in} - h_{out}}{1 - \left(\frac{A_{out}}{A_{in}}\right)^2 \cdot \left(\frac{q_{in}}{q_{out}}\right)^2}}$$

To determine orders of magnitude, ideal flow is assumed.

Therefore:

$$A-9a \quad s_{in} = s_{out}$$

The solution for a typical set of conditions is given below. Other conditions have been computed in a similar fashion and are tabulated in figure A-4.

Assume:

$$\begin{aligned} P_{in} &= 600 \text{ psig} \\ T_{in} &= 490^\circ\text{F} \text{ (4}^\circ \text{ superheat)} \\ w &= 7000 \text{ lbm/hr} \\ A_{in} &= .00849 \text{ ft}^2 \end{aligned}$$

$$P_{out} = 150 \text{ psig}$$

From the steam tables:

$$\begin{aligned} h_{in} &= 1206.7 \text{ BTU/lbm} \\ q_{in} &= 0.7768 \text{ ft}^3/\text{lbm} \\ s_{in} &= 1.4492 \text{ BTU/}^\circ\text{F lbm} \end{aligned}$$



By equation A-9a:

$$S_{out} = S_{in} = 1.4492$$

For a mixture of saturated vapor and saturated liquid basic thermodynamics provides the relation:

$$S_{out} = S_f + XS_{fg}$$

A-10

where:

S_f = entropy of sat. liquid

S_{fg} = entropy change

X = quality of steam = $\frac{\text{mass vapor}}{\text{mass mixture}}$

Solving this expression for X and using S_f and S_{fg} from the steam tables for $P_{out} = 150$ psig:

$$\begin{aligned} X &= \frac{S_{out} - S_f}{S_{fg}} \\ &= \frac{1.4492 - .5138}{1.0556} \\ X &= .877 \end{aligned}$$

With this quality relation and the f and fg properties from the steam tables for $P_{out} = 150$ psig :

$$\begin{aligned} h_{out} &= h_f + Xh_{fg} \\ h_{out} &= 330.51 + .877(863.6) \\ h_{out} &= 1086 \\ q_{out} &= .01809 + .877(2.997) \\ q_{out} &= 2.638 \end{aligned}$$

Noting that $\left(\frac{q_{in}}{q_{out}}\right)^2 = \left(\frac{.7768}{2.638}\right)^2 = (.295)^2 = .087$

the denominator of A-9 is therefore essentially one and:

$$V_{out} = 223.7 \sqrt{h_{in} - h_{out}}$$

$$V_{out} = 223.7 \sqrt{1206.7 - 1086.0}$$

A-11

$$V_{out} = 2550 \text{ ft/sec}$$

The throat area is obtained from continuity, A-8:

$$A_{out} = \frac{wq_{out}}{V_{out}}$$

$$= \frac{7000}{3600} \cdot \frac{2.638}{2550}$$

A-12

$$A_{out} = 2.01 \times 10^{-3} \text{ ft}^2$$

From Appendix B, the average speed of sound in steam C_o is:

$$C_o = 1800 \text{ ft/sec}$$

Therefore this throat Mach number is:

$$M_{out} = \frac{V_{out}}{C_o} = \frac{2550}{1800}$$

A-13

$$M_{out} = 1.42$$

These relations give only order of magnitude values.

The assumption of ideal flow (A-9a) and approximating the

denominator of equation A-9, as one, certainly influenced the resultant velocity even though these assumptions have been conservative. Also no consideration is given in equation A-9 to the phenomenon of a critical state, characteristic of nozzle flow which is known empirically to exist when the outlet pressure is below a certain fraction of the stagnation pressure. The complications of condensation and thus two phase flow prevent using perfect gas relations. However empirical expressions do permit approximations: (37)

$$A-14 \quad P_c \text{ (Initially wet steam)} = 0.58P_{in}$$

$$P_c \text{ (superheated)} = 0.545P_{in}$$

The minimum throat area required at the critical point can also be estimated from empirical relations: (38)

$$A-15 \quad w = \frac{A \cdot P_o}{70} \quad (\text{Napier's equation})$$

$$w(\text{Moist}) = \frac{60 A \cdot p_o^{0.97}}{\sqrt{X}}$$

$$W(\text{superheated}) = \frac{60 A \cdot P_o^{0.97}}{1 + 0.0065t_o}$$

Values from equations A-14a and A-15c are tabulated in figure A-4.

P _{in}	P _c	U _{out}	M	A*	A _{out}
Inlet Pressure	Critical Pressure	Throat Velocity	Mach Number	Minimum Throat Area	Throat Pipe Area
psig	psig	ft/sec		inch ²	inch ²
600	340	2550	1.42	.234	.282
500	290	2300	1.28	.266	.248
400	232	2120	1.17	.314	.366
300	174	1650	.95	.457	.487
200	116	1380	.77	.684	.593

Figure A-4 Approximate Throat Velocities

APPENDIX B

FLUID CHARACTERISTICS

1. Static properties:

Fluid properties in the domain of interest here are tabulated in figure B-1.

2. Pipe velocities for air:

The air flow, Q , in SCFM (cubic feet per minute at standard conditions of 14.7 psig and 70°F) is obtained from the calibration chart, figure C-2 for a given P_2 . This flow can then be used to determine the pipe velocities as shown below:

The equation of state for air (and for nitrogen) for practical applications is (25):

$$B-1 \quad \frac{P}{\rho} = RT$$

where:

$$\begin{aligned} p &= \text{pressure (psia)} \\ \rho &= \text{density (lbm/ft}^3\text{)} \\ R &= \text{Gas constant} \left(\frac{\text{ft} \cdot \text{lb}_f}{\text{lb}_m \cdot ^\circ\text{R}} \right) \\ T &= \text{Temperature (}^\circ\text{Rankine)} \end{aligned}$$

Isothermal flow is assumed from V-A which reduces B-1 to:

$$\begin{aligned} \frac{P}{\rho} &= \text{constant} \\ B-1a \quad \frac{\rho_{atm}}{\rho} &= \frac{P_{atm}}{P} \end{aligned}$$



		Steam		Air		N ₂	
		600 490°	150 358°	600 80°	150 80°	600 80°	150 80°
P	psig						
T	°F						
ρ	(lbm/ft ³)	1.29	.33	3.17	.797	3.9	.742
μ	(lbf sec/ft ²)	3.89×10^{-7}	2.49×10^{-7}	3.9×10^{-7}	3.9×10^{-7}	3.7×10^{-7}	3.7×10^{-7}
R	$\frac{\text{ft}^2 \text{f-lbm}}{\text{lb}^{\circ} \text{R}}$	70.9	107.0	53.3	53.3	55.2	55.2
k	Specific Heat Ratio	1.29	1.3	1.4	1.4	1.40	1.4
C _O	(ft/sec)	1850	1740	1150	1150	1168	1168

Figure B-1 Static Properties



Mass continuity of the flow gives:

$$w_{\text{pipe}} = w_{\text{atm}}$$

$$(v \cdot A \cdot \rho)_{\text{pipe}} = (Q \cdot \rho)_{\text{atm}}$$

B-2

$$v_{\text{pipe}} = \frac{Q_{\text{atm}} \cdot \rho_{\text{atm}}}{A_{\text{pipe}} \cdot \rho_{\text{pipe}}}$$

WHERE:

w = mass flow rate (lbm/sec)

v_{pipe} = average pipe velocity (ft/sec)

A_{pipe} = cross section area of pipe (ft²)

Q_{atm} = SCFM from figure C-2 (ft³/min)

ρ_{atm} = air density at 14.7psig (lb_m/ft³)

Substituting B-1a this becomes:

B-2a

$$v_{\text{pipe}} = \frac{Q_{\text{atm}}}{A_{\text{pipe}}} \frac{P_{\text{atm}}}{P_{\text{pipe}}}$$

Applying equation B-2a to an inlet pipe of diameter 13/16 inches with $P_{\text{pipe}} = p_{\text{in}} = 600$ psig and a representative Q_{atm} of 27 scfm gives:

$$v_{\text{in}} = v_{\text{pipe}} = \frac{27}{3.56 \times 10^{-3} \left(\frac{60}{60} \right) \left(\frac{14.7}{600} \right)}$$

$$v_{\text{in}} = 3.15 \text{ feet/sec.}$$



Reynolds number for pipe flow is

$$B-3 \quad Re = \frac{D \cdot v}{\nu}$$

where:

D = pipe diameter (ft)

ν = kinematic viscosity (ft²/sec)

Therefore for the inlet pipe:

$$Re_{in} = \frac{.0677 \times 3.15}{3.96 \times 10^6}$$

$$Re_{in} = 5.39 \times 10^4$$

Similarly for the outlet conditions : ($P_{pipe} = P_{out} = 150$ psig,
D = 13/16 inches and Q = 27 scfm) equation B-2a becomes:

$$v_{out} = v_{pipe} = \frac{1}{3.56 \times 10^{-3}} \times \frac{27}{60} \times \frac{14.7}{150}$$

$$v_{out} = 12.0 \text{ ft/sec}$$

$$Re_{out} = \frac{.0677 \times 12.0}{16 \times 10^{-6}}$$

$$Re_{out} = 5.09 \times 10^4$$



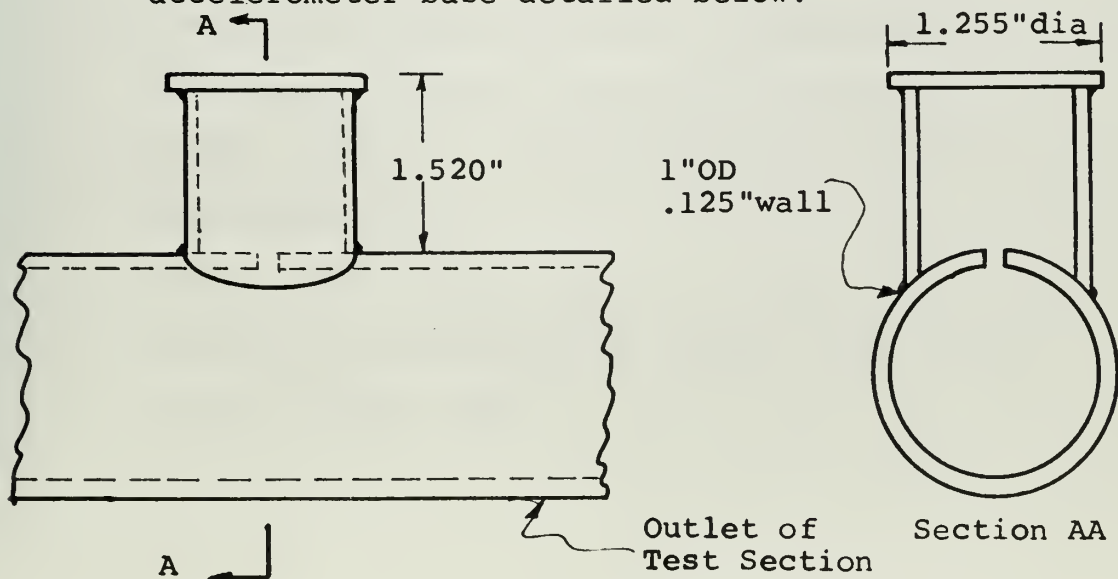
APPENDIX C
TEST APPARATUS

1. Piping arrangement:

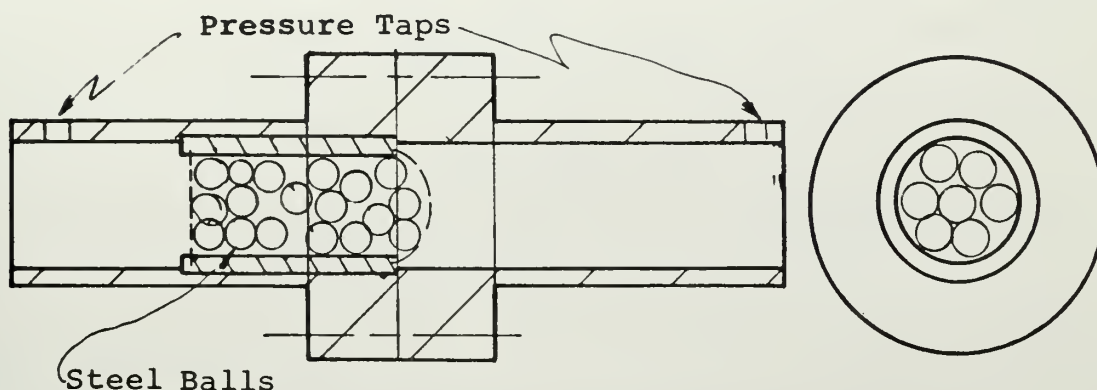
The various schemes considered are sketched in figure C-1.
Nomenclature definitions are in appendix D.

2. Description of piping components:

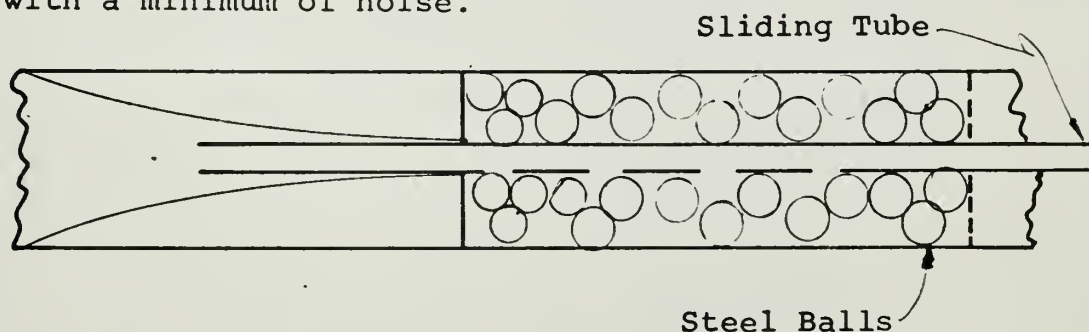
- a. Solenoid valve and filter: A battery powered orifice type valve primarily for quick start and stop of air flow from a Nitrogen bottle. The filter is fiber composition.
- b. Inlet and outlet hoses: Rubber, composition 3/4 inch ID, designed for high pressure use.
- c. Inlet test section: Steel tubing, 1 inch OD, 1/8 inch wall, 5000 psig designed working pressure, 10½ inches long. End connectors: 37° flare nuts.
- d. Outlet test section: Same as inlet plus an accelerometer base detailed below.



- e. Calibrated maze: Designed by Sanders using small spheres. Calibration curve-figure C-2.



- f. Backpressure nozzle: A special design utilizing small sphere maze for controlling the backpressure with a minimum of noise.



- g. Backpressure control valve: A conventional orifice valve used to extend the range of the backpressure nozzle, item f. Manufactured by Greer Hydraulics (VII 62200-1-1)
- h. Outlet pipe: Steel tubing, 5/8 OD, 37° fittings. (Contain the backpressure nozzle). Two pieces-- 9 and 6 inches long.

Gauges:

Inlet: Two inch circular faced, Bourdon,
0 to 1000 psig.

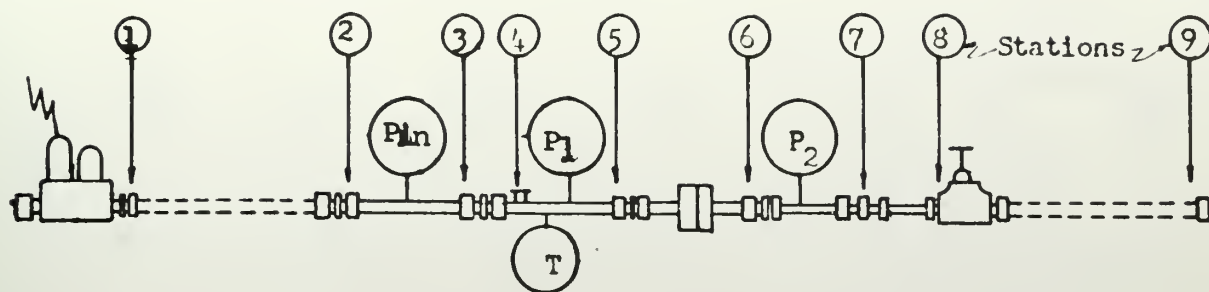
Outlet: Five inch circular faced, precision,
Bourdon, 0 to 200 psig.

P_1 and P_2 : Two inch circular faced, Bourdon,
0 to 250 psig.

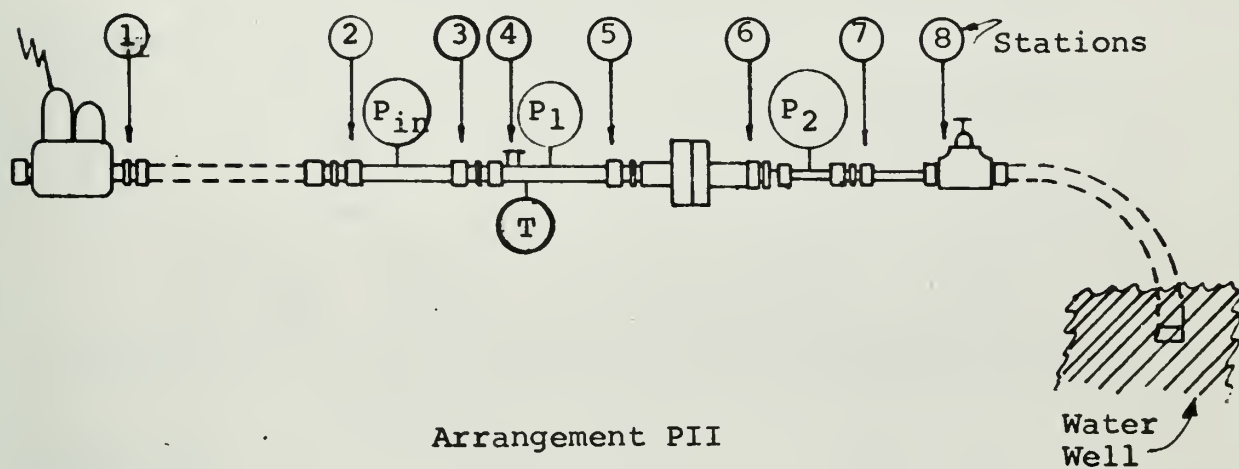
(All gauges initially calibrated on a dead-
weight tester)

3. Test plugs and seats:

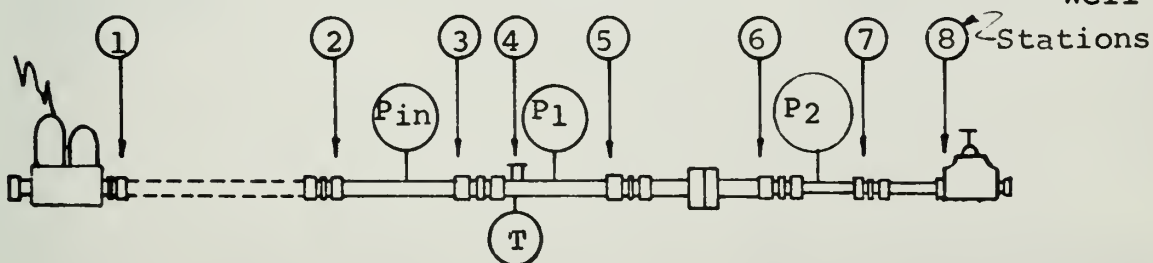
Shapes and dimensions are given in figure C-3.



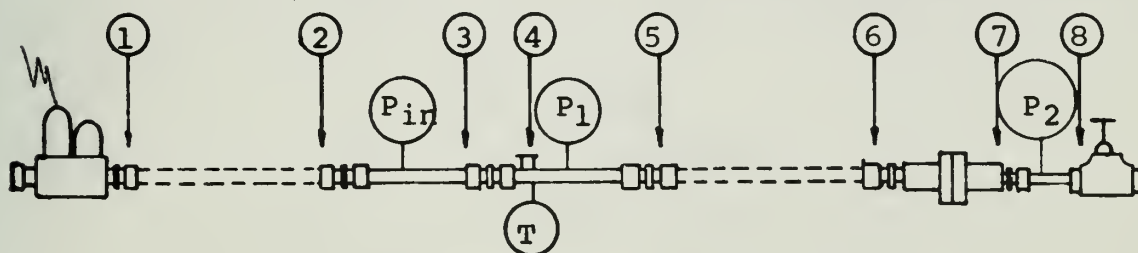
Arrangement PI



Arrangement PII

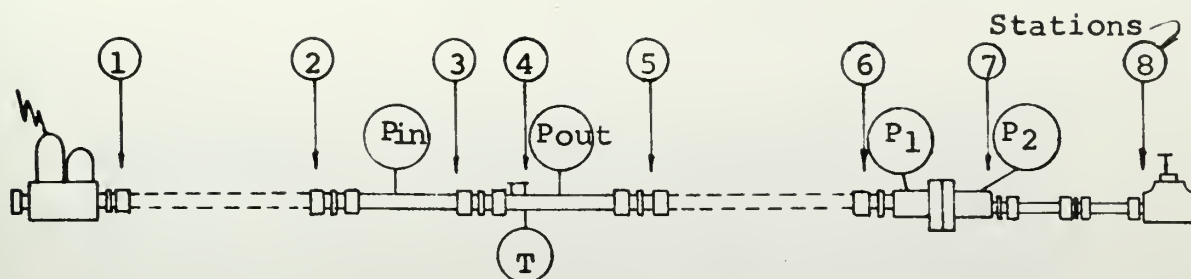


Arrangement PIII

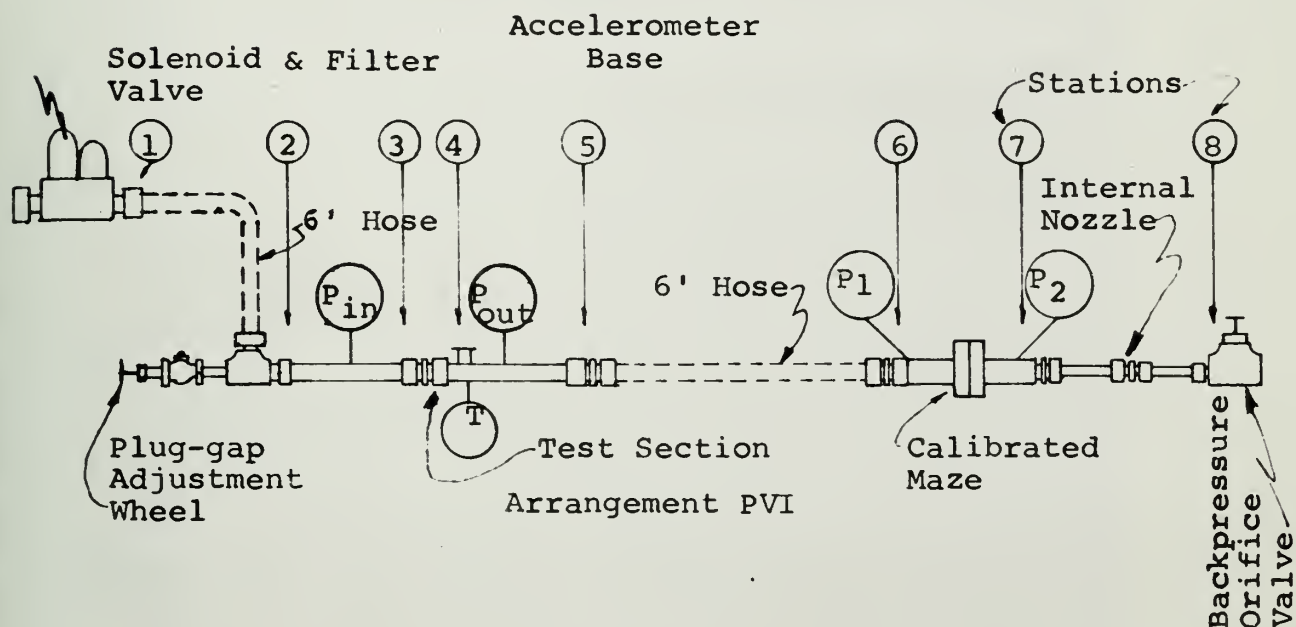


Arrangement PIV

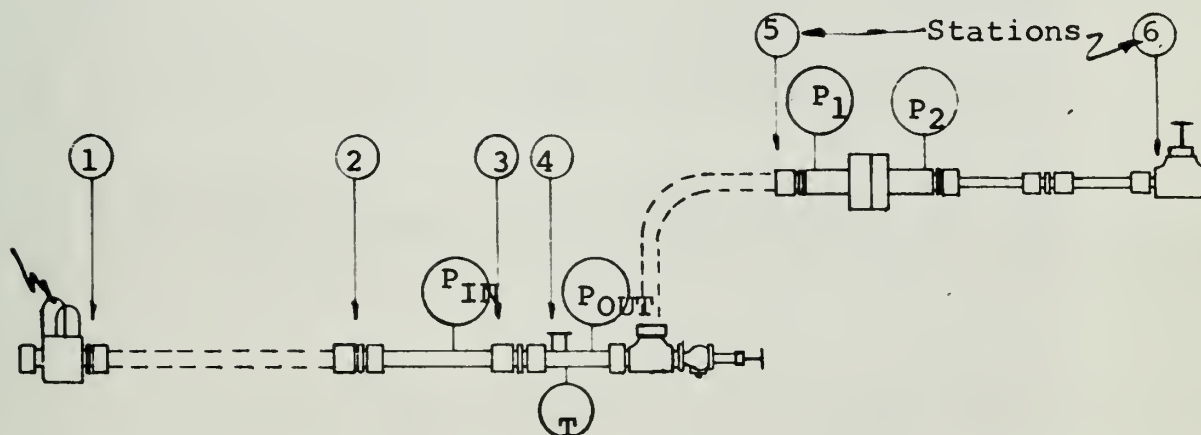
Figure C-1a Test Apparatus Arrangements



Arrangement V



Arrangement PVI



Arrangement PVII

Figure C-1b Test Apparatus Arrangements

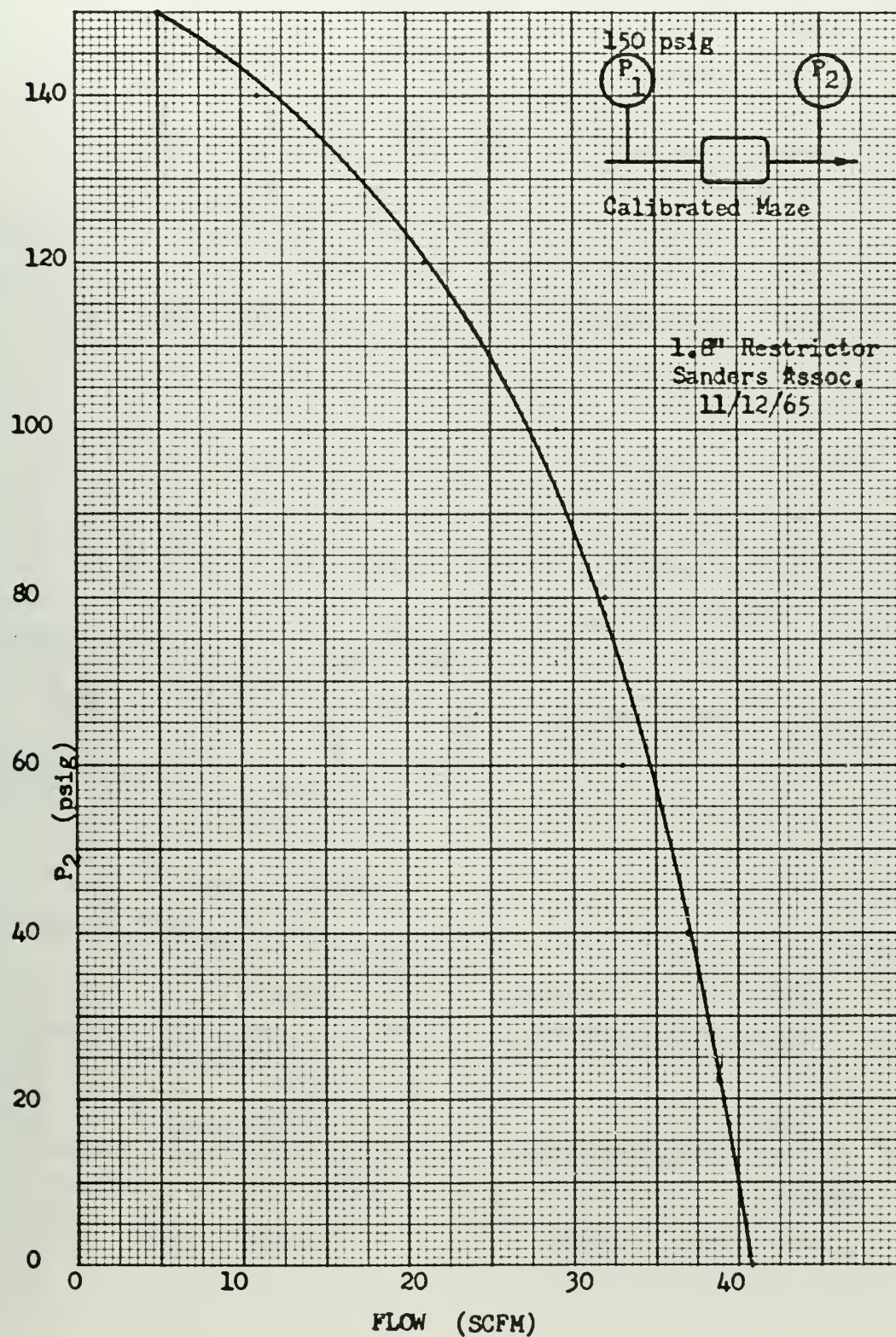
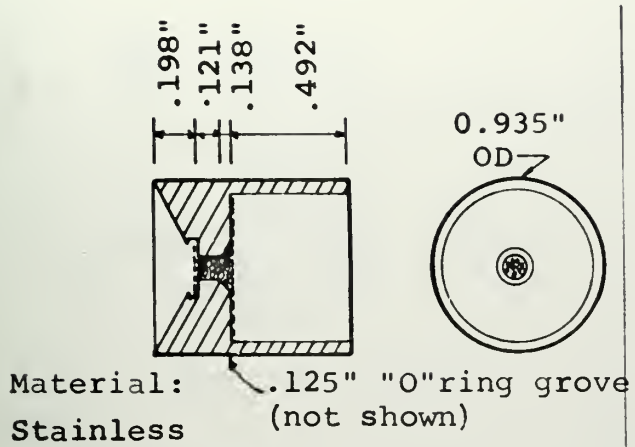
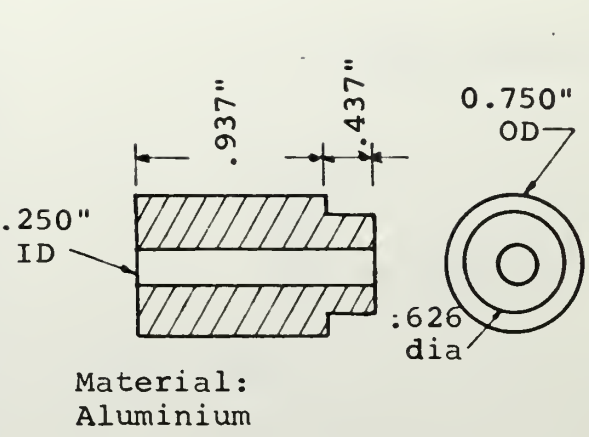


Figure C-2 Calibrated Maze Characteristic

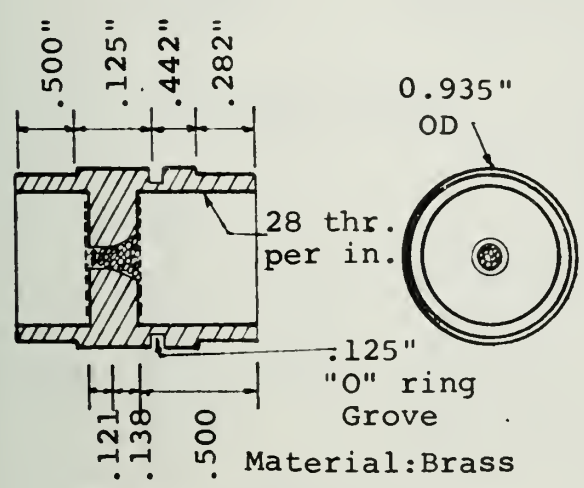




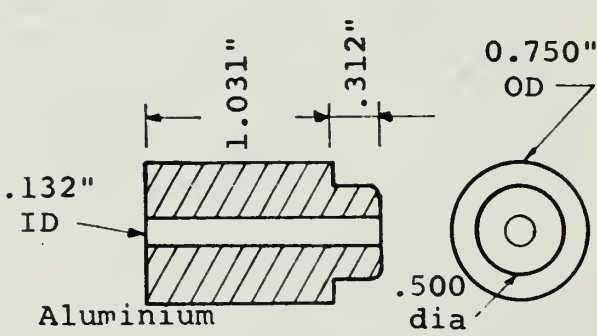
MAZE NUMBER ONE



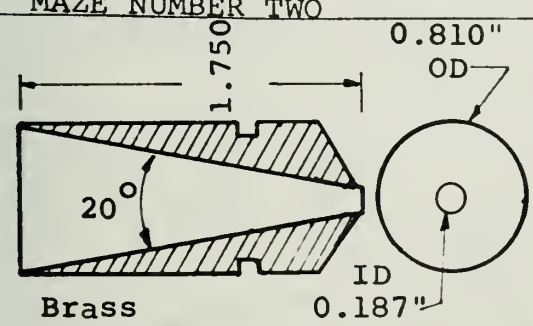
SQUARE SEAT (outlet)



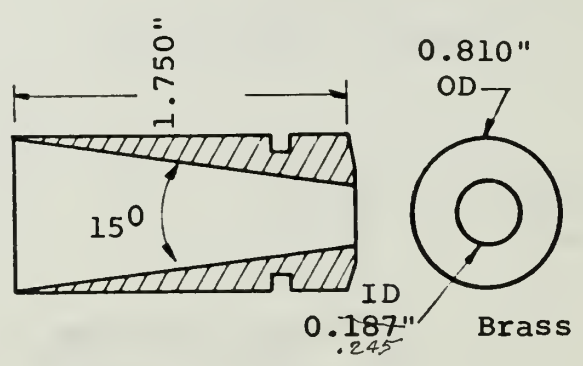
MAZE NUMBER TWO



SQUARE SEAT (inlet)



TAPER SEAT (inlet)



TAPER SEAT (outlet)

Figure C-3a: Plug-seat and Maze Details

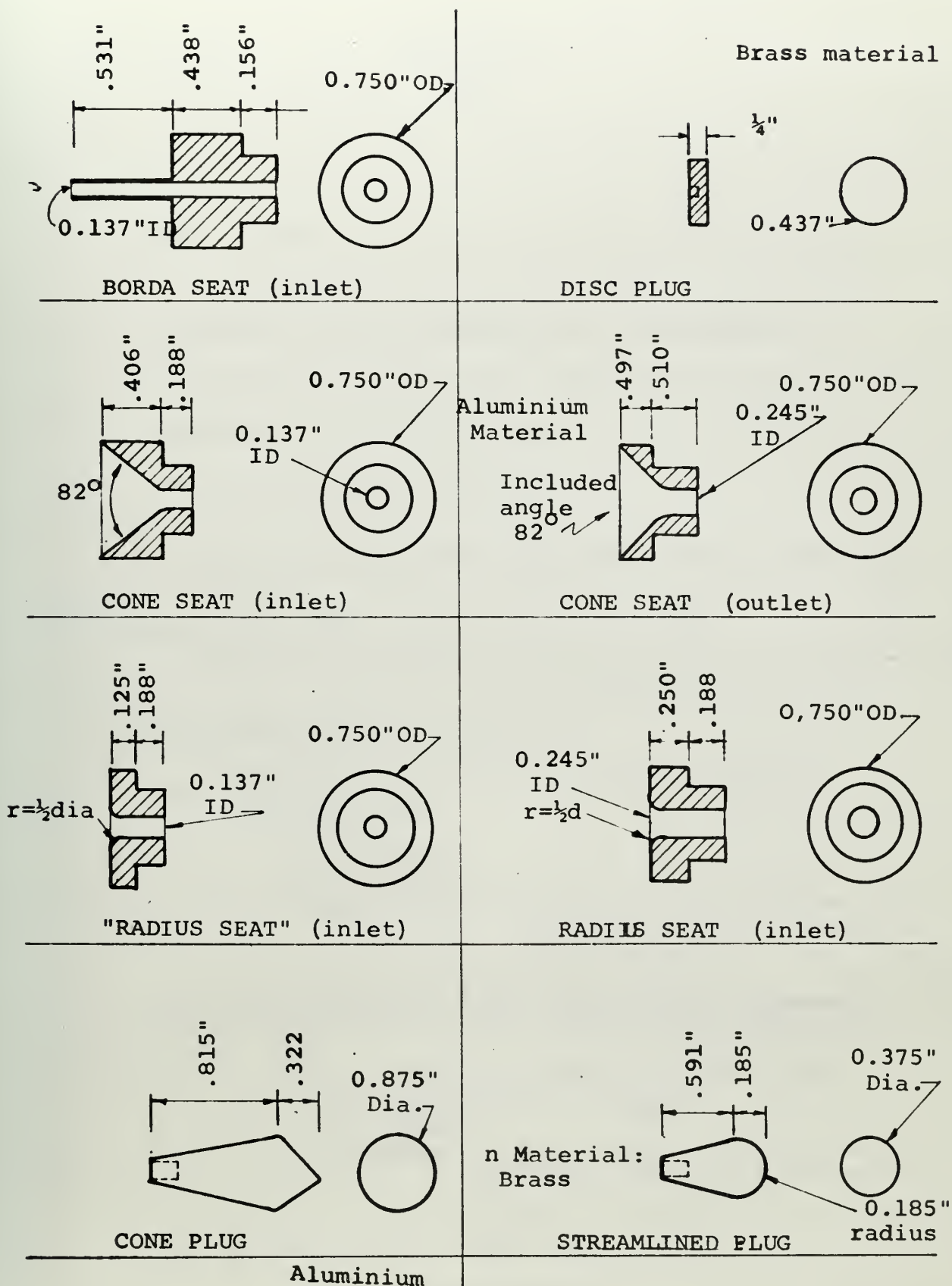


Figure C-3b plug-seat and Maze Details

Q. 1

2

3

4

5

6

7

8

9

10

11

12

13

14

15

16

17

18

APPENDIX D

DATA

1. Nomenclature:

a. Test acronym:

To account for the large number of variables inherent in this experimental investigation, a concise yet all inclusive notation was developed and found to be extremely helpful. This acronym can best be explained by an example:

	PVI	(Air-p6)	(Accel4)	(X-taper-maze2-taper-X)
Group Designation	α	\mathcal{E}	\mathcal{T}	δ

b. Group designation explanation:

α Experimentor and overall test arrangement identification:

S = Sanders

P = Porter

Roman numeral = accounts for variances in the over all test apparatus.
See figure C-1.

\mathcal{E} Fluid media and test section inlet pressure (in units of 100 psig)

Air = Laboratory high pressure system

N = Bottled, dry nitrogen

S = Steam

p number = inlet pressure in units of 100 psig (i.e. p6 = 600 psig at P_{in})

\mathcal{T} Pickup type and location:

Accel - accelerometer

Mike - sound pressure microphone (atmosp)

Tran - sound pressure sensor (high static pres)

Numerical = identifies location of pickup device. For axial positions see figure C-1.

8 Test section configuration:

- 1st position identifies the plug up stream of the maze
- 2nd position identifies the seat up stream of the maze
- 3rd position identifies the pressure reducer maze design
- 4th position identifies the seat downstream of the maze
- 5th position identifies the plug downstream of the maze

() = specifies the gap between the plug and seat

X = nothing installed

2. Summary of Data runs:

More than 250 individual runs were made. However data was not recorded on a few initial runs, also some runs had to be discarded. With runs redesignated, summaries of those runs considered appropriate for the objectives of this thesis are tabulated on the following page.

3. Graphs and recordings:

Data from the Octave Band Analyzer is plotted in figures D-1 to D-8. The recordings from the narrow band analyzer have been compiled into mosiacs and reduced to page size for presentation as figures D-10 to D-23. All scales are identified on each page. Broadband readings are given as

"B.B." with the decibel reference according to the scale of that plot. The volume flow rates, Q , in SCFM (Standard cube feet per minute at 14 psia, and 70°F) can be obtained with a given P_2 from figure C-2.

Data Run #	Test Acronym	Results Presented
1	PI (Air-p6) (Accel4) (X-X-Orifice-X-X)	Fig D1-9
2	" (" -p5.5)	Similar Run 1
3	" (" p5)	" "
4	" (" p4)	" Run 2
5	" (" p3)	Fig D1-9
6	" (Air-p6) (X-taper-mazel-taper-X)	
7	" (" p5.5)	Fig D3
8	" (" p5)	Similar Run 7
9	" (" p4)	" "
10	" (" p3)	Fig D3
11	PII (Air-p5)	Fig D2
12	" (" p3)	" "
13	PIII (" -p5)	" "
14	" (" ")	" "
15	" (Air-p2) (X-taper-less balls-taper-X)	" "
16	" (" p5.5) (X-taper-maze2-taper-X)	Fig D3
17	" (" p5)	Similar Run 16
18	" (" p3)	Fig D3
19	" (" p2.5)	Similar Run 18
20	" (" p4) (X-taper-mazel-taper-X)	Fig D4
21	" (" P2)	" "
22	" (N2-P4)	" "
23	" (" p2)	" "
24	PI (Air-p5.5) (Accell) (X-taper-maze2-taper-X)	Fig D6
25	" " (" 2)	" "
26	" " (" 3)	" "
27	" " (" 4)	" "
28	" " (" 5)	" "
29	" " (" 6)	" "
30	" " (" 7)	" "
31	" " (" 8)	" "
32	" " (" 9)	" "
33	" (Air-p4) (Accell)	Similar Run 24
34	" " (" 2)	" "
35	" " (" 3)	" "
36	" " (" 4)	" "
37	" " (" 5)	" "
38	" " (" 6)	" "
39	" " (" 7)	" "
40	" " (" 8)	" "
41	" (Air-p3) (Accell)	Fig D6
42	" " (" 2)	" "
43	" " (" 3)	" "
44	" " (" 4)	" "
45	" " (" 5)	" "
46	" " (" 6)	" "
47	" " (" 7)	" "
48	" " (" 8)	" "
49	" " (" 9)	" "
50	" (Air-p2) (Accell)	Similar Run 40
51	" " (" 2)	" "

52	PI (Air-p2)	(Accel3)	(X-taper-maze2-taper-X)	Similar Run 40
53	"	"	(Accel4)	"
54	"	"	(" 5)	"
55	"	"	(" 6)	"
56	"	"	(" 7)	"
57	"	"	(" 8)	"
58	"	"	(" 9)	"
59	PIII (N2-p5.5)	(Accel4)	(X-Square-maze2-taper-X)	Taped
60	"	(" p4)	"	"
61	"	(" p3)	"	"
62	"	(" p2)	"	"
63	"	(Air-p6)	"	"
64	"	(" p5.5)	"	"
65	"	(" p5)	"	"
66	"	(" p4)	"	"
67	"	(" p3)	"	"
68	"	(" p2)	"	"
69	PV	(Air-p6)	(X-taper-maze2-taper-X)	"
70	"	(" p5.5)	"	"
71	"	(" p5)	"	"
72	"	(" p4)	"	"
73	"	(" p3)	"	"
74	"	(" p2)	"	"
75	"	(" p6)	(X-Square-maze2-taper-X)	Fig D5
76	"	(" p5.5)	"	"
77	"	(" p5)	"	"
78	"	(" p4)	"	"
79	"	(" p3)	"	"
80	"	(" p2)	"	"
81	PI	(Air-p5.5)	"	"
82	"	(" p4)	"	"
83	"	(" p3)	"	"
84	"	(" p2)	"	"
85	PIII	(Air-p5.5)	"	"
86	"	(" p4)	"	"
87	"	(" p3)	"	"
88	"	(" p2)	"	"
89	PIII	(" p5.5)	(Accel1) (X-taper-maze2-taper-X)	Fig D8
90	"	"	(" 2)	"
91	"	"	(" 3)	"
92	"	"	(" 4)	"
93	"	"	(" 5)	"
94	"	"	(" 6)	"
95	"	"	(" 7)	"
96	"	"	(" 8)	"
97	"	(Air p3)	(" 1)	"
98	"	"	(" 2)	"
99	"	"	(" 3)	"
100	"	"	(" 4)	"
101	"	"	(" 5)	"
102	"	"	(" 6)	"
103	"	"	(" 7)	"
104	"	"	(" 8)	"

105	PIV(Air-p5.5)	(Accel1)	(X-taper-maze2-taper-X)	Fig D7
106	"	"	(" 2)	"
107	"	"	(" 3)	"
108	"	"	(" 4)	"
109	"	"	(" 5)	"
110	"	"	(" 6)	"
111	"	"	(" 7)	"
112	"	(Air-p3)	(Accel1)	"
113	"	(Air-p3)	(Accel2)	"
114	"	"	(" 3)	"
115	"	"	(" 4)	"
116	"	"	(" 5)	"
117	"	"	(" 6)	"
118	"	"	(" 7)	"
119	PV(Air-p5.5)	(Accel4)	"	Fig D7
120	"	"	(" 5)	"
121	"	"	(" 6)	"
122	"	"	(" 7)	"
123	"	(Air-p3)	(" 4)	"
124	"	"	(" 5)	"
125	"	"	(" 6)	"
126	"	"	(" 7)	"
127	PV1(Air-p6)	(Accel4)	(X-X-Orifice-X-X)	Fig D12
128	"	(" p3)	"	"
129	"	(" p6)	(" 7) (X-taper-maze2-taper-X)	Fig D13
130	"	"	(" 2)	"
131	"	"	(" 3)	"
132	"	"	(" 4)	Similar 132
133	"	"	(" 5)	Fig D13
134	"	"	(" 6)	"
135	"	(Air-p6)	(Accel4)	Fig D12
136	"	(" p5)	"	Similar 135
137	"	(" p3)	"	Fig D12
138	"	(" p6)	(X-sharp-maze1-taper-X)	Fig D21
139	"	(" p3)	"	Similar 138
140	"	(" p6)	(X-cone-maze2-taper-X)	Fig D17
141	"	(" p5)	"	Similar 140
142	"	(" p3)	"	Fig D17
143	"	(" p6)	(X-Borda-maze2-taper-X)	Fig D18
144	"	(" p3)	"	"
145	"	(" p6)	(Disc(1/16)-Borda-maze2-taper-X)	"
146	"	(" p3)	"	Similar 145
147	"	(" p6)	(Disc(5/8)-Borda-maze2-taper-X)	Fig D18
148	"	(" p3)	"	Similar 147
149	"	(" p6)	(Cone(1/16)-Cone-maze2-taper-X)	Fig D17
150	"	(" p3)	"	Similar 149
151	"	(" p6)	(Cone(9/16)-cone-maze-taper-X)	Fig D17
152	"	(" p6)	(SL(1/32)-radius-maze2-taper-X)	Fig D19
153	"	"	(" -Borda-maze2- ")	Fig D20
154	"	"	(" -cone-maze2- ")	"
155	"	"	(" -square-maze- ")	Fig D19
156	"	"	(SL(1/2)-cone-maze2-taper-X)	Fig D20

157	PVI	(Air-p6)	(Accel4)	(SL(1/2) -borda-maze2-taper-X)	Fig D20
158	"	"	"	(" -square- ")	Fig D19
159	"	"	"	(" -radius- ")	"
160	"	(" -p6)	"	(X-radius-maze2-taper-X)	Fig D14
161	"	(" -p3)	"	"	"
162	"	(" -p6)	"	(Disc(1/16) -radius-maze2-taper-X)	Fig D15
163	"	(" -p3)	"	"	"
164	"	(" -p6)	"	(Disc(1/2) -radius- ")	"
165	"	(" -p3)	"	"	"
166	"	(" -p6)	"	(X-square-maze2-taper-X)	Fig D14
167	"	(" -p3)	"	"	"
168	"	(" -p6)	"	(Disc(1/16) square-maze2-taper-X)	Fig D16
169	"	(" -p3)	"	"	"
170	"	(" -p6)	"	(Disc(1/2) ")	"
171	"	(" -p3)	"	"	"
172	PVII	(Air-p6)	"	(X-square-maze2-square-X)	Fig D22
173	"	"	"	(" " -cone-X)	"
174	"	"	"	(" " -radius-X)	"
175	"	"	"	(" " -taper-X)	"
176	"	"	"	(X-sharp-mazel-round-X)	Fig D21
177	"	"	"	(" " -square-X)	"
178	"	"	"	(" " -cone-X)	"
179	"	"	"	(" " -taper-X)	"
180	"	"	"	(X-taper-maze2-taper-X)	Fig D10
181	"	(N ₂ -p6)	"	"	"
182	"	(Air-p6)	"	(X-square-maze2-square-disc(1/16)	Fig D23
183	"	"	"	(" (1/2)	"
184	"	"	"	(" -cone SL(1/16)	"
185	"	"	"	(" (1/2)	"
186	PVI	(Air-p6)	(Mike 3"from 4')	(X-radius-maze2-taper-X)	Fig D11
187	"	(" -p3)	"	"	"
188	Typical	Laboratory	Background (Accel4)	(No airflow)	"
189	"	"	"	(Mike 3 "from4) (")	"
190	Noisy	"	"	"	Fig D10
191	"	"	"	"	"
192	PVI	(Air-p6)	(Accel7)	(X-Taper-Maze2-taper-X)	Fig D13
193	PVI	(Air-p6)	(Accel8)	(")	"

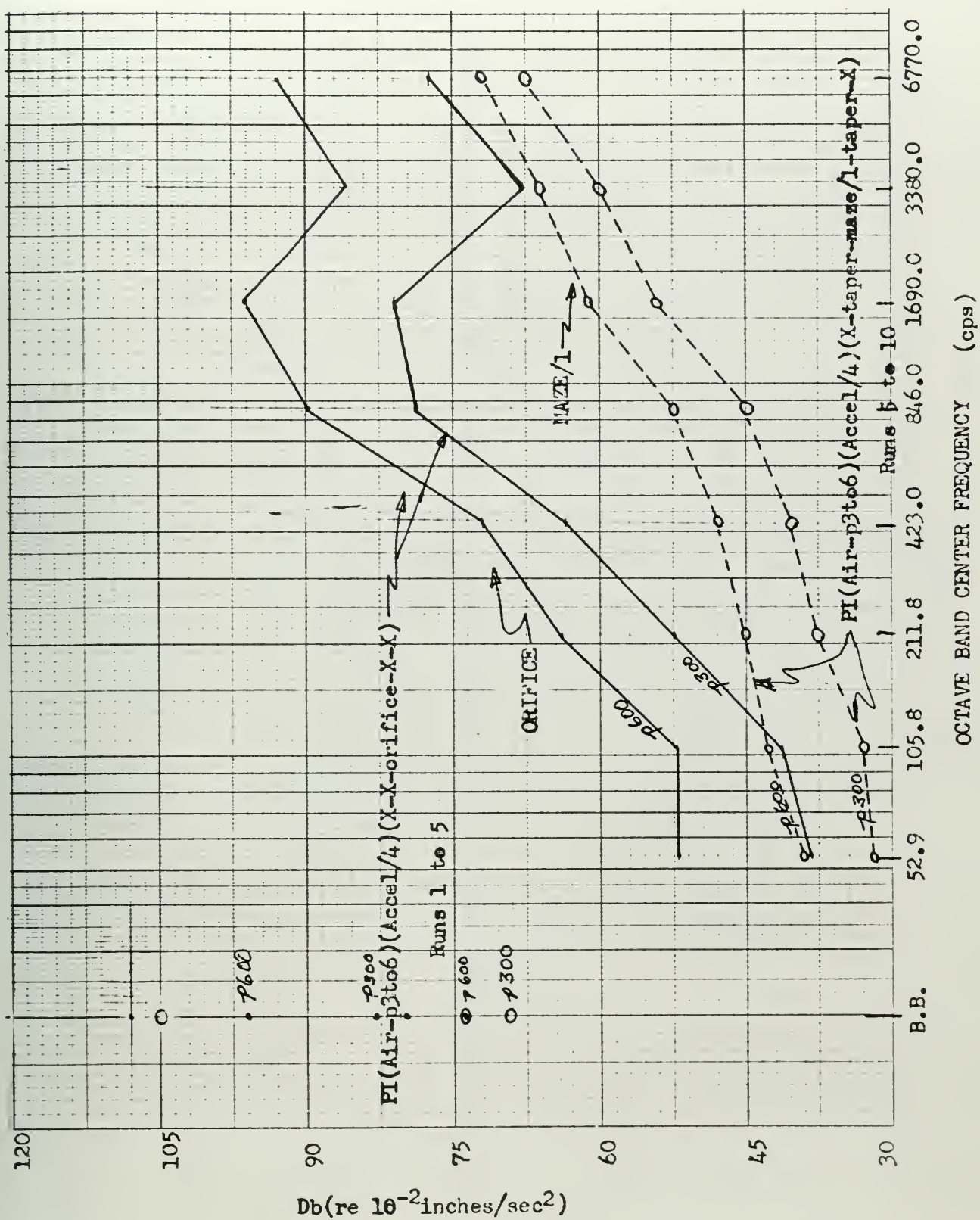


Figure D-1 Run 1 - 10

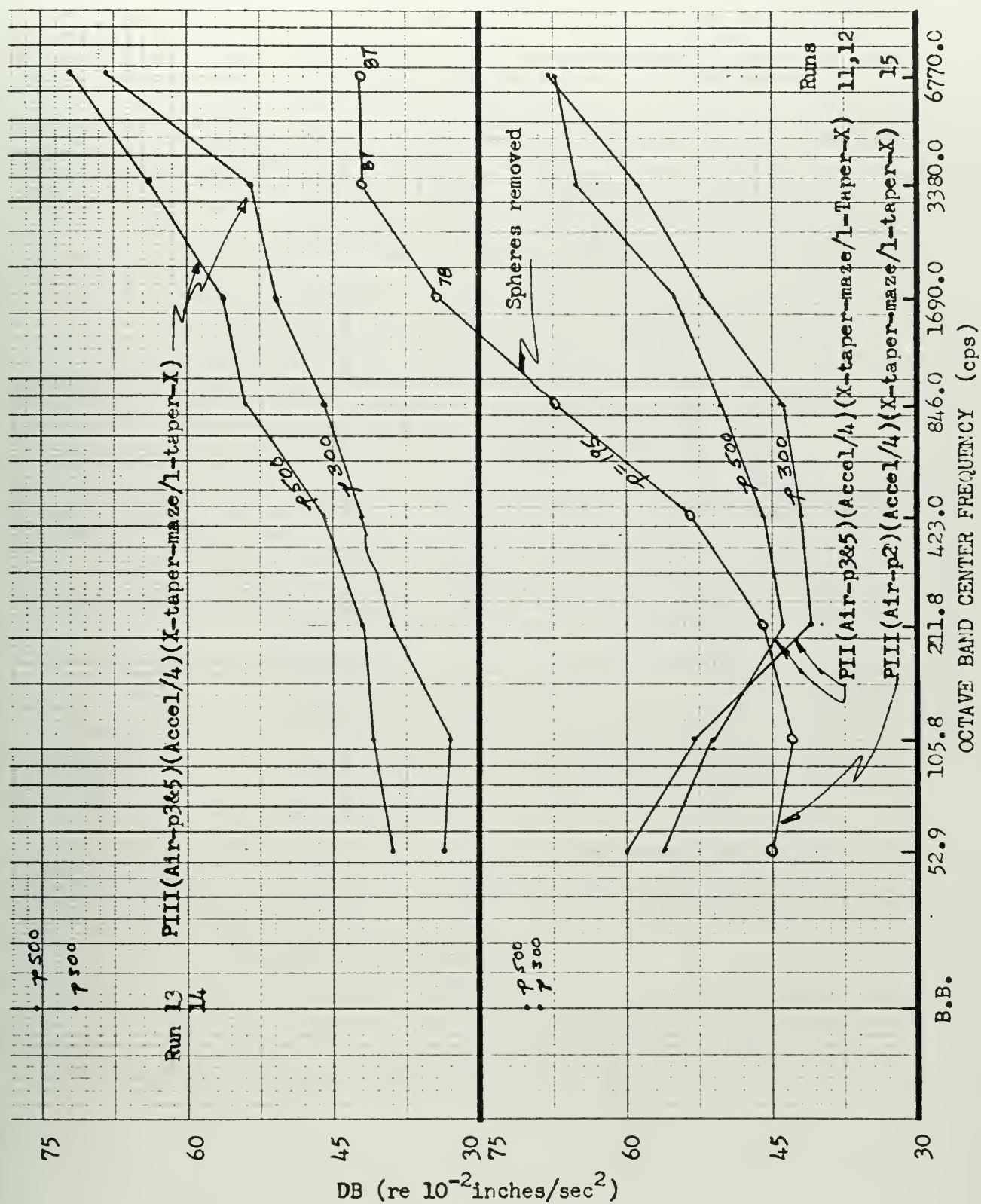


Figure D-2 Run 11-15

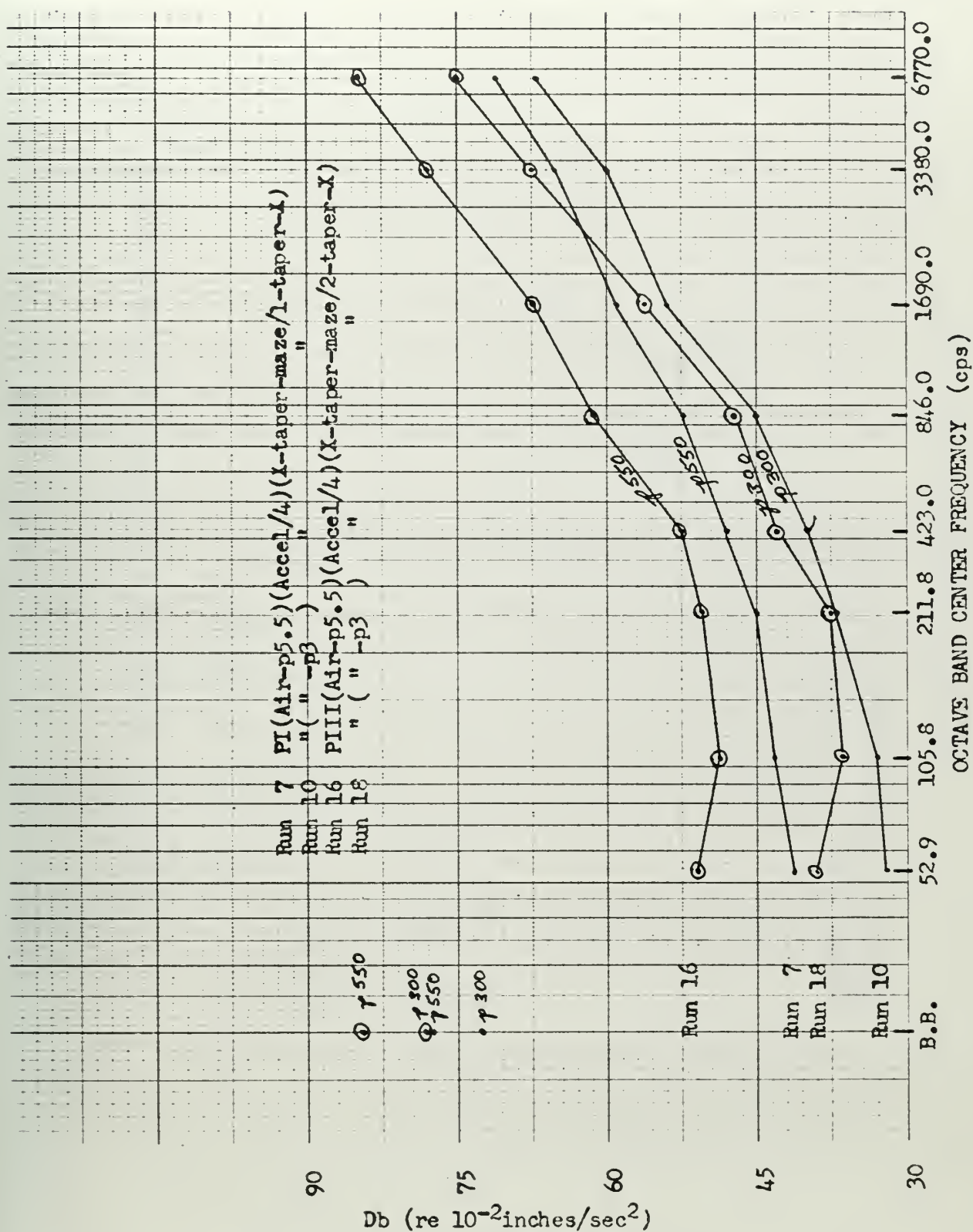


Figure D-3a Run 7, 10, 16, 18

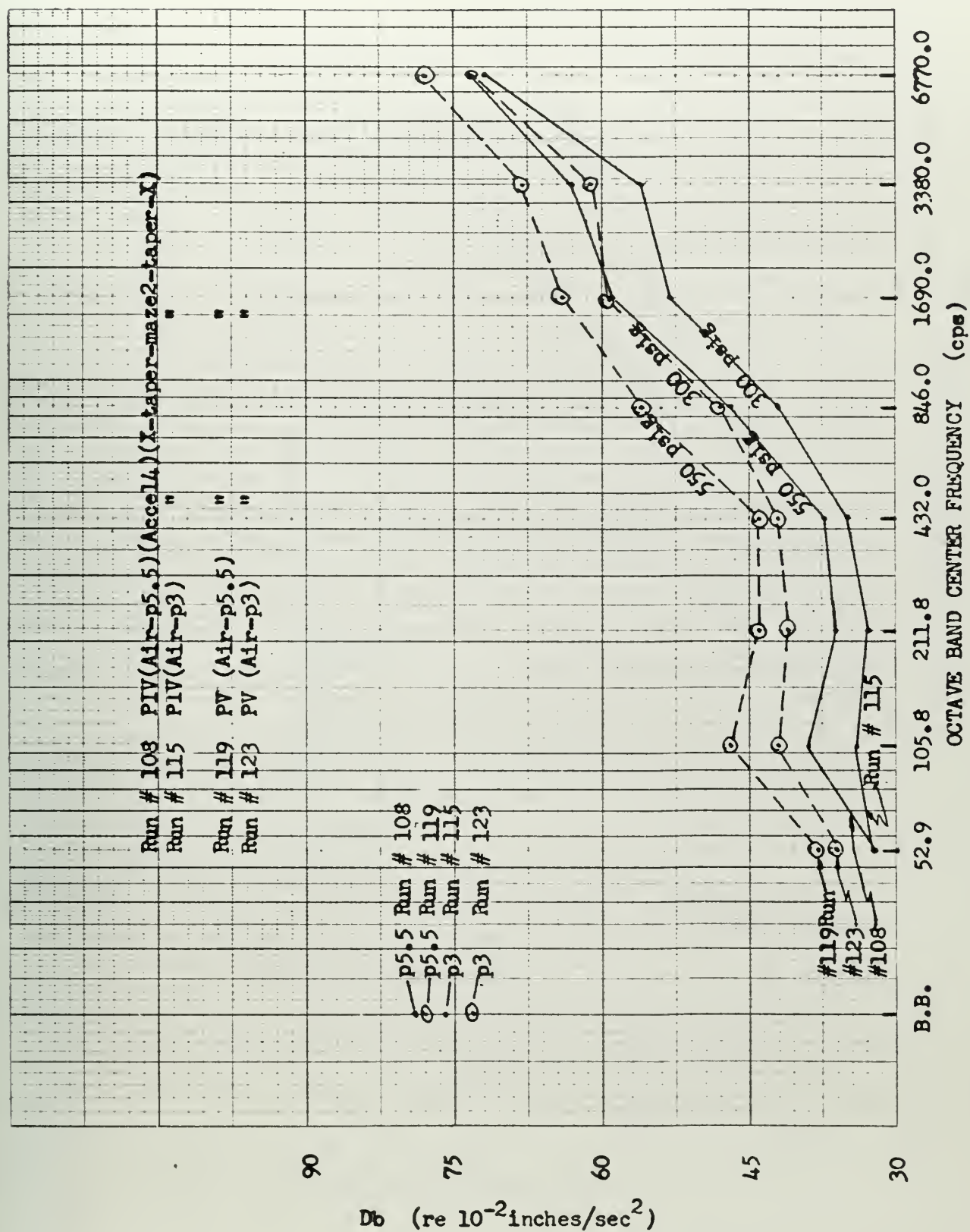


Figure D-3b Run 108, 119, 115, 123

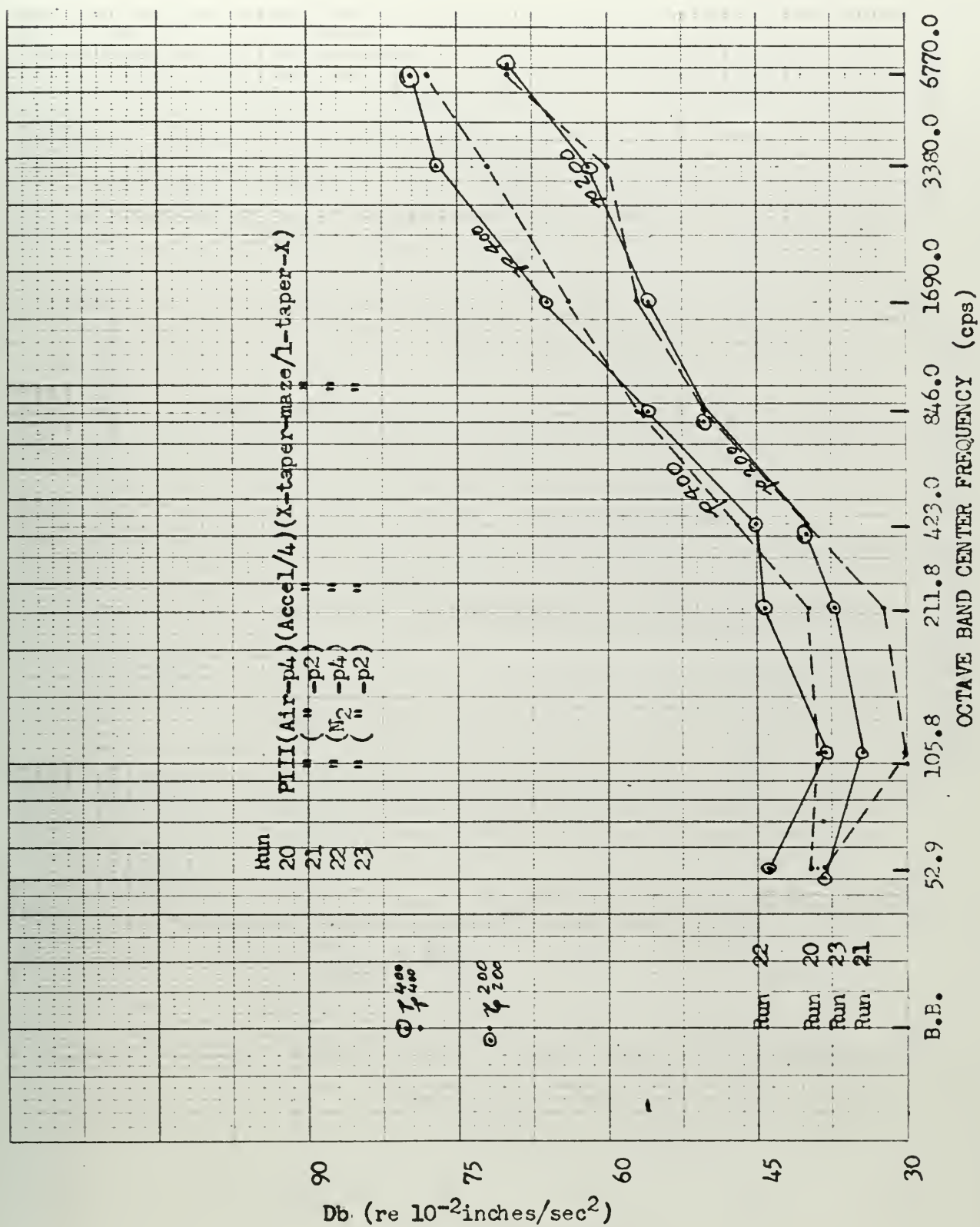


Figure D-4 Run 20 - 23

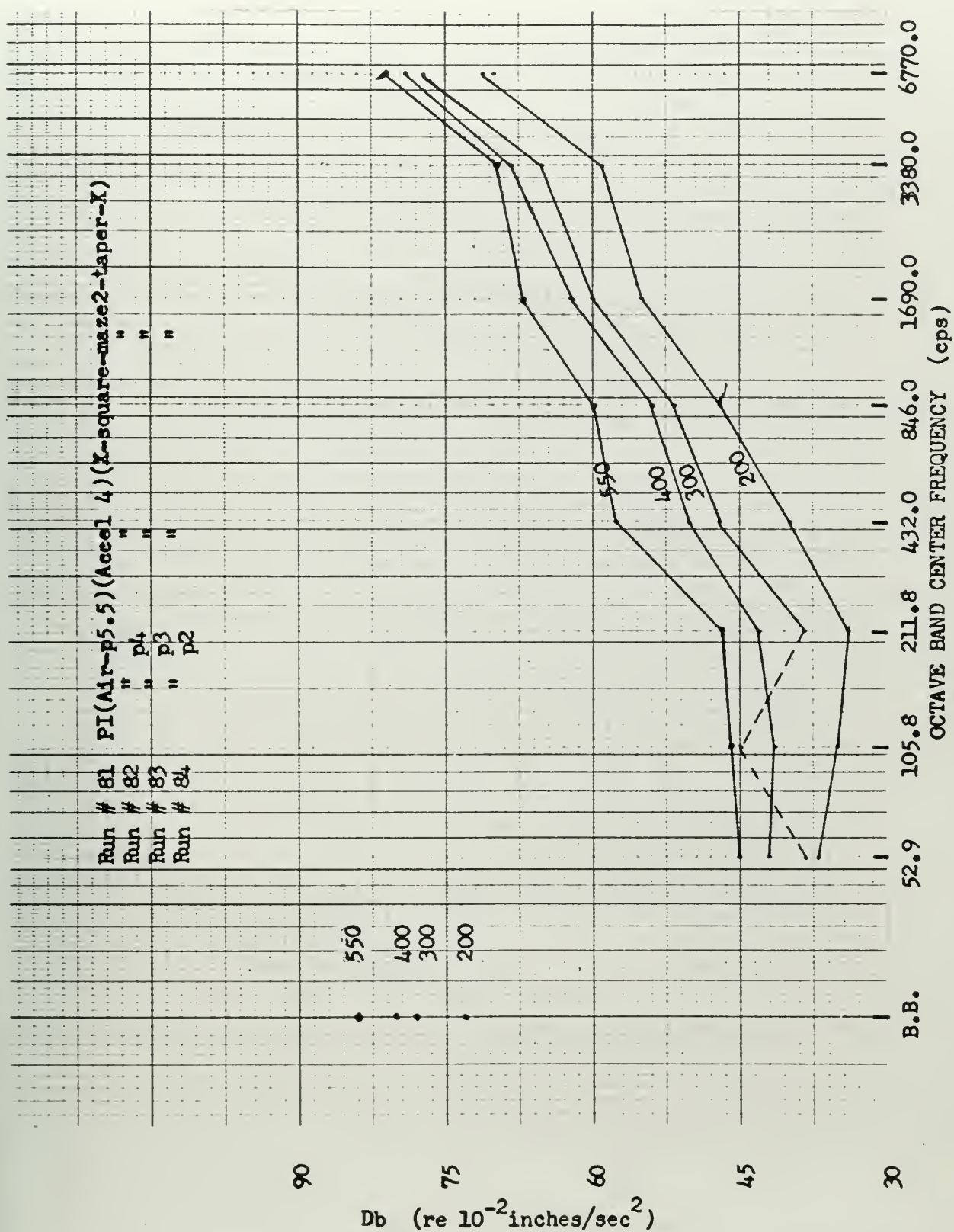


Figure D-5a Run 81 - 84

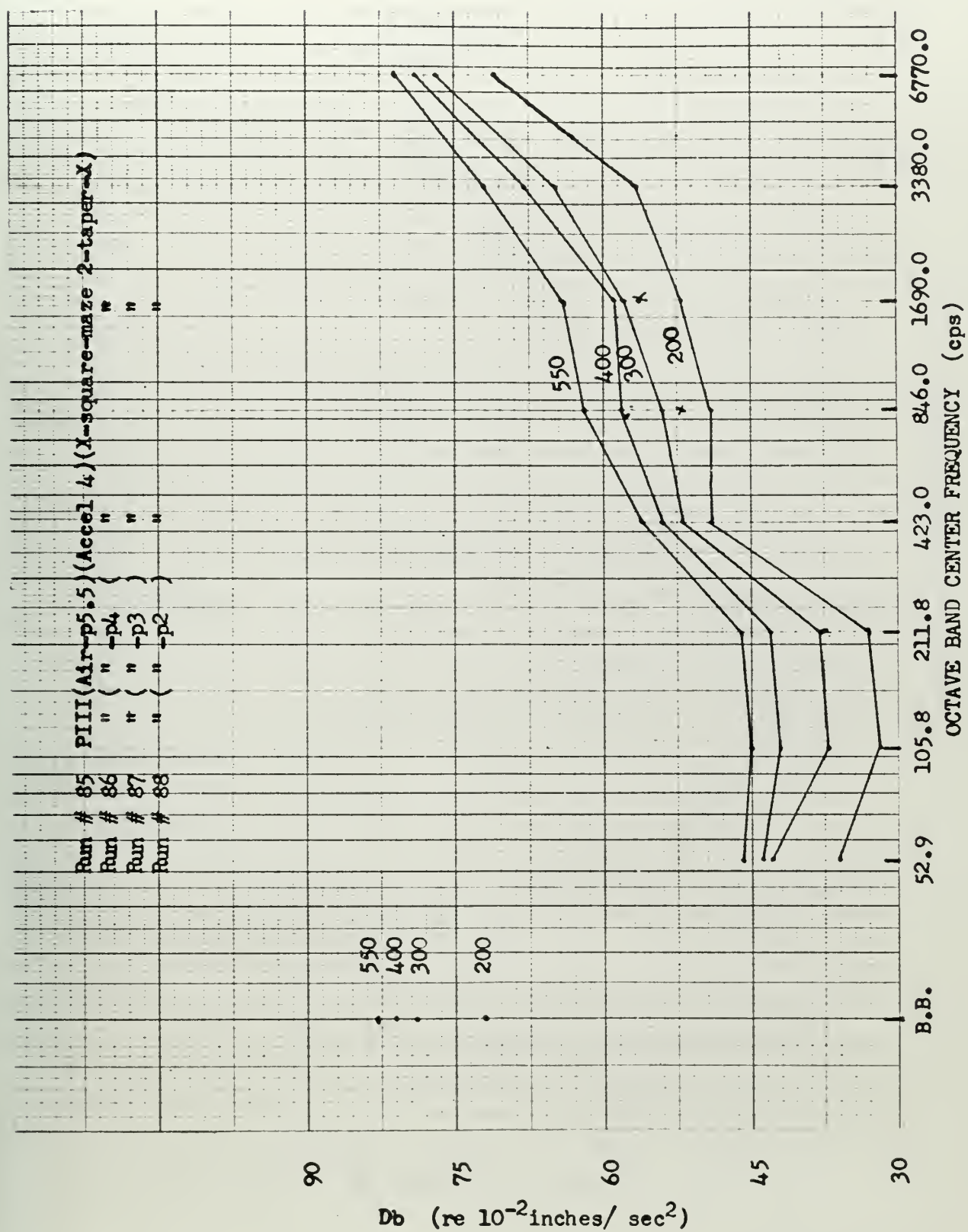


Figure D-5b Run 85 - 88

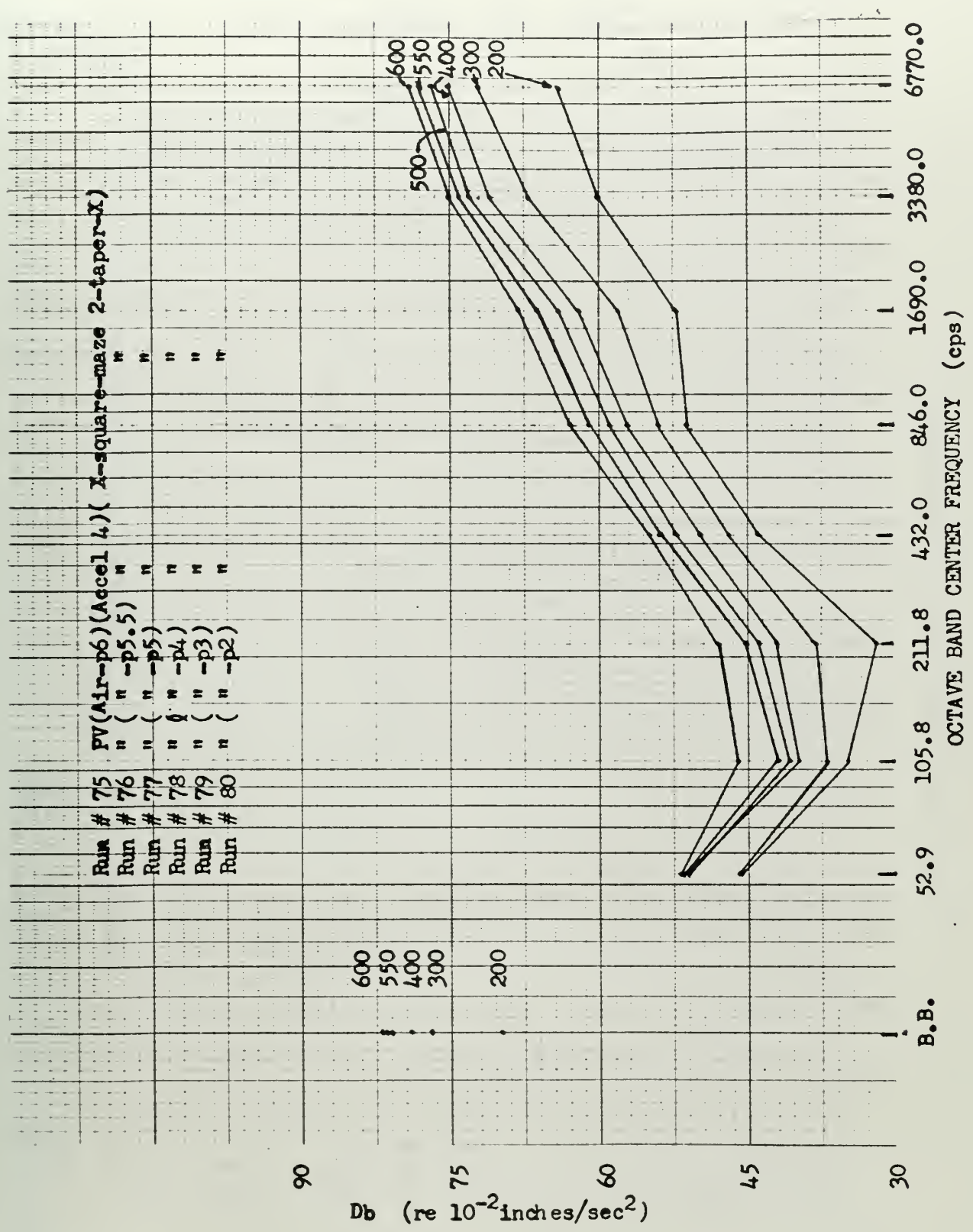


Figure D-5c Run 75 - 80

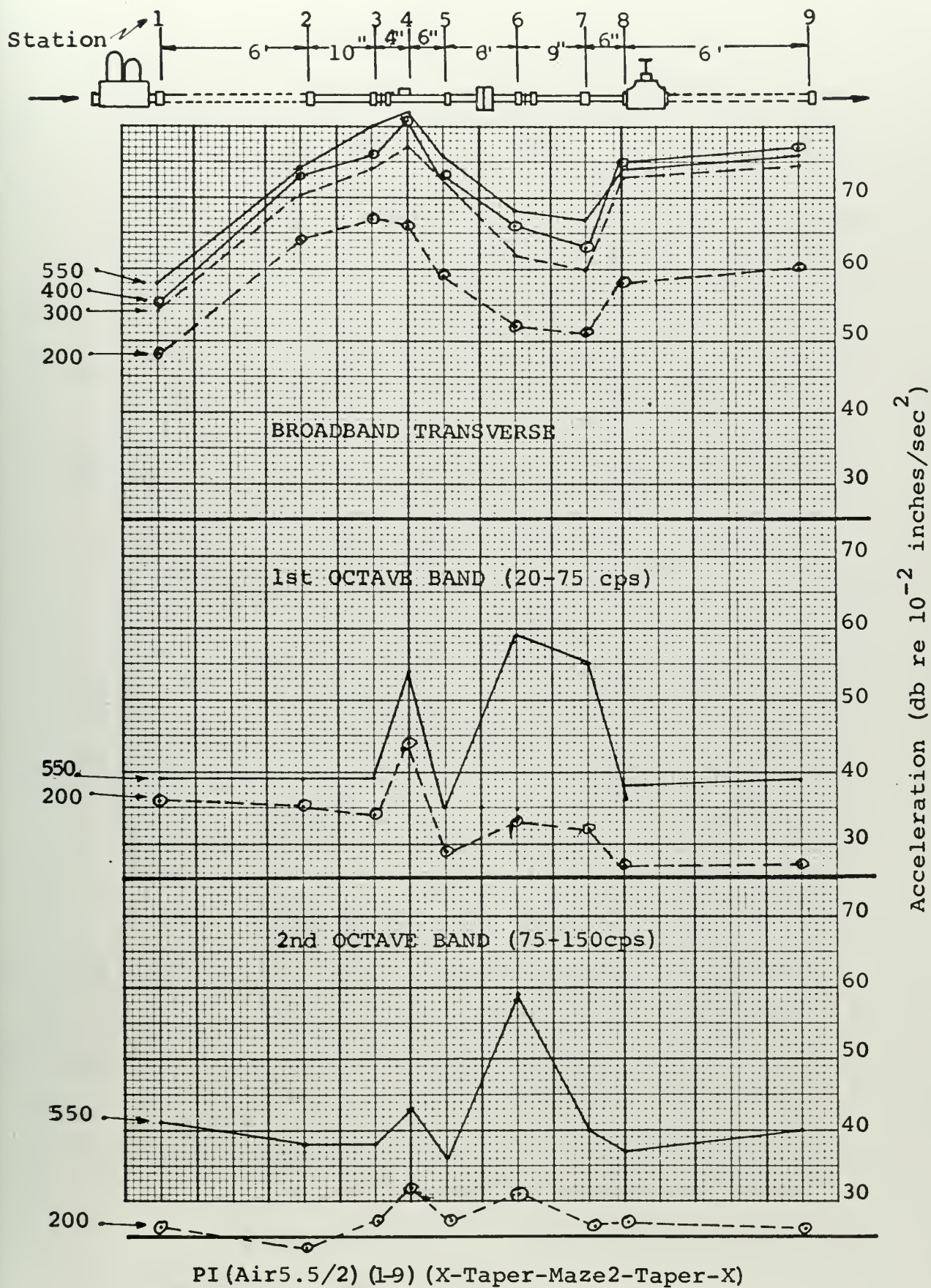
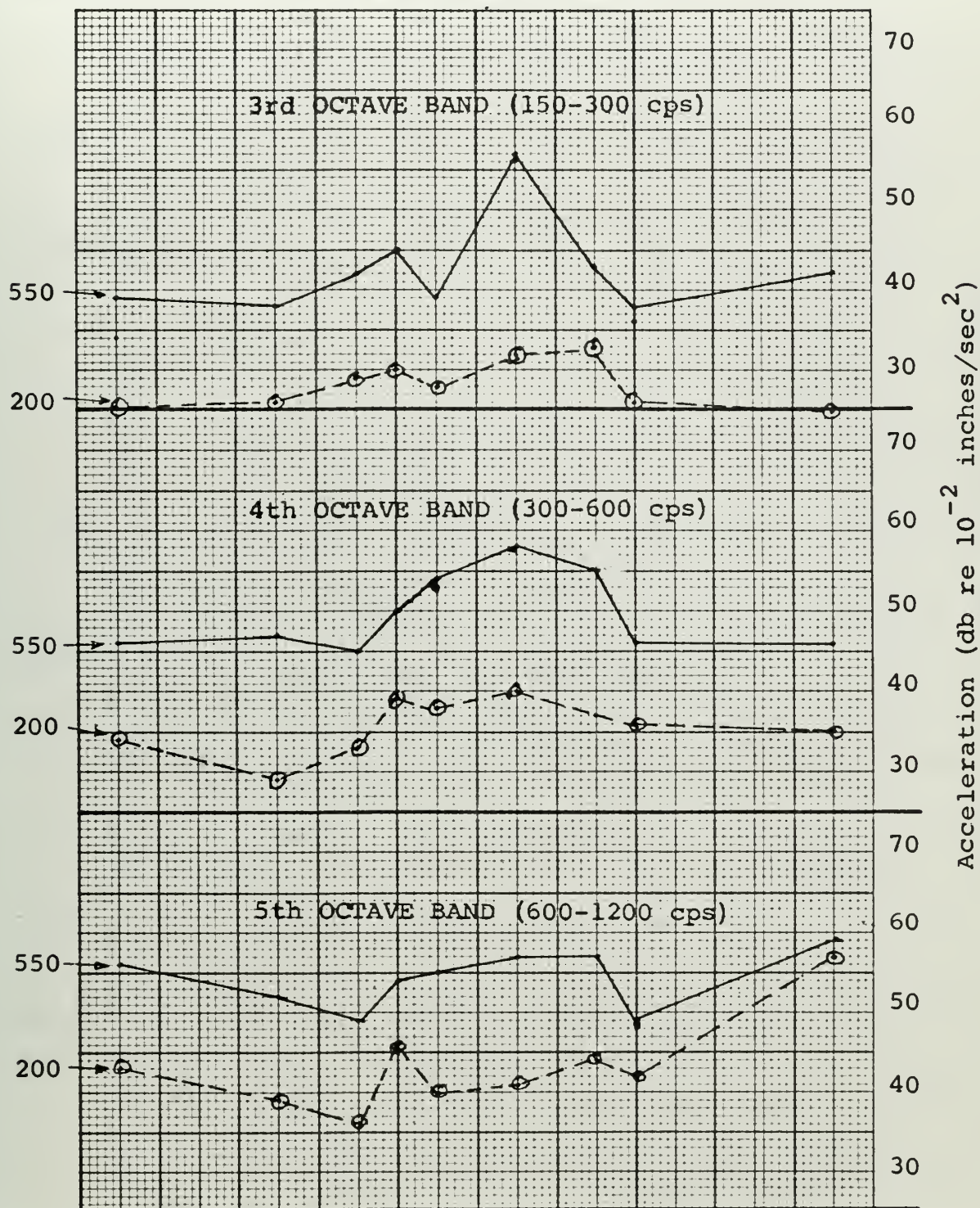
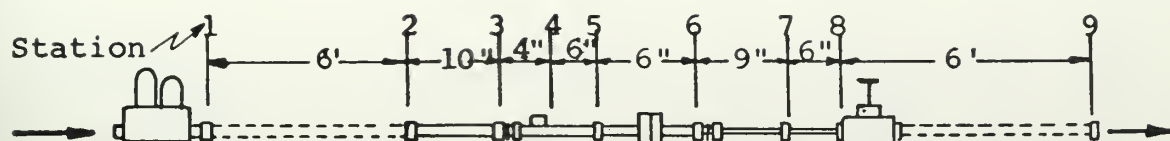


Figure D-6a Run 24 - 49



PI (Air-p5.5/2) (1 to 9) (X-Taper-Maze2-Taper-X)

Figure D-6b Run 24 - 49

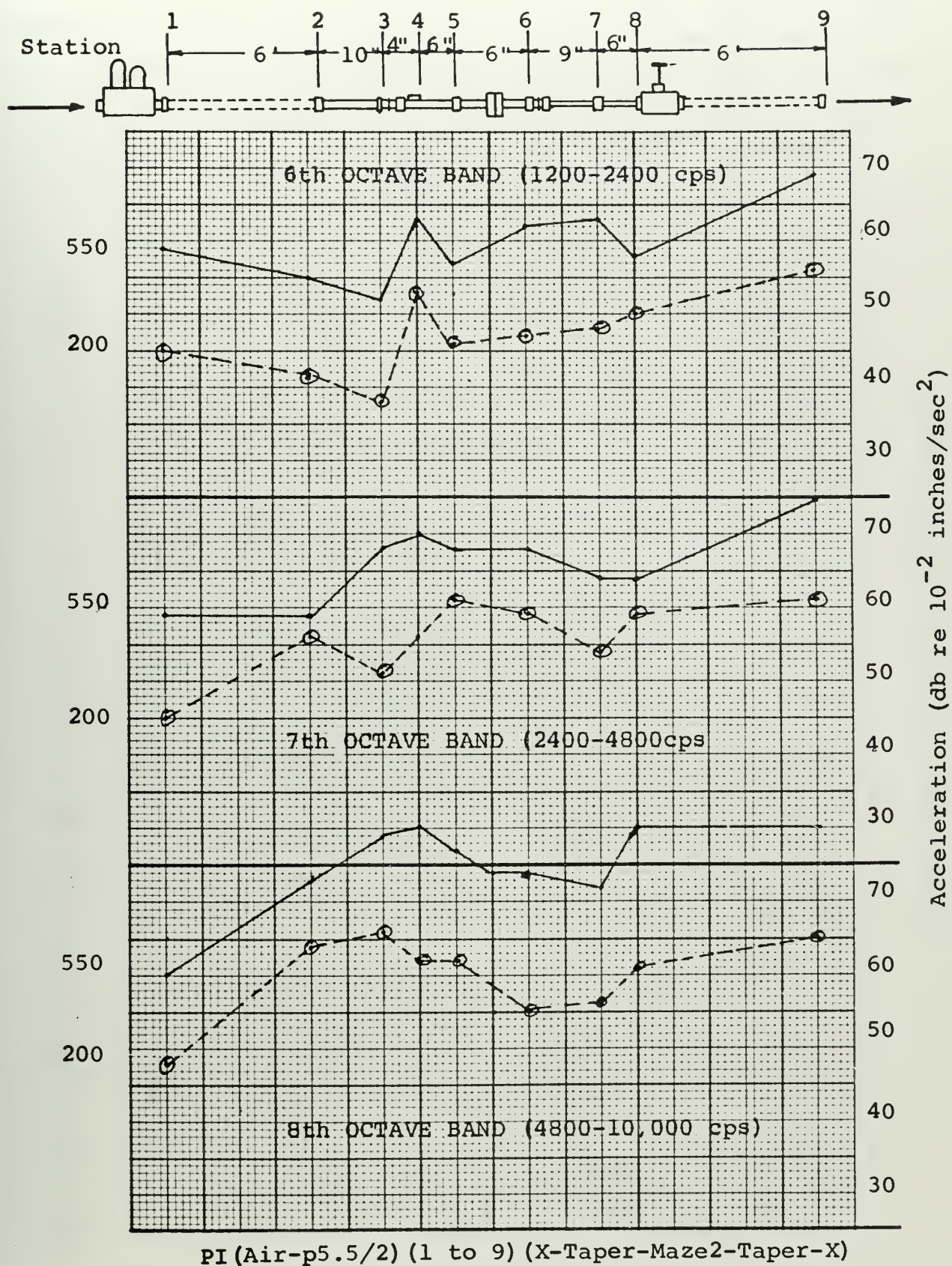
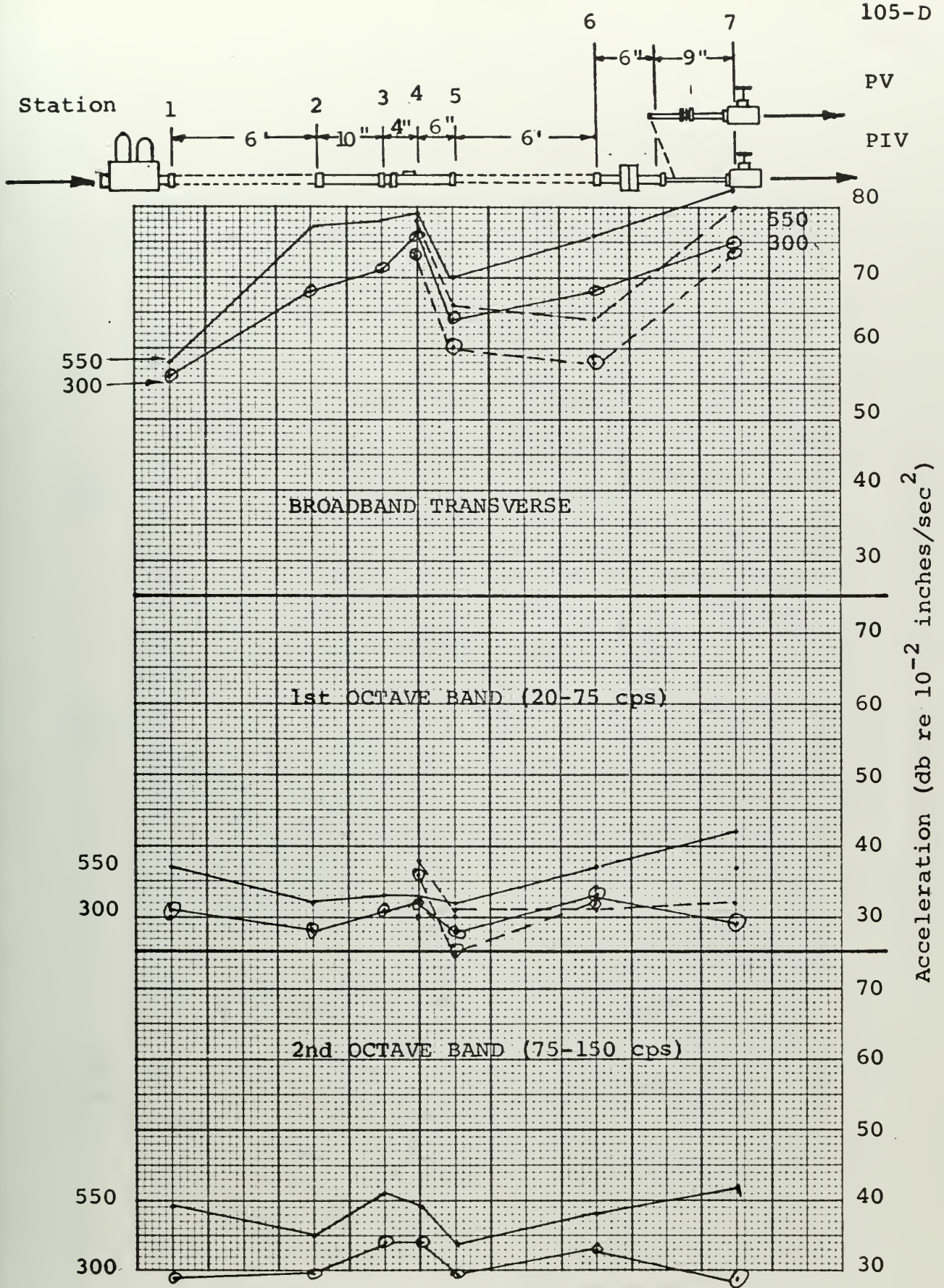


Figure D-6c Run 24-49



— PIV(Air-p5.5/3) (1 to 7) (X-taper-Maze 2-taper-X)
 - - - PV(Air-p5.5/3) (1 to 7) (X-taper-Maze 2-taper-X)

Figure D-7a Run 105 - 126

Station \nearrow 1

2

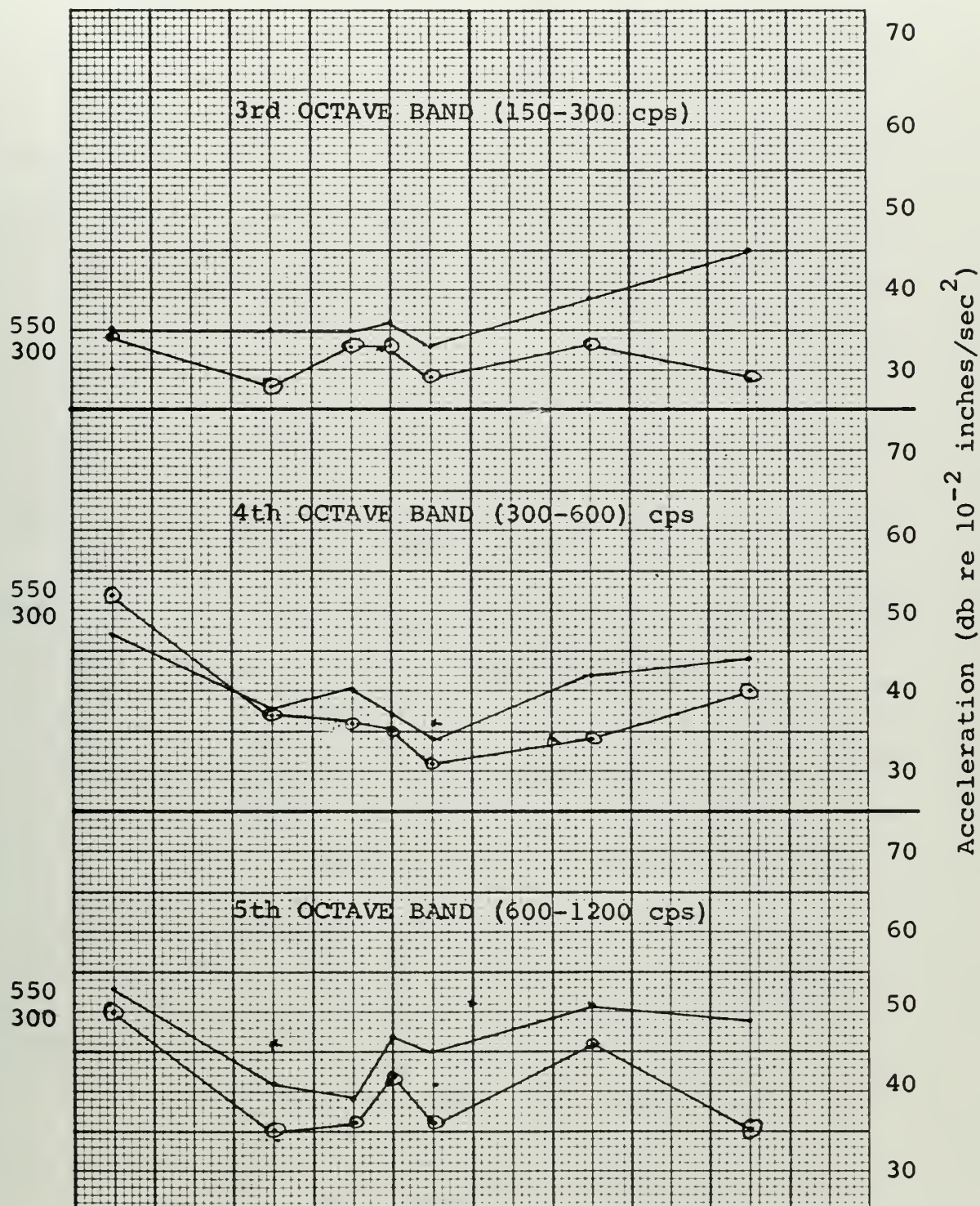
3

4

5

6

7



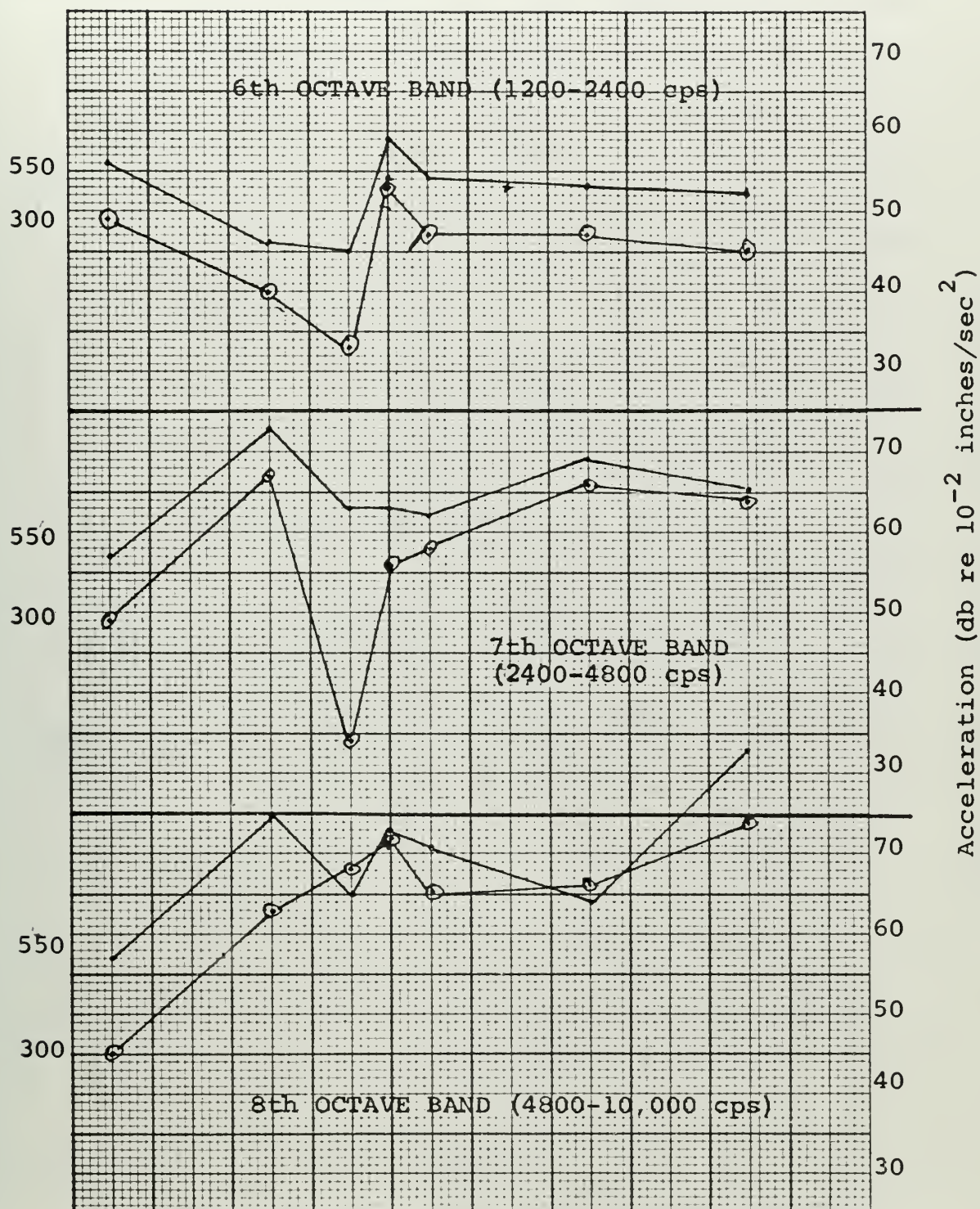
PIV (Air-p5.5/3) (1 to 7) (X-taper-Maze2-taper-X)

PV (Air-p5.5/3) (1 to 7) (X-taper-Maze2-taper-X)

Figure D-7b Run 105 - 126

Station 1 2 3 4 5 6 7

 | | | | | | |

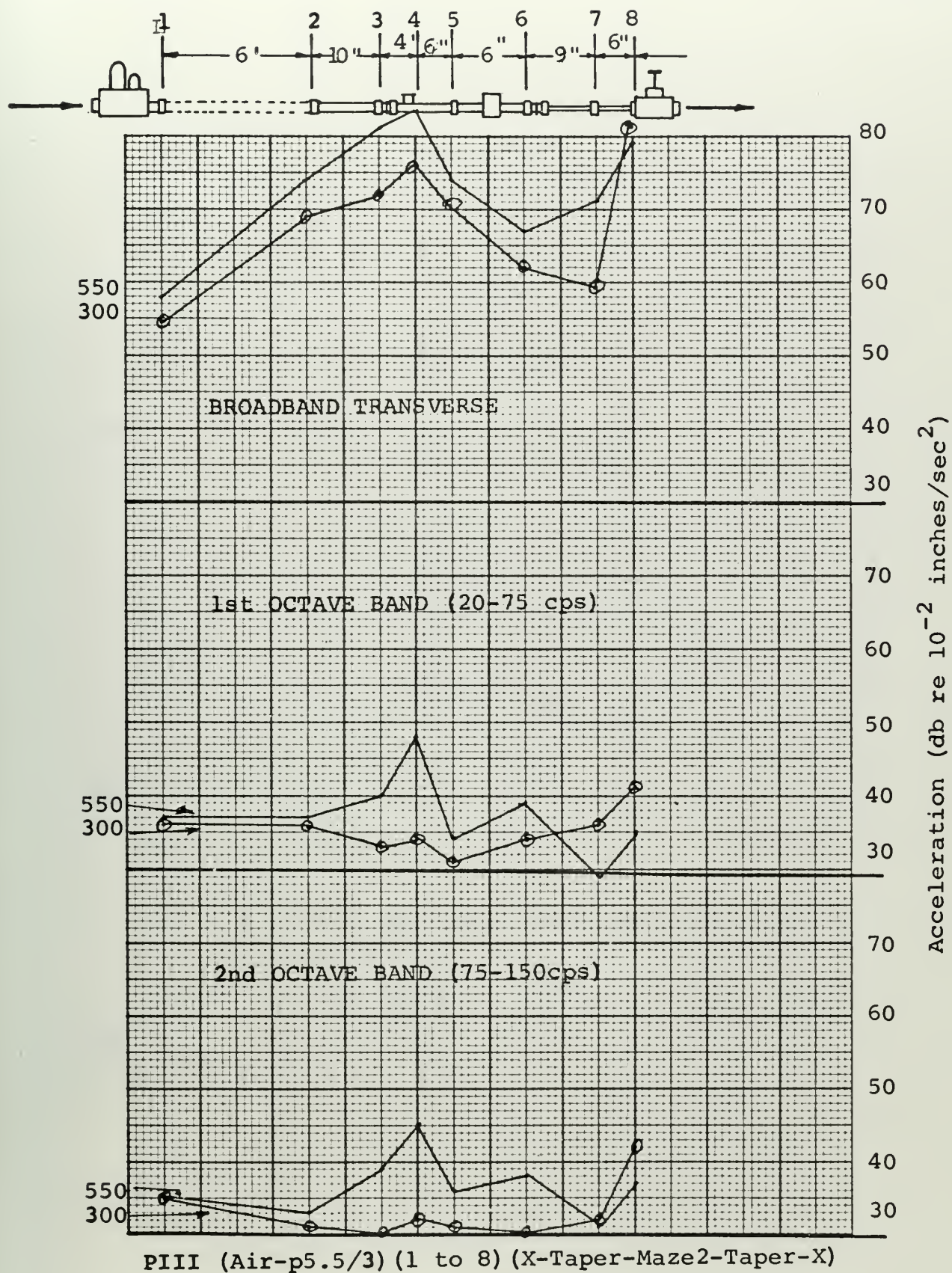


PIV (Air-p5.5/3) (1 to 7) (X-taper-Maze2-taper-X)
 PV (Air-p5.5/3) (1 to 7) (X-taper-Maze2-taper-X)

Figure D-7c Run 105 to 126



Station

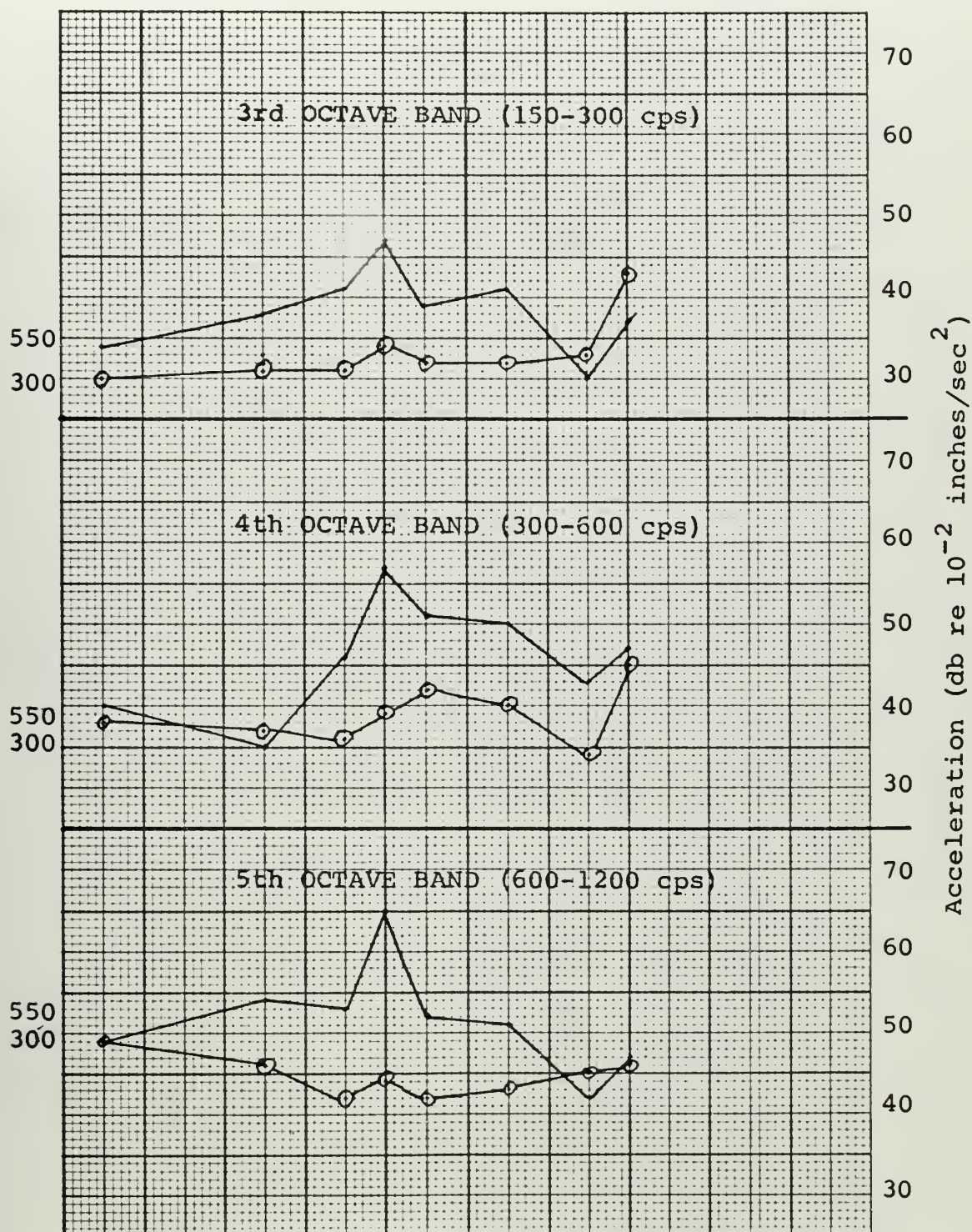


PIII (Air-p5.5/3) (1 to 8) (X-Taper-Maze2-Taper-X)

Figure D-8a Run 89 - 104

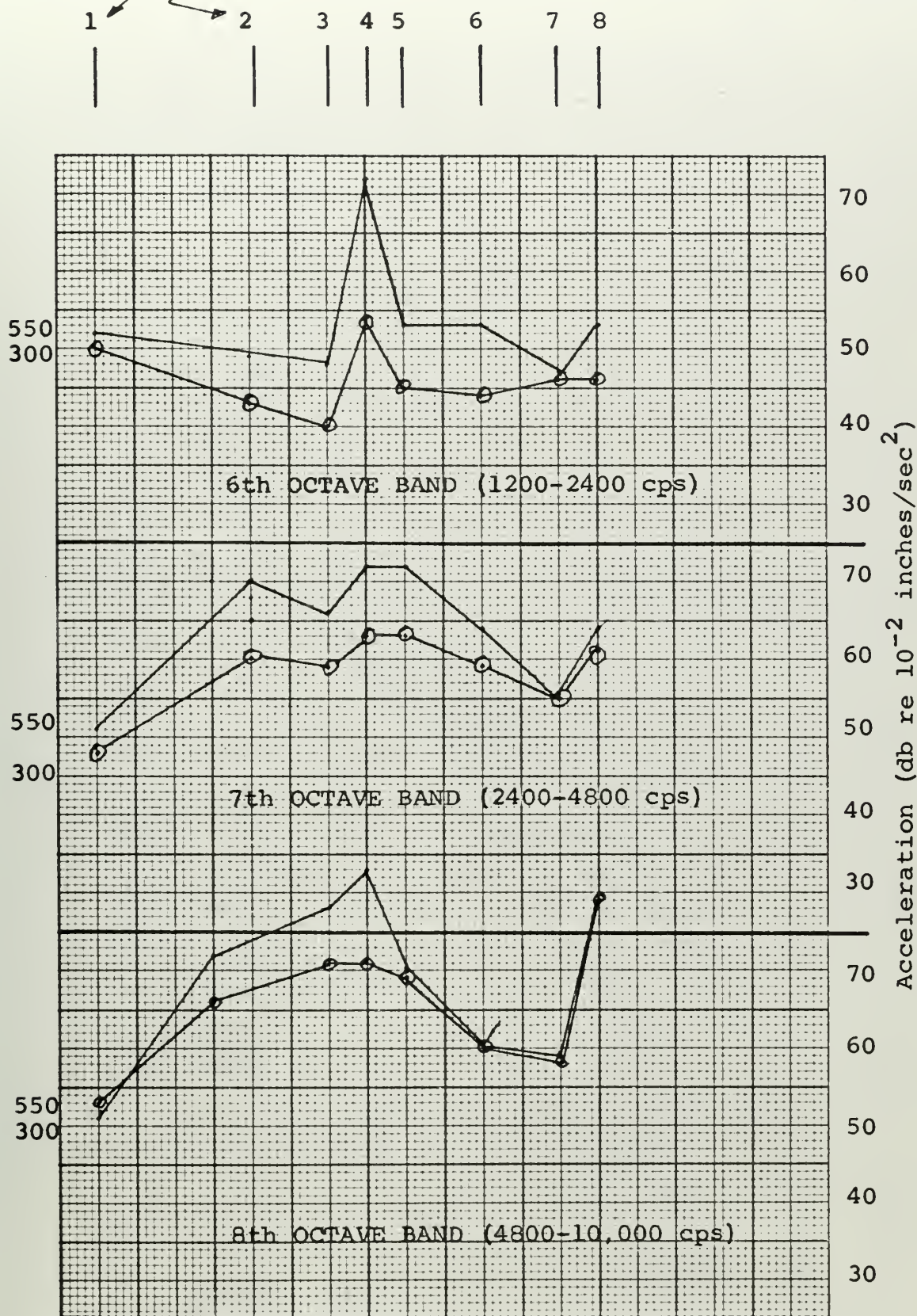
Station

1	2	3	4	5	6	7	8



PIII (Air-p5.5/3) (1 to 8) (X-Taper-Maze2-Taper-X)

Figure D-8b Run 89-104



PIII (Air-p5.5/3) (1 to 8) (X-Taper-Maze2-Taper-X)

Figure D-8c Run 89 - 104

Run # 1 PI(Air p6)(Accel 4)(X-X-orifice-X-X)
 Run# 2 " (" p5.5) "
 Run# 3 " (" p.5) "
 Run# 4 " (" p4) "
 Run# 5 " (" p3)

600
550
500
400
300

DECIBEL (re 10⁻² inches/sec²)

30

45

60

75

90

B.B.

52.9

105.8

211.8

423.0

846.0

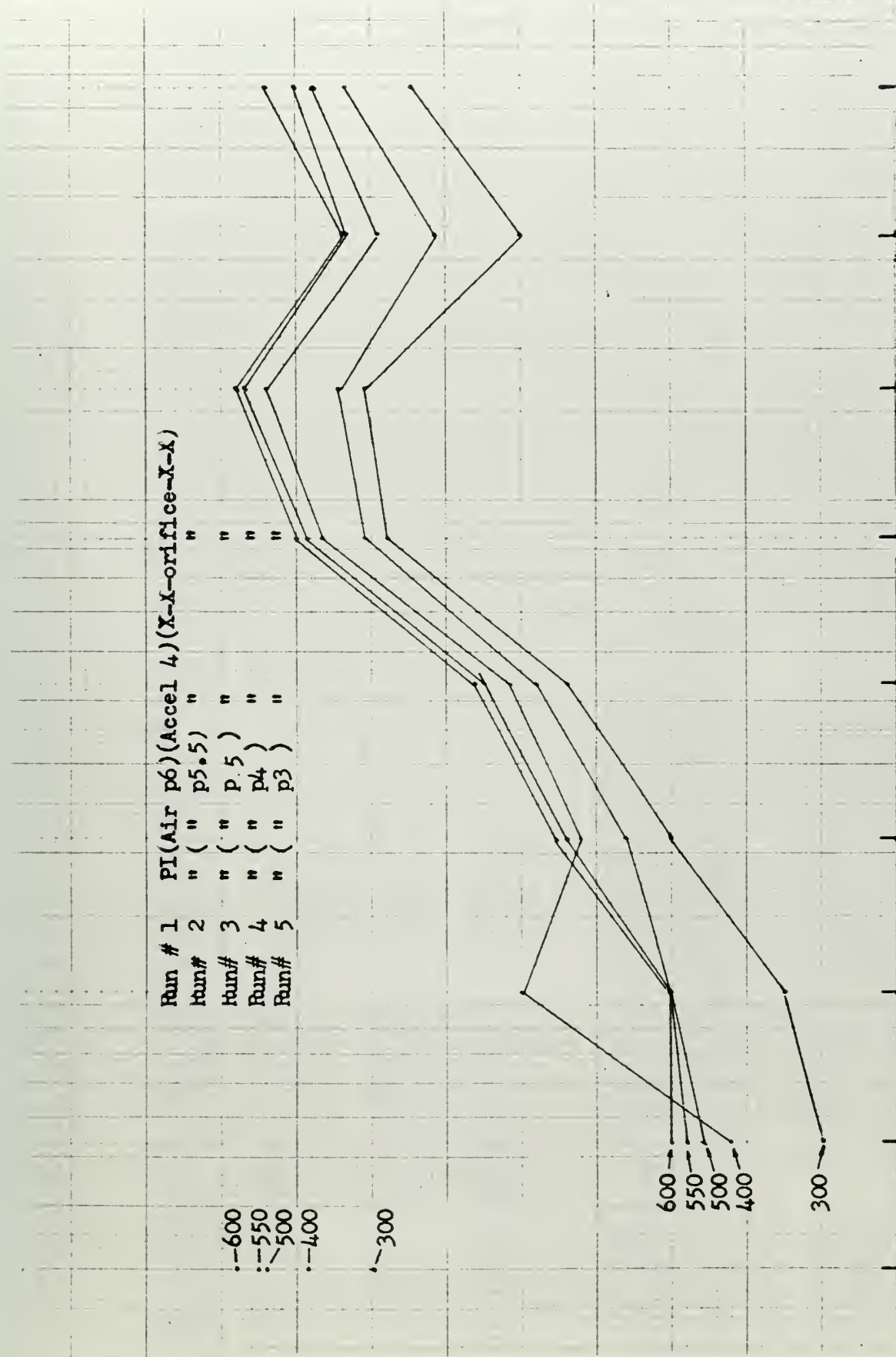
1690.0

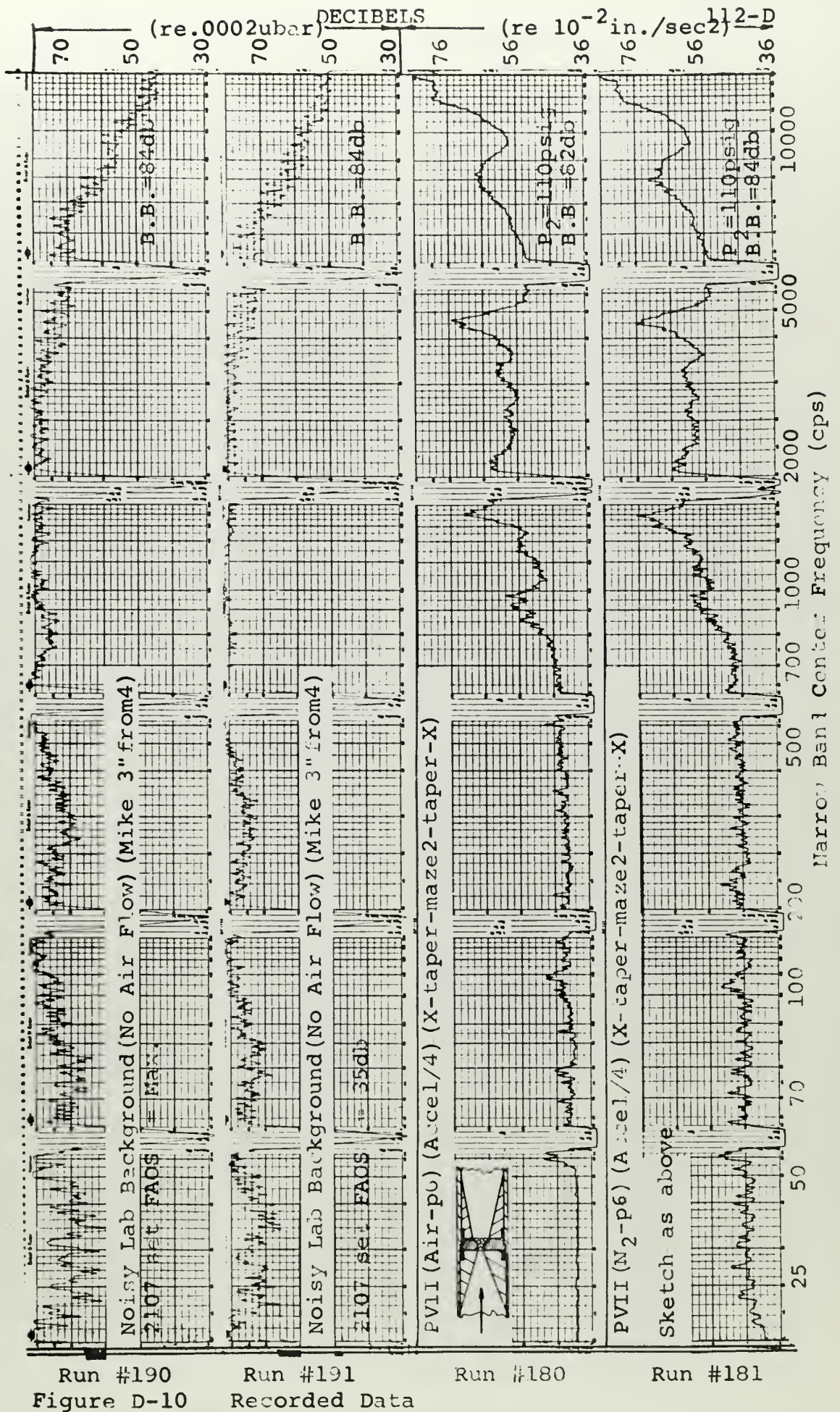
3380.0

6770.0

OCTAVE BAND CENTER FREQUENCY (cps)

600
550
500
400
300





Run #190
Figure D-10

Run #191
Recorded Data

Run #180

Run #181

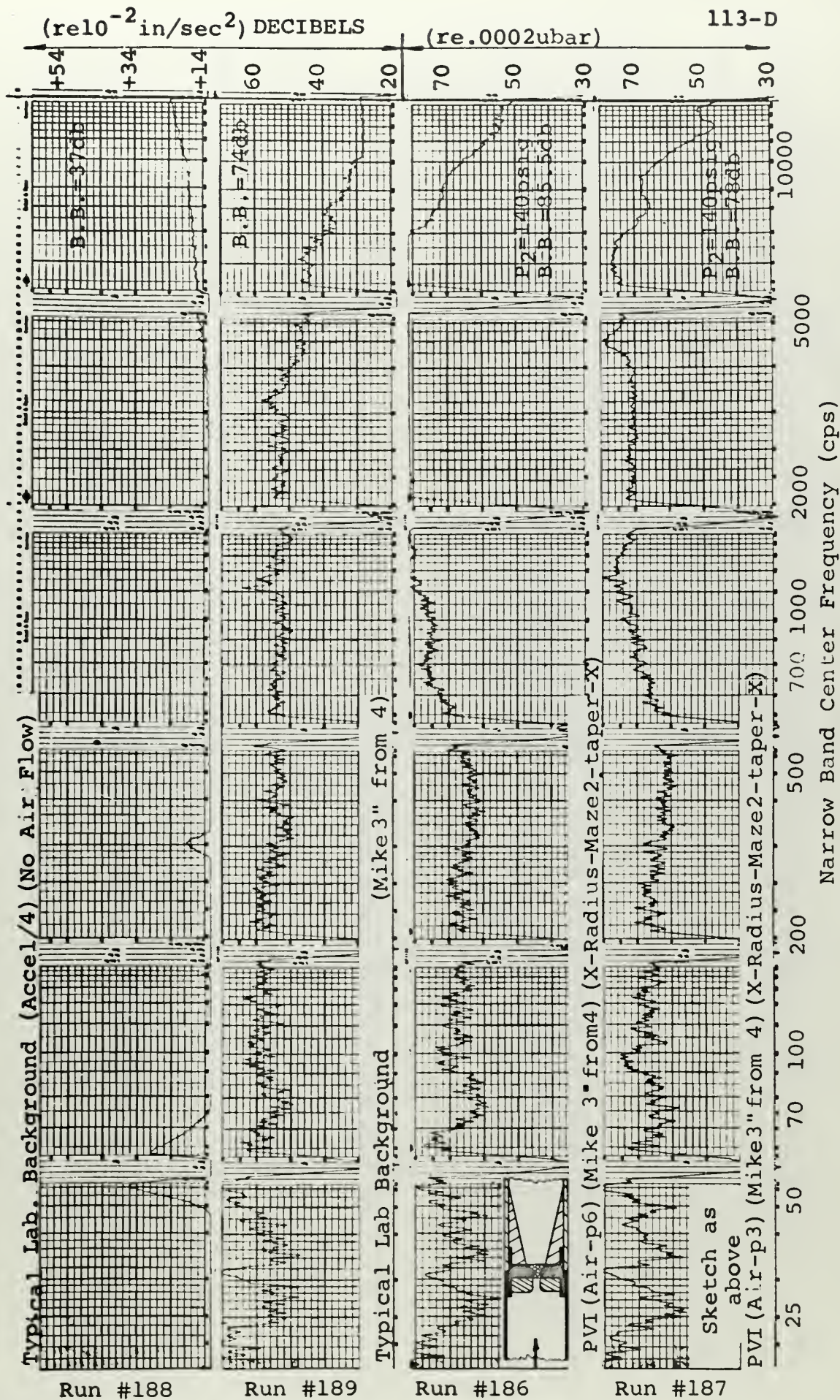


Figure D-11 Recorded Data

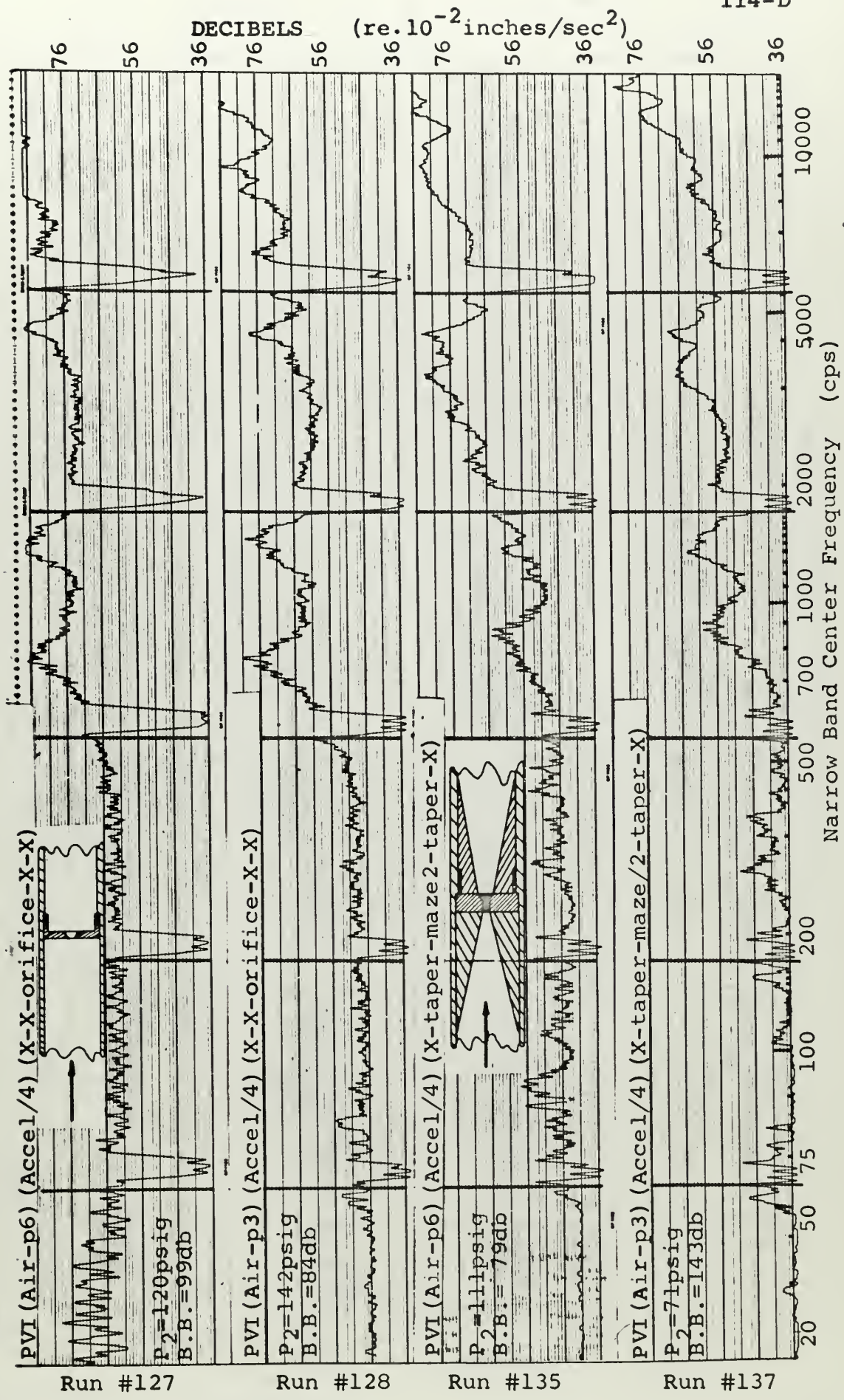


Figure D-12 Recorded Data

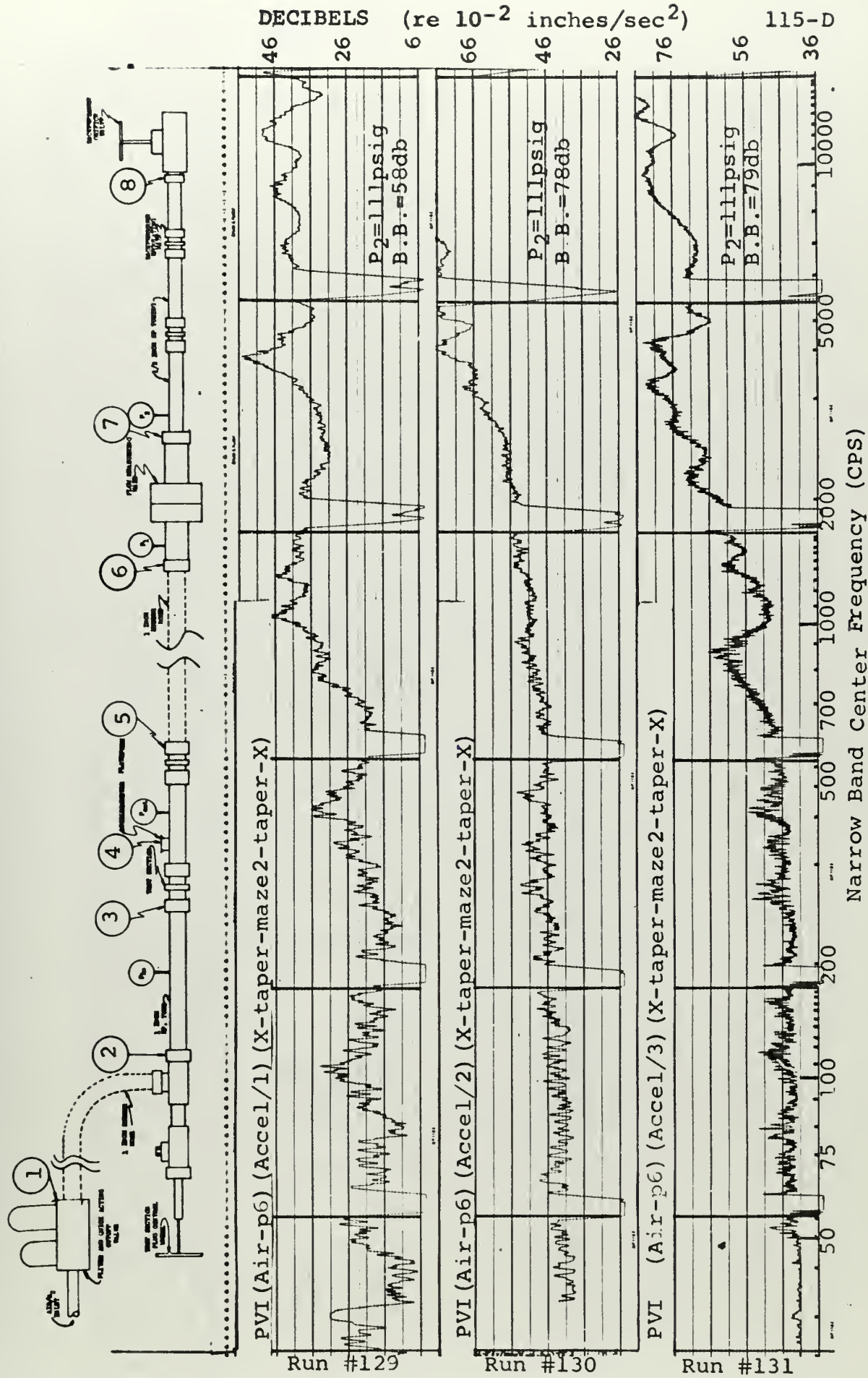


Figure D-13a Recorded Data

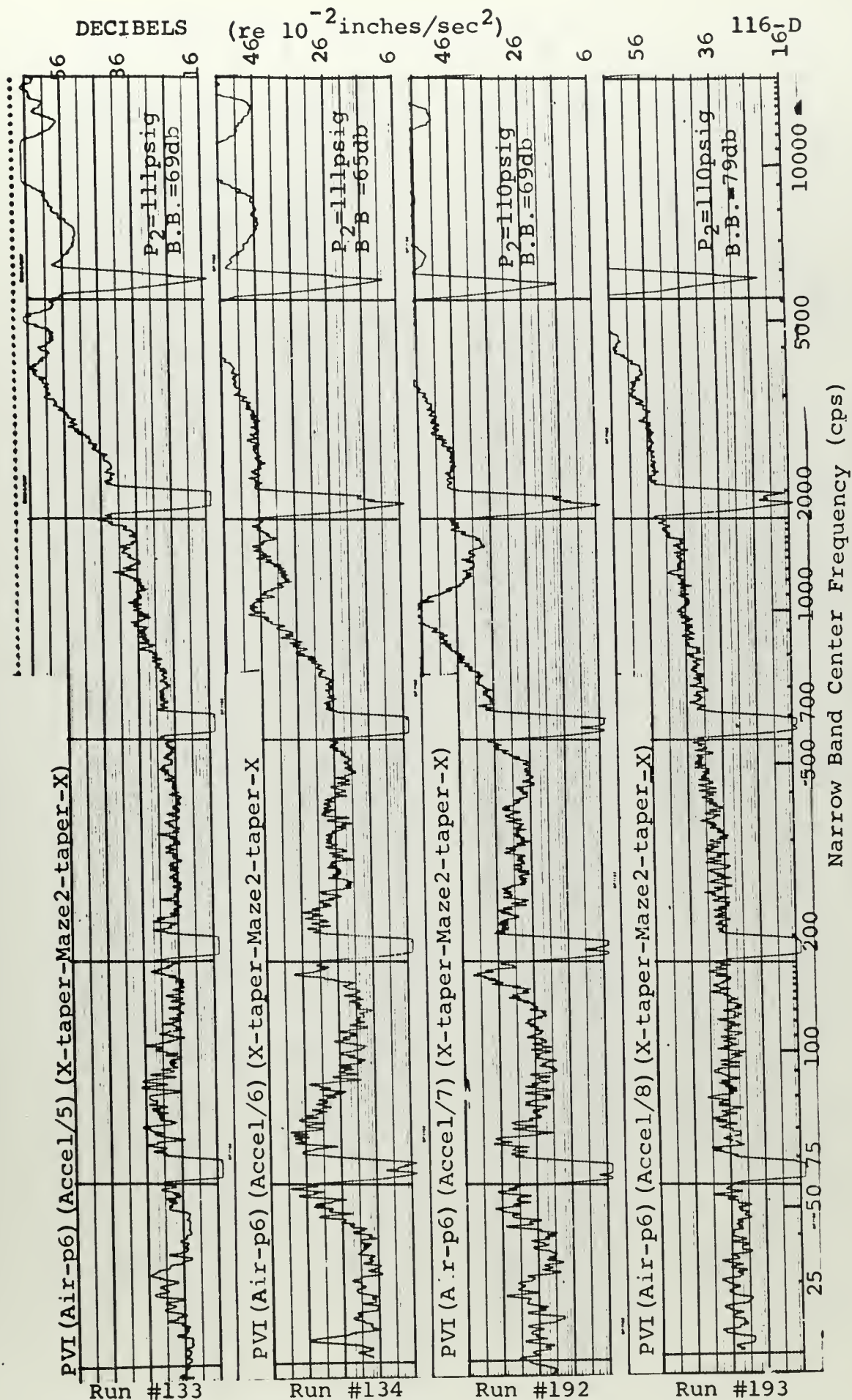


Figure D-13b

Recorded Data

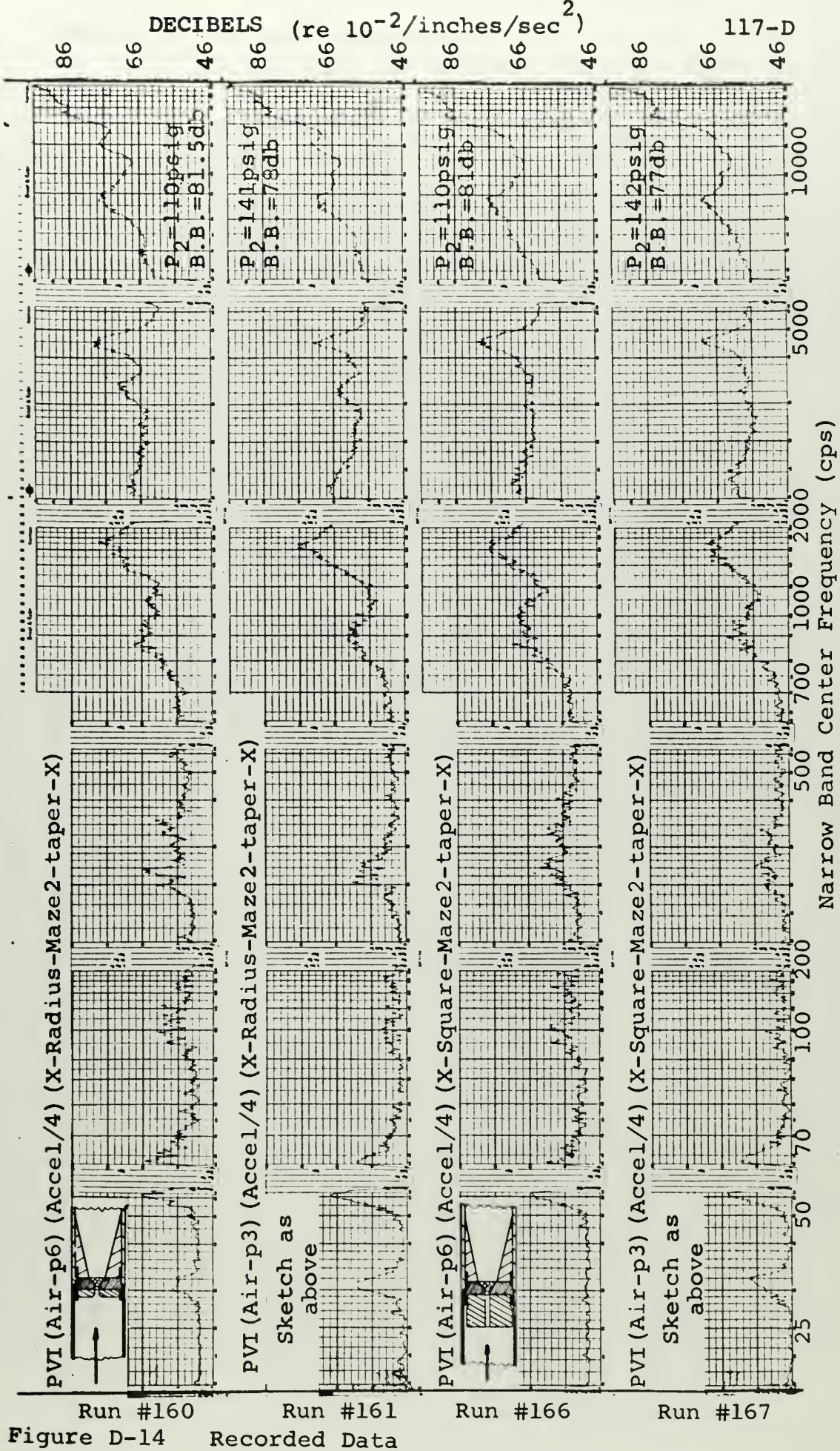


Figure D-14 Recorded Data

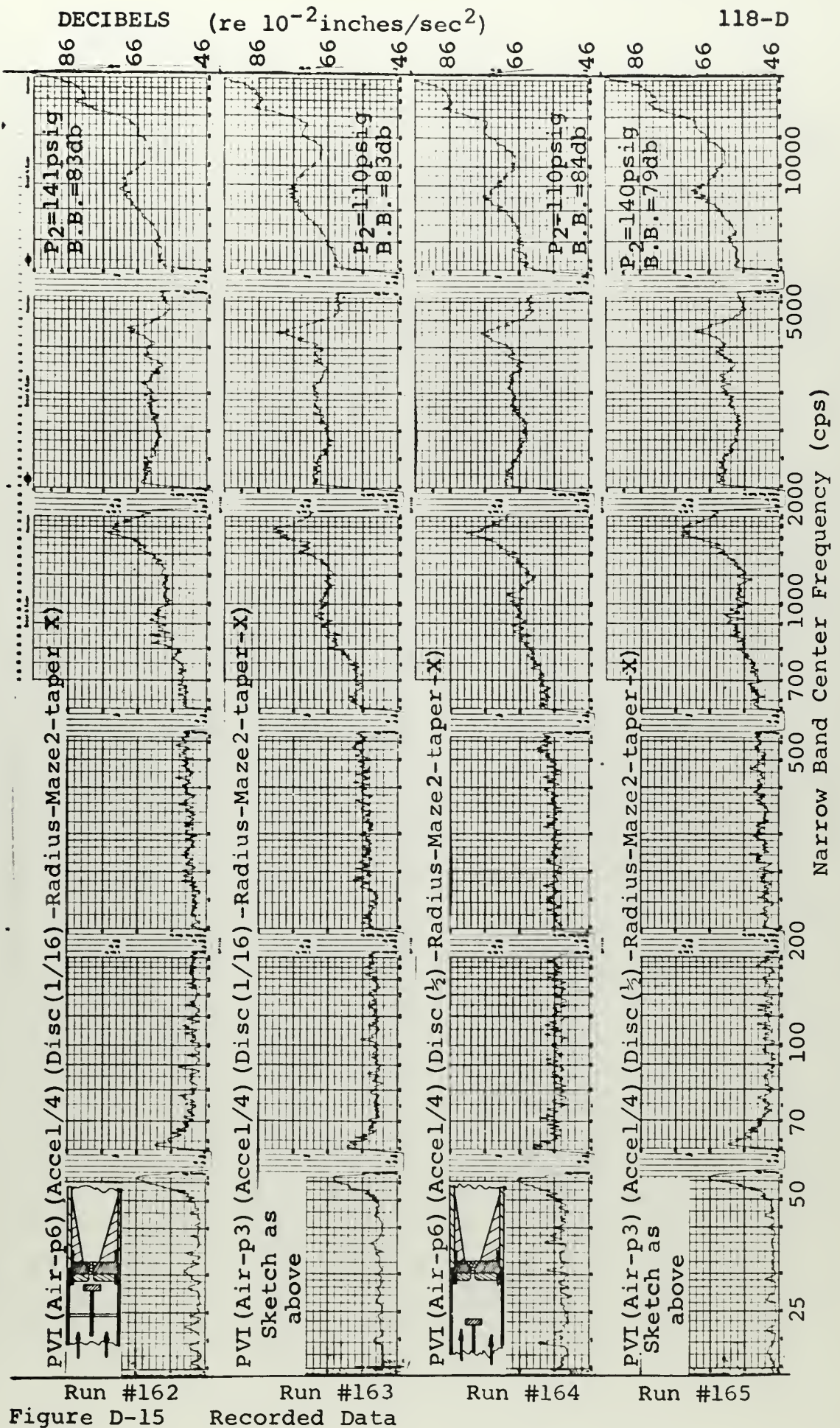


Figure D-15 Recorded Data

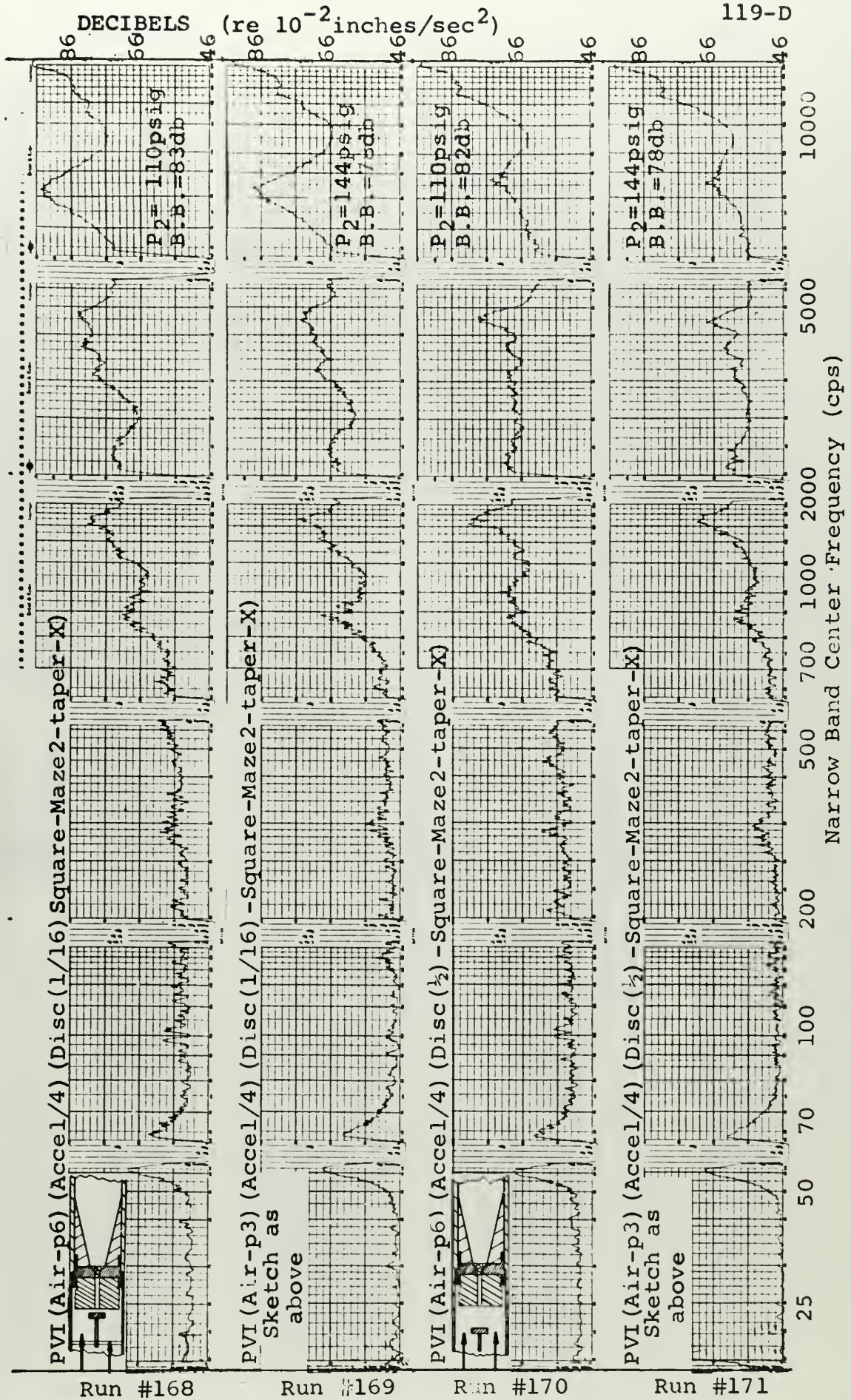


Figure D-16 Recorded Data

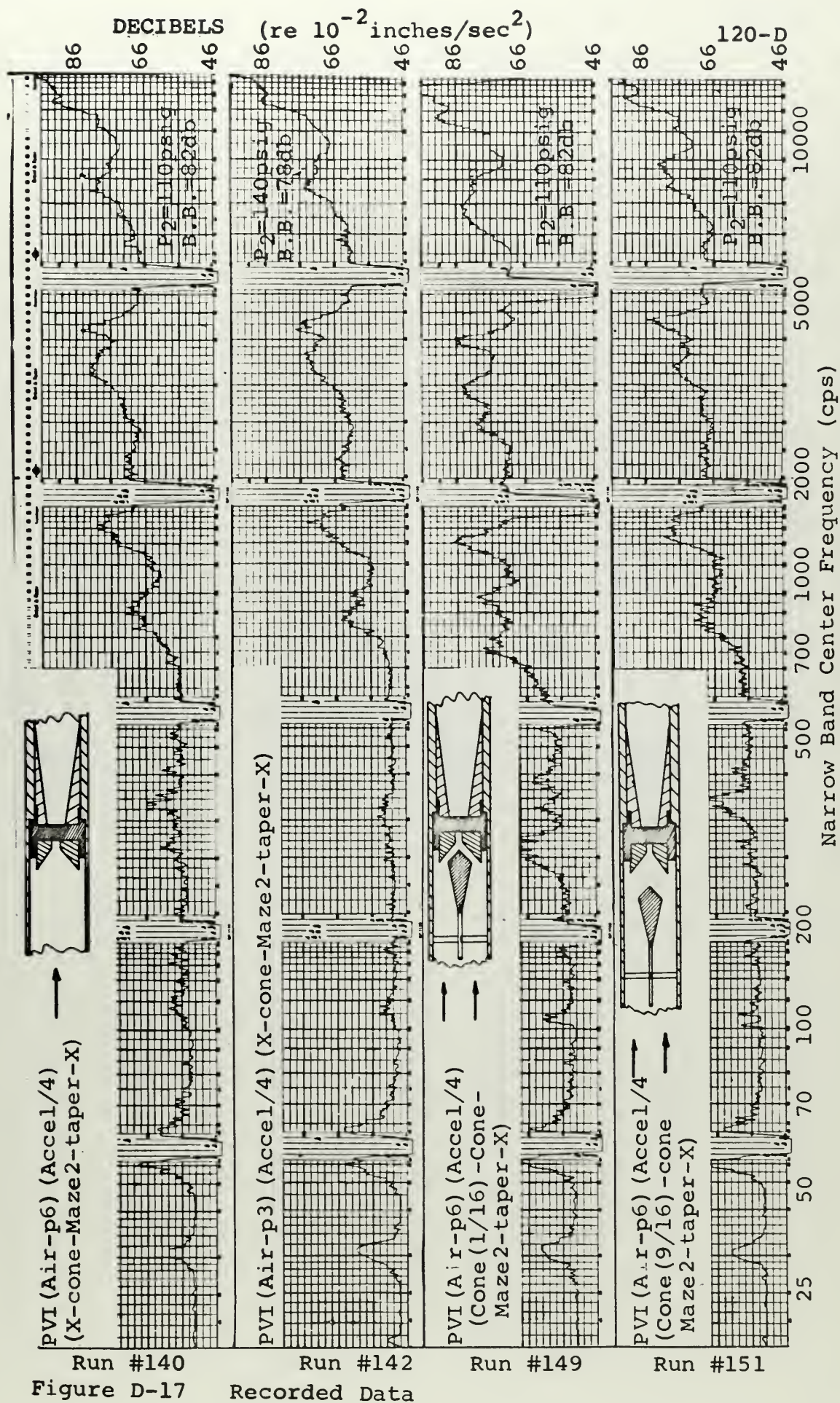
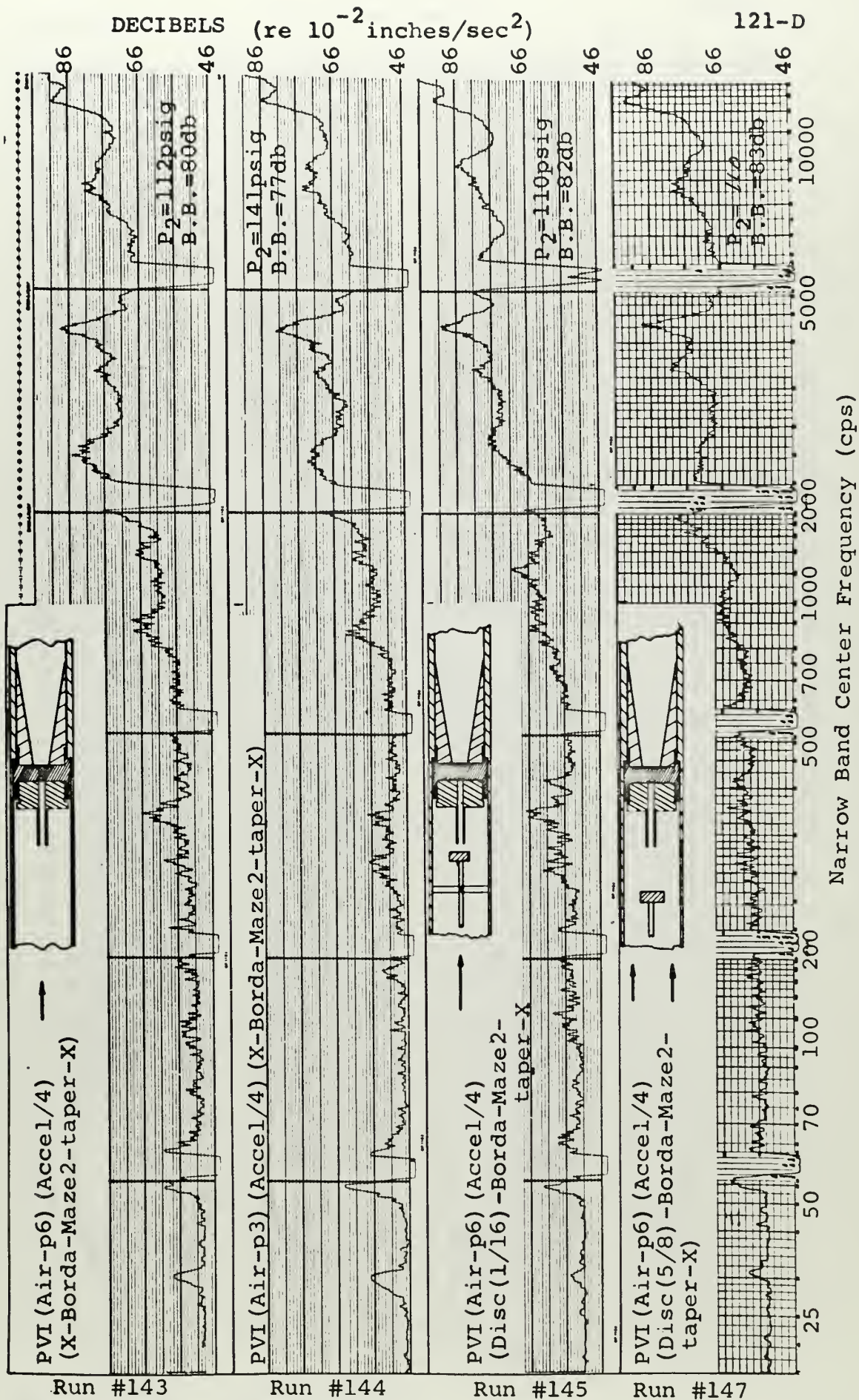
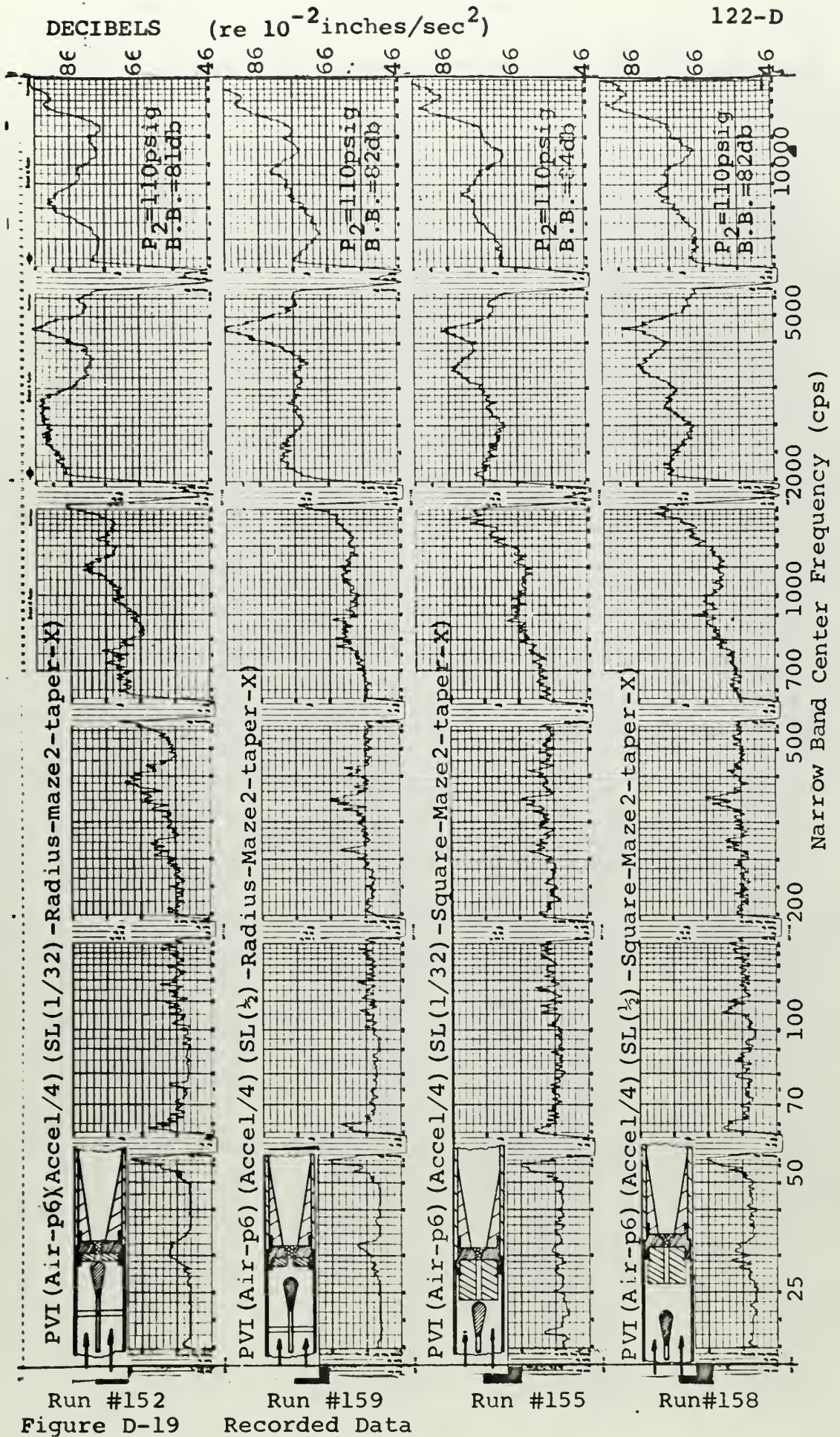


Figure D-17

Recorded Data



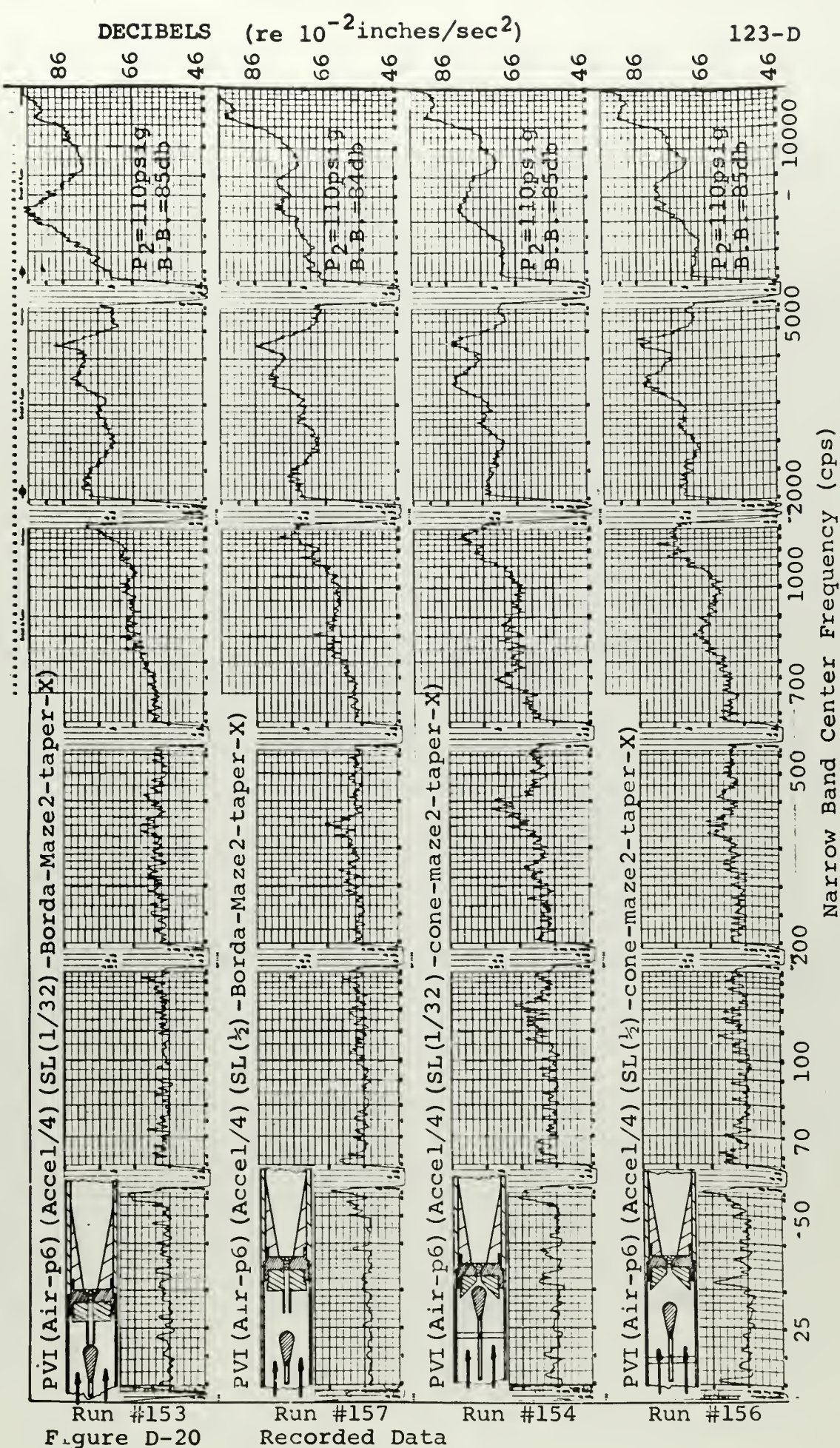


Run #152
Figure D-19

Run #159
Recorded Data

Run #155

Run#158

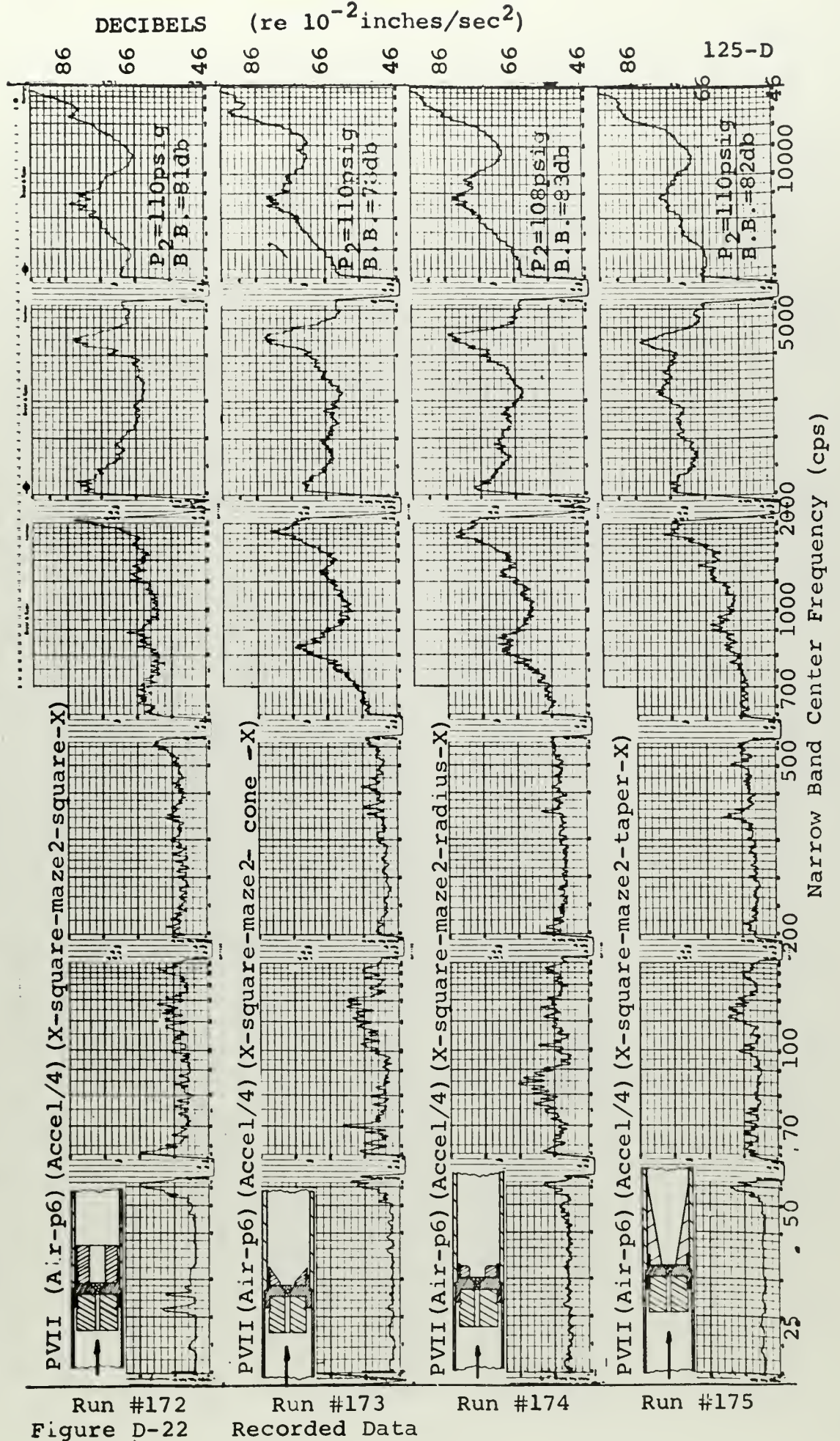


Run #153
Figure D-20

Run #157
Recorded Data

Run #154

Run #156



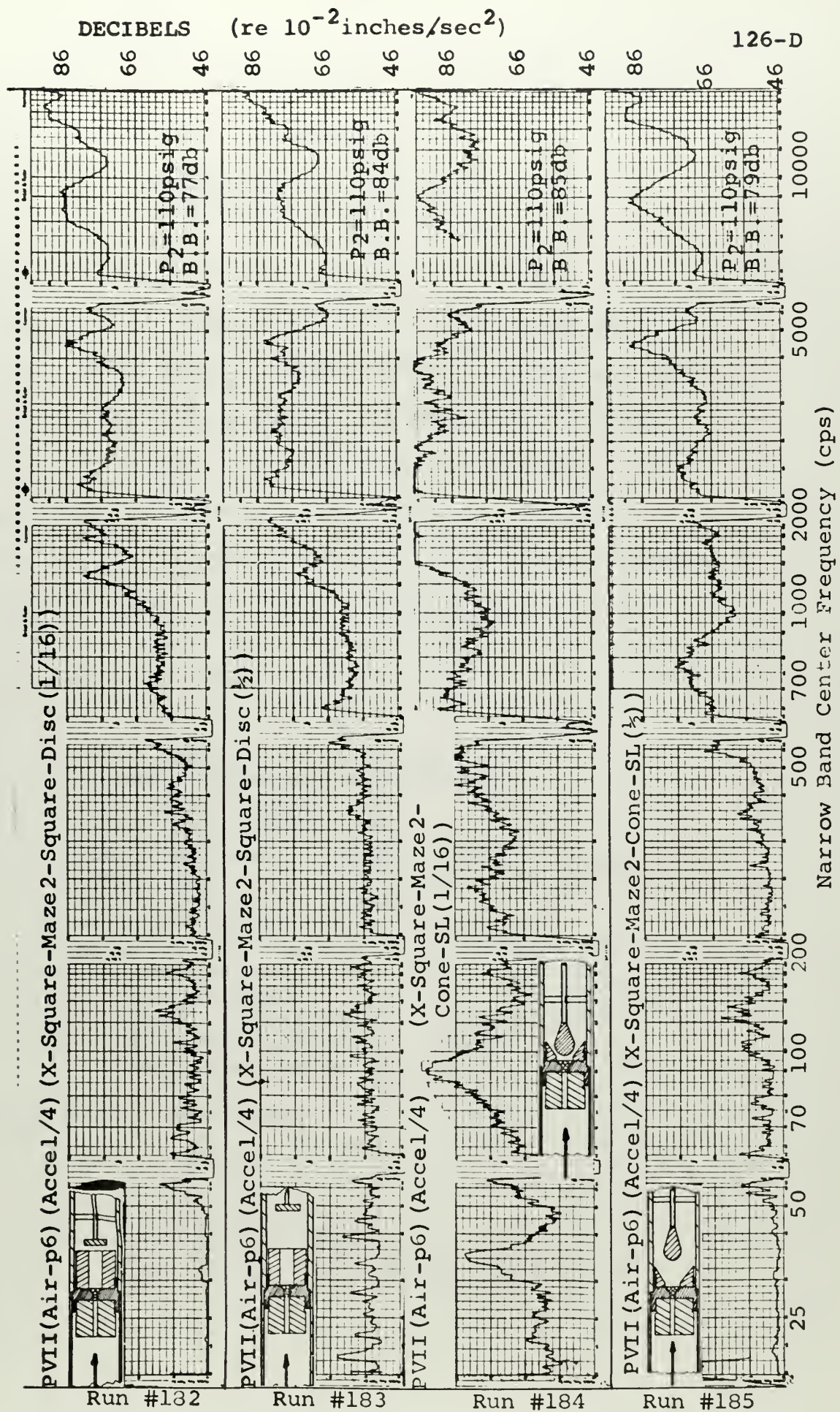


Figure D-23 Recorded Data

APPENDIX E

INSTRUMENT SPECIFICATIONS

1. Pick-up system:

General Radio type 1560-pl3 Vibration Pick-up System consisting of an Endevco, model 2217C accelerometer and a control box. The accelerometer is mounted on a strong magnet for attachment to the vibrating structure. The control box integrates the accelerations to provide velocity and displacement, but all tests for this project were made in the direct, acceleration mode.

Accelerometer characteristics:

Piezo-electric ceramic material
 Resonate frequency: 28,000 cps
 Max. accel. 1000g
 Capacitance: 337pf (Cp)
 Operating temp. -65 to +250°F
 Temp. coeff. of sensitivity: .01 db/°F
 Weight 1,2 oz (34 grams)
 Size 5/8 inches hex. x .7 inches
 Sensitivity (nominal 60 millivolt /g)
 peak mv/peak g 76.2 (Es)
 rms mv/peak g 53.9 (Ec)
 peak p cmbs/peak g $Es(Cp + 180)10^{-3} = 39.4$
 External capacity 180 pf
 Max. transverse sensitivity in % 4.2

System characteristics:

Acceleration:

20-20,000 cps
 -2 db at 20 cps .
 + 1 db at 10,000 cps
 RMS accel 0.3 to 300,000 inches/sec²)

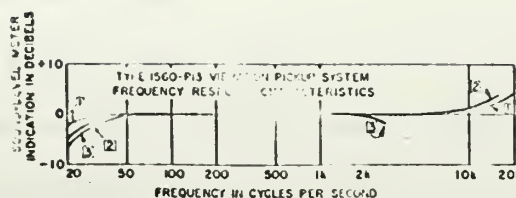


Figure E-1 Frequency Response of Pick-up System for Constant Applied Acceleration

2. Sound Level Meter:

General Radio type 1551-C consisting of a omnidirectional microphone (removed to connect the accelerometer), a calibrated attenuator, an amplifier, standard weighing networks and an indicating meter.

Characteristics:

Sound level range: 24 to 150 db (re 0.0002 μ bar)

Frequency characteristics: Four response modes selected by panel switch providing A,B,C, weighing in accordance with ASA S1.4-1961, and a flat (figure E-2) response in the fourth mode. (The later was used throughout these tests.)

Output: 1.4v into 7000 Ω

Input impedance 25 M in parallel with 50 pf

Temp: range 0 to 60°C

Humidity range 0 to 90%

Weight 7.7 lb

Size 6x7x9 inches

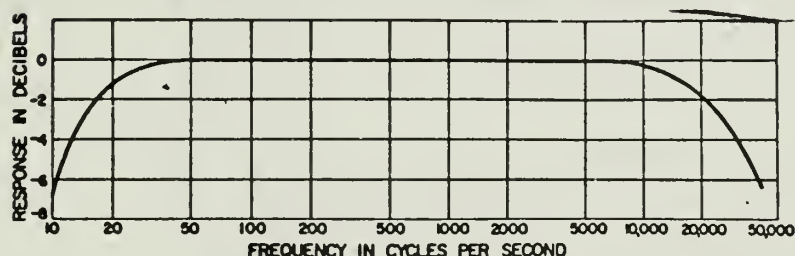


Figure E-2 Frequency Response of Sound Level Meter with Weighing Switch at 20kc.

3. Octave Band Analyzer:

General Radio type 1550-A consisting of 8 bandpass filters, an attenuator and an amplifier.

Characteristics:

Frequency bands:

Broadband	20 to 10,000 cps
20 to 75 cps	600 to 1200 cps
75 to 150 cps	1200 to 2400 cps
150 to 300 cps	2400 to 4800 cps
300 to 600 cps	4800 to 10,000 cps

Input voltage: 1 to 10v

Input Impedance: 20,000 ohms

Output voltage: 1v across 20,000 ohms

Weight 27lb

Size 9x11x12

4. Narrow Band Analyzer:

Bruel and Kjaer type 2107 constant-relative bandwidth frequency analyzer consisting of an input amplifier, frequency weighing networks, a selective amplifier, an output amplifier and a rectifier and meter circuit.

Characteristics:

Frequency range:

20 to 20,000 cps

Frequency bands:

20-63 cps	630-2000 cps
63-200 cps	2000-6300 cps
200-630 cps	6300-20,000 cps

Weighing networks:

A,B,C, in accordance standards for precision SLM

20-40,000 cps (Used throughout these tests)

2-40,000 cps

Selectivity:

Of amplifier (3 db bandwidth) is variable in six steps of 6, 8.5, 12, 16, 21, and 29%. (6% used here)

Octave selectivity (attenuation \pm octave away from the tuned center freq.) is 45, 40, 35, 25, and 20 db respectively - see figure E-3.

Output of amplifier: 45v
 Amplifier output impedance: 50 ohm (24 uf in parallel)
 Input voltage range: 100 micro to 1000 volts
 Input impedance: 2.22 megaohms (30 pf across terminals)

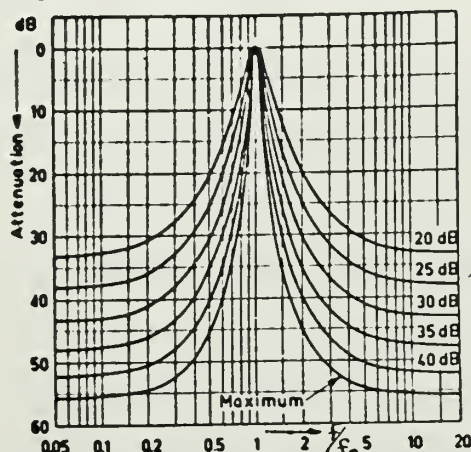


Figure E-3 Selectivity Curves of B & K, 2107,
 (Attenuation one octave from tuned in freq.)

5. Automatic Recorder:

Bruel and Kjaar type 2305 Level Recorder:

Characteristics:

Frequency range:

2 to 200,000 cps (See figure E-4)

Writing speeds:

4mm to 2000mm/sec for 100mm paper width
 (200/sec used here) (also 2 to 1000mm/sec
 for 50mm paper)

Paper speed:

0.0003 to 100mm/sec (10mm/sec used here)

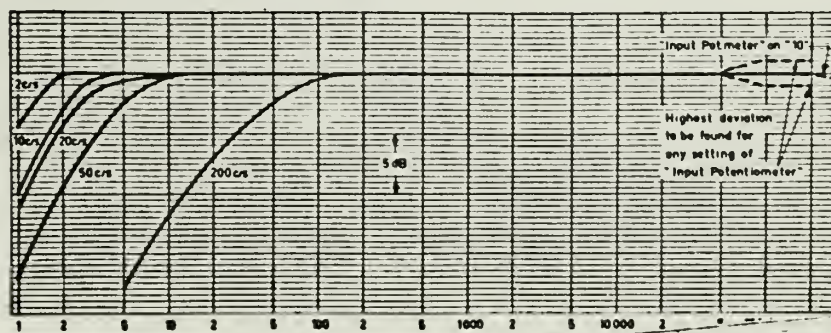


Figure E-4 Typical Frequency Characteristics (20 cps curve)

6. Calibrations:

- a. The accelerometer and sound level meter as a system was calibrated with a General Radio type 1557-A vibration calibrator at the start of testing and checked again at the end. (Calibrator subjects pickup to an acceleration of $1g$ at 100 cps)
- b. Known input voltages were also passed through the analysis train and read on the recorder paper at the input oscillator frequencies (400 and 8500 cps). The results and components used for this check are shown in figure E-5.

7. Instrument settings held constant (except when noted)

- a. Vibration pickup system:

Control box selector switch: Acceleration

- b. Sound level meter:

Meter/Batteries switch: Fast meter
Weighing switch: 20 kc

- c. Octave Band Analyzer:

Batteries switch: Fast

- d. Narrow Band Analyzer:

Input potentiometer: 2
Input selector: Direct
Meter switch: RMS, Fast
Frequency Analysis Octave Select.: Max.
Weight switch: Linear 20-40,000 cps
Frequency range: automatic scan
Function switch: automatic

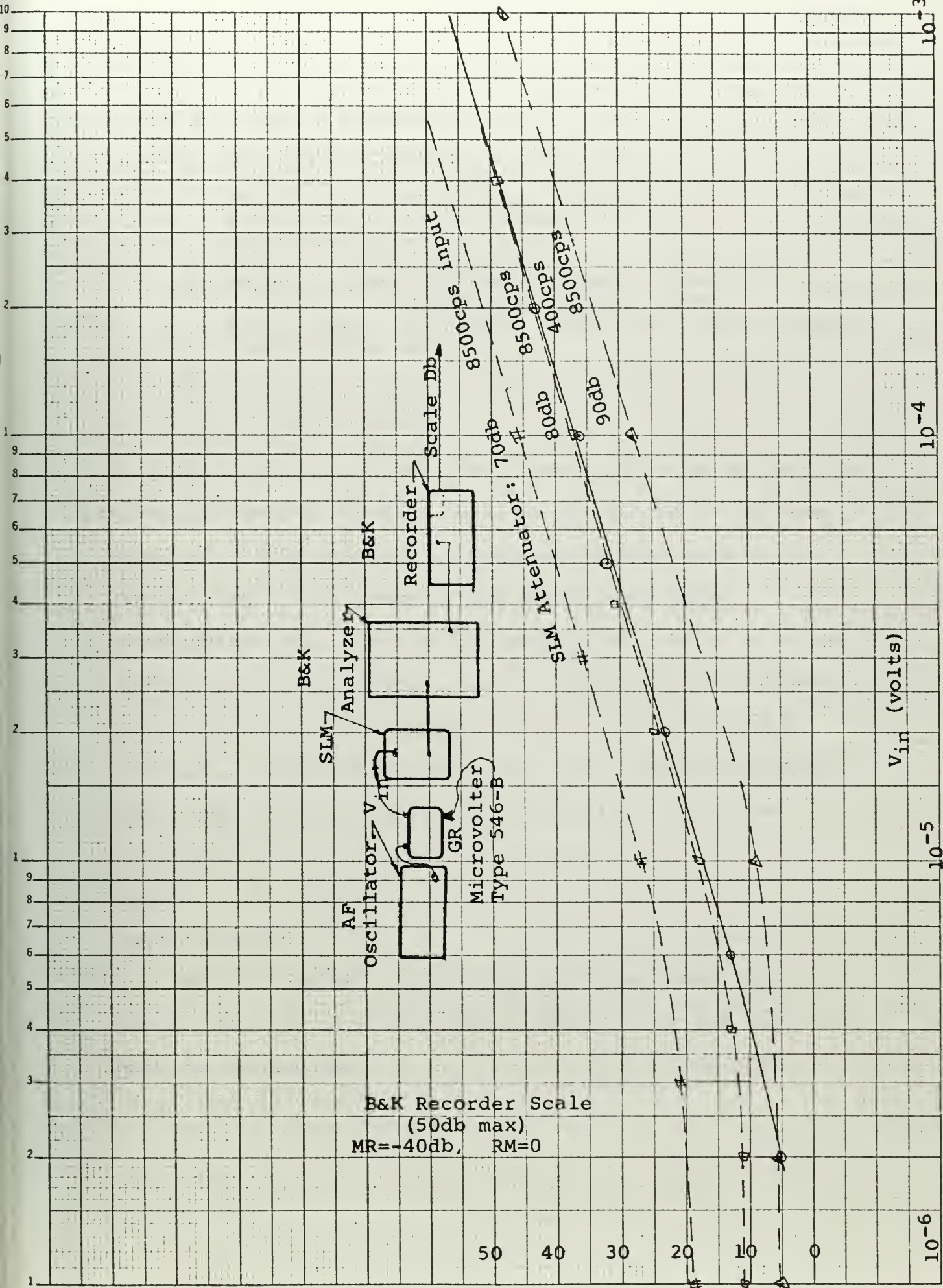


FIGURE E-5 Calibration checks

f. Automatic Recorder:

Input potentiometer: $6.6 \pm .4$
 Input attenuator : 10
 Replacable potentiometer: 50db
 Potentiometer range: 50 db
 Range recorder: RMS
 Lower limiting frequency: 20 cps
 Writing speed: 200 mm/sec (small numbers)
 (100 mm/sec large numbers)
 Paper speed: 10 mm/sec (100 mm/sec large numbers)
 Paper width: 100 mm

9. Decibel scale conversion:

The entire instrument chain was calibrated so that all plot and recording scales could be referenced to the same standard. This standard corresponds to that used in the General Radio Accelerometer and Sound Level Meter combination- (i.e. all decibel scales for acceleration are referenced to 10^{-2} inches / sec²). Since the GR equipment provides only decibel values which can be translated by instruction book conversion tables into absolute quantities and since the B & K equipment reads only in decibels referenced to a standard input voltage of 10v, Figures E-6 and E-7 were developed for determining the relationships outlined below:

From figure E-6 the gain of the Sound Level Meter can be obtained for each attenuator setting. For use here this gain is defined as:

A_i = gain of SLM for i^{th} attenuator setting

V_{out} = output voltage of SLM

V_{in} = input voltage of SLM

E-1

$$A_i = 20 \log \frac{V_{\text{out}}}{V_{\text{in}}}$$

This relation and figure E-6 have been used to determine the following:

A	Decibel gain
100	28.96
90	39.10
80	49.56
70	59.1
60	68.96

Although the instruction book gives the accelerometer sensitivity, the overall system sensitivity was not known but has been determined with the aid of figures E-7 to be 1.8×10^{-5} volts input/inch/sec² for a meter reading of 80 db.

The B & K recorder paper scale can be referenced to 10^{-2} inches/sec² acceleration as follows:

- S = recorder paper scale (50db max)
- RM = range multiplier switch setting on B&K analyzer (db)
- MR = meter range switch setting on Analyzer (db)
- P = Recorder range potentiometer (db)

V_a = input voltage to analyzer (volts)

V_{oa} = input ref. voltage for analyzer (10 volts)

I_a = input voltage in decibel (re 10v)

E-2

$$I_a = 20 \log \frac{V_a}{V_{oa}}$$

When the analyzer and recorder are used together the following relationship converts the recorded decibel reading to input volts: (manufacturers instruction book)

E-3

$$I_a = S + RM + MR - P = 20 \log \frac{V_a}{V_{oa}}$$

Subtracting E-1 from E-3:

$$\begin{aligned} I_a - A &= 20 \log \frac{V_a}{V_{oa}} - 20 \log \frac{V_{out}}{V_{in}} \\ &= 20 \log \frac{V_a}{V_{oa}} \frac{V_{in}}{V_{out}} \end{aligned}$$

When the output from Sound Level Meter is connected to the Analyzer:

$$V_a \equiv V_{out}$$

So that

E-4

$$I_a - A = 20 \log \frac{V_{in}}{V_{oa}}$$

Transforming E-4 into acceleration variables:

$$I_a - A = 20 \log \frac{V_{in}/1.8 \times 10^{-5}}{V_{oa}/1.8 \times 10^{-5}} \frac{10^{-2}}{10^{-2}}$$

Now let

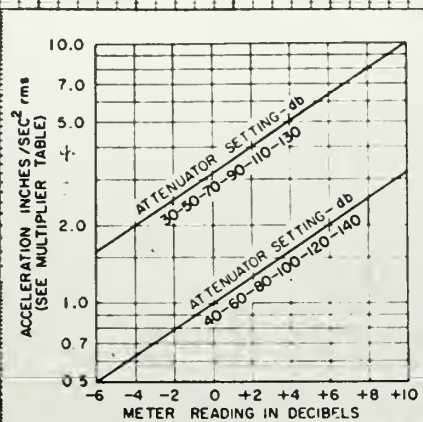
α = unknown acceleration (inches/sec²)

α_r = reference acceleration (10⁻² in./sec²)

Then:

$$E-5 \quad I_a - A = 20 \log \left(\frac{\alpha}{\alpha_r} \right) - 155 \text{db}$$

All recorder scales are determined from E-5.



Attenuator Setting - db	Multiply Inches/Sec ² By
30	10 ⁻¹
40 or 50	1
60 or 70	10
80 or 90	10 ²
100 or 110	10 ³
120 or 130	10 ⁴
140	10 ⁵

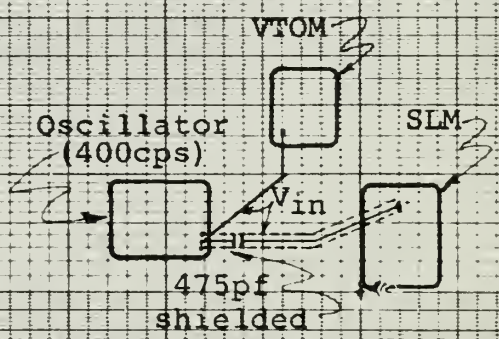
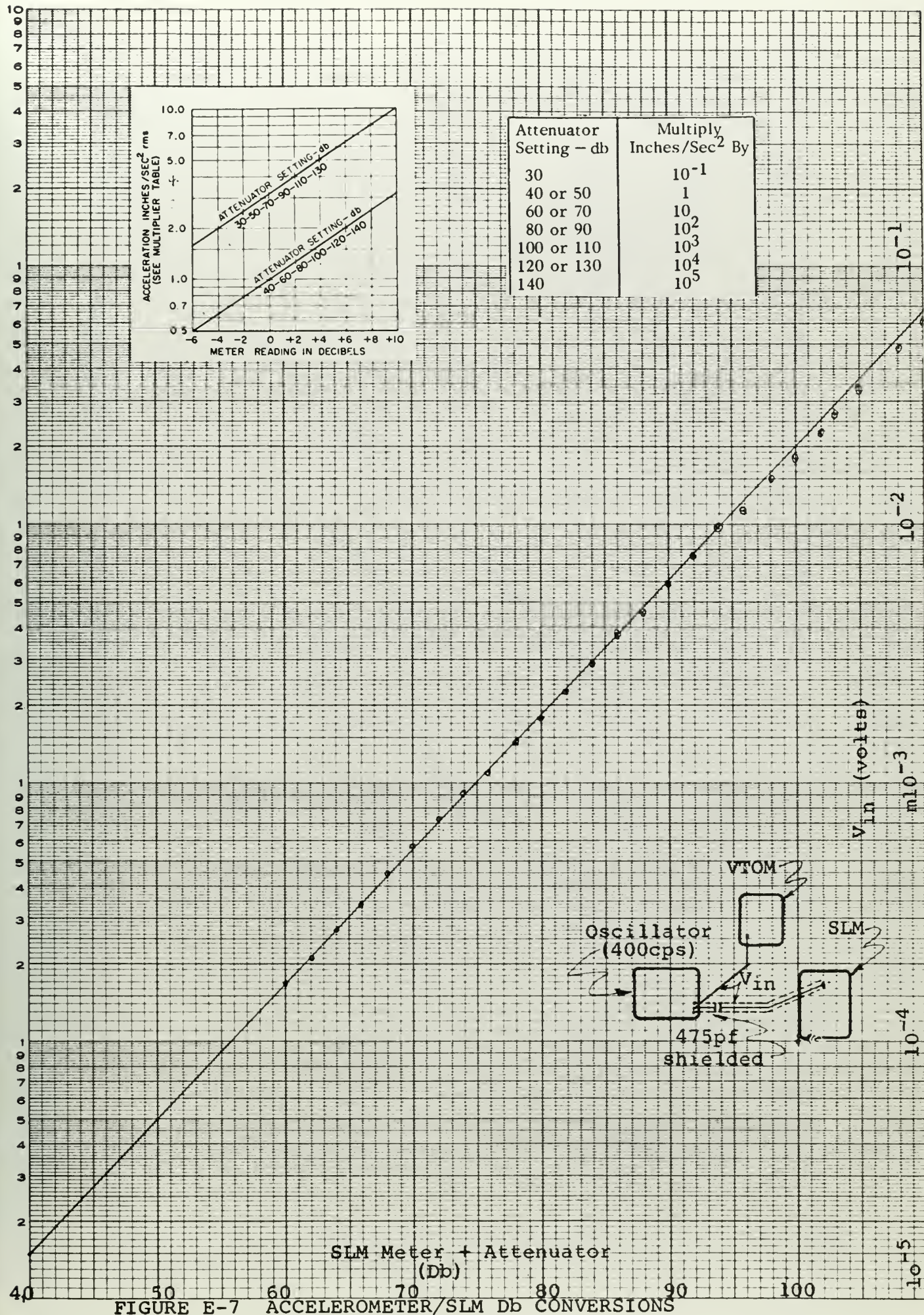


FIGURE E-7 ACCELEROMETER/SLM Db CONVERSIONS

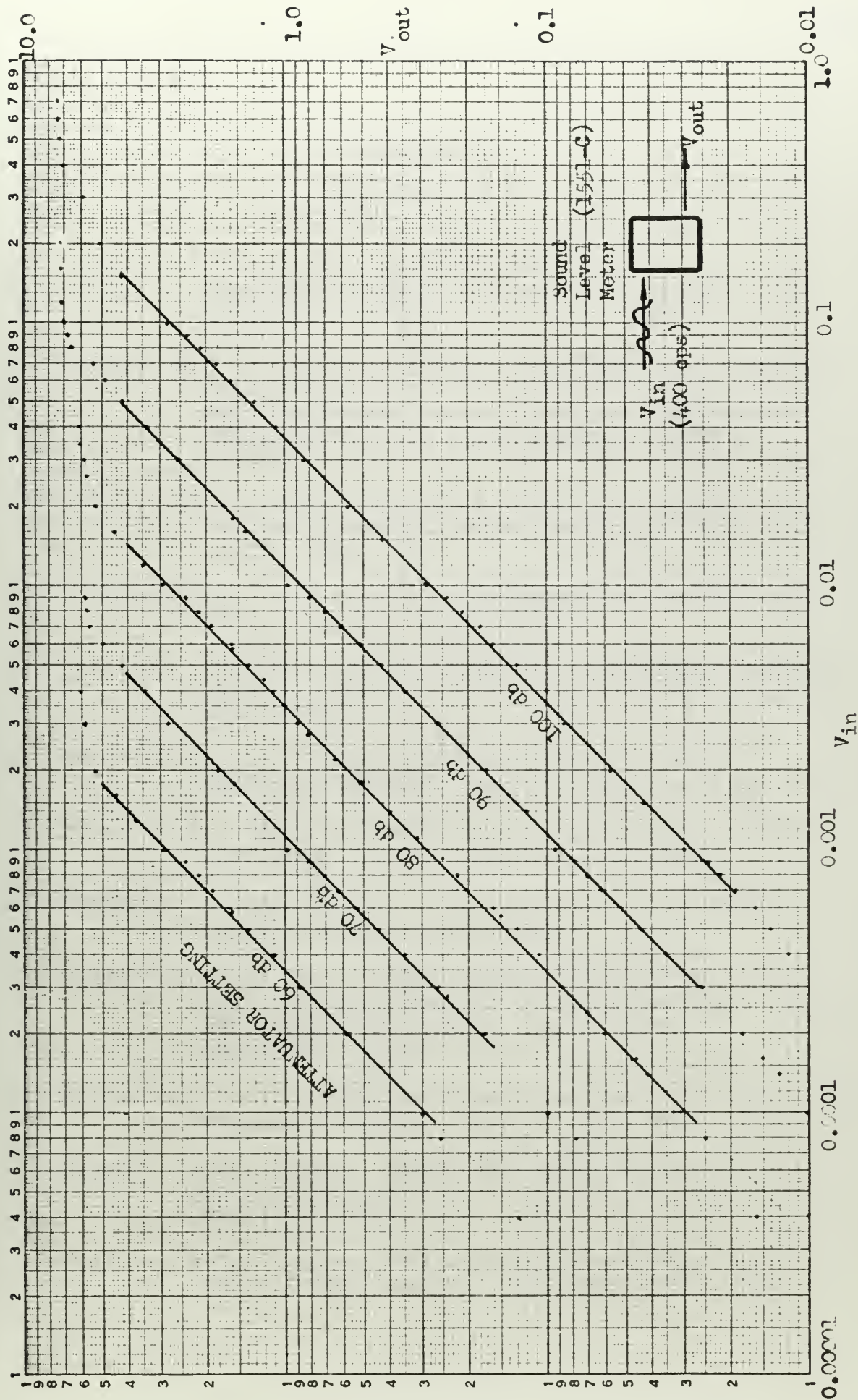


FIGURE E-6

Sound Level Meter (SL-551-C) amplifier gain

REFERENCES

Appendix F

1. _____, Handbook of Noise Control, Editor, Harris, CM McGraw-Hill 1957.
2. Muller, E.A., "Some Experimental and Theoretical Results Relating to Production of Noise by Turbulence and the Scattering of Sound by Turbulence or Single Vortices", 2nd Symposium, Naval Hydrodynamics, Aug 25-29, 1958, ONR, ACR-38.
3. "Principles and Applications of Underwater Sound", National Defense Research Council Technical Report, Vol 7, 1946.
4. Kinsler, L.E., and Frey, "Fundamentals of Acoustics", John Wiley and Sons, 1962.
5. _____, "Installations and Piping of Pressure Reducing Valves", Heating and Ventilation Vol 45, #12, Dec 1948, p85.
6. Hostedler, D.E., "Control Valve Design and Use" Petroleum Refiner, Vol 31, #12, Dec 1952, p116.
7. Beard, C.S., "Control Valves and Positioners", Industry and Power, Vol 64, #3, Mar 1953, p67.
8. Handbook of Instrumentation and Control, H.P. Kallen, editor, McGraw Hill, 1961.
9. Keikiti, T., "Air Flow Through Exhaust Valves of Conical Seat", Proceedings of 3rd International Congress for Applied Mechanics, Vol I, p278, Stockholm, 1930.
10. Hostedler, D.E., "Design and Construction of Control Valves" Petroleum Refiner, Vol 32, Aug 1953, p133.
11. Valstar, J.E., "Sizing Valves for Maximum Flow and Control Rangeability," Control Engineer, Vol 6, May 1959, p120.
12. Valstar, R.E., "Selecting Control Valve Characteristics", Control Engineering, Vol 6, Mar 1959, p104.

13. Collins, R.E., "Flow of Fluids Through Porous Materials, Reinhold Publishing, 1961.
14. _____, "Technical Report of Phase I of Pressure Reducer Maze Development", PRDR-23, Sanders Associates, Nashua, N.H. 1966.
15. Blackburn, J.F., Reethof, G., Shearer, J.L., "Fluid Power Control," MIT Press, 1960.
16. Munk, M.M., "Aerodynamics Theory Series", Vol 1, Editor Duram Berlin -Springer, 1934.
17. Lamb, H., "Hydrodynamics", Dover, 1945.
18. Hess, J.L., Smith, A.M., "Calculations of Non Lifting Potential Flow About A Arbitrary 3D Body., J. Ship Research, Vol 3, #2, Sept 1964.
19. Robertson, J.M., "Hydrodynamics In Theory and Application" Prentice-Hall, 1965.
20. Birkhoff, G., Zarantonello, E.H., "Jets, Wakes, and Cavities", Academic Press, 1957.
21. Ehrick, F.F. "The Hydrodynamics of Flow Regulation", PhD Thesis, MIT, 1951.
22. Keenan, J.H., "Thermodynamics," J.Wiley & Sons, 1941.
23. Lighthill, M.J., "On Sound Generated Aerodynamically," Proc. The Royal Society, Series A, #1107, Vol. 211, 1952, p 565.
24. Lighthill, M.J., "On Sound Generated Aerodynamically," Part 2 Proc. The Royal Society, Series A, # Vol. 222, 1954, p 1.
25. Faires, V.M. "Thermodynamics," McMillan, 1957.
26. Bateman, H. "Partial Differential Equations," Dover Publications, 1944.
27. Stratton, J.A. "Electromagnetic Theory" McGraw-Hill, 1941.
28. Curle, N., "The Influence of Solid Boundries Upon Aerodynamic Sound," Proc. the Royal Society, Series A, vol 231, Ap 1955, p 505.
29. Schlechting, H., "Boundry Layer Theory," McGraw-Hill Translation from German, 1955.

30. Batchelor, G.K., "Theory of Homogenous Turbulence," Cambridge Univ. Press, 1953.
31. Townsend, A.A., "The Structure of Turbulent Stream Flow," Cambridge Univ. Press, 1956.
32. Hinze, J.D., "Turbulence," McGraw-Hill, 1959.
33. Beard, C.S. "Control Valves and Positioners," Industry and Power, vol 64, #3, Mar 53, p67.
34. Valstar, J.E., "Selection of Control Valve Characteristics" Control Engineer, vol 6, #3,4,5, Mar, Apr, May 1958.
35. Ross, D. and Robertson, J.M., "Water Tunnel Paper," T-SNAME, 1956.
36. Lee, S.Y., "Contributions to Hydraulic Control - Six New Valve Configurations for High Performance Hydraulic and Pneumatic Systems," Trans. ASME, vol 76, 1954, p905.
37. Hutchinson, F.W., "Thermodynamics of Heat Power System," Addison-Wesley, 1957.
38. Potter, "Steam Power Plants," Ronald Press, 1949.
39. Callaway, D.B., Tyzzer, F.G., and Hardy, H.C., "Resonant Vibrations in a Water-Filled Piping System," J. Accoustical Society of America, vol 23, #5, Sept 1951, p550.
40. Ehenoweth, J.M. and Martin, W.W., "Turbulent 2-Phase Flow," Petro. Refiner, vol 34, Oct 1955, pl51.
41. Jacobi, W.J. , "Propagation of Sound Waves Along Liquid Cylinders", J. Accoustical Society of America, vol 21, #2, Mar 1949, pl20.
42. Callaway, D.B., Tyzzer, F.G., and Hardy, H.C. "Techniques for Evaluation of Noise-Reducing Piping Components", J. Accoustical Society of America, vol 24, #6, pp 725-730.



thesP7426

Investigation of noise caused by flow co



3 2768 001 92334 5

DUDLEY KNOX LIBRARY